Durham E-Theses

Pressure measurement by Piezo-electric transducers in reciprocating combustion engines
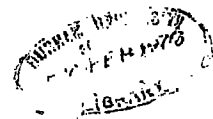
Khayat, Masin N.

PRESSURE MEASUREMENT BY PIEZO-ELECTRIC TRANSDUCERS
IN RECIPROCATING COMBUSTION ENGINES

by

Mazin N. Khayat

Thesis submitted for the Degree of Master of Science
in the University of Durham

Engineering Science Department
December, 1969

ABSTRACT

The properties, use and construction of quartz Piezo-electric transducers are briefly described. The dynamic calibration of quartz pressure transducers have been investigated using a Balanced-Disc pressure pick-up as a standard. The temperature effect on the static and dynamic output of these transducers has also been examined. Various types of engine indicators and their limitations are discussed.

Piezo-electric pressure transducers and strain gauges were used for constructing an inertia-free pressure-volume indicator to produce a P-V diagram on an oscilloscope screen from which the trace was recorded. This included a simple and accurate method for obtaining top-dead-centre on pressure-time records.

Some aspects of diesel combustion were consdiered using P-T diagrams from a variable compression Lister F.R.1 diesel engine running at different loads and compression ratios. The effect of the shape of transducer passage on the accuracy of P-T diagrams is observed.

Volumetric efficiency was measured using a crystal pressure transducer. The assumptions of this method was checked by comparison with the volumetric efficiency obtained by two other established methods.

- i -

ACKNOWLEDGEMENT

CONTENTS

1. INTRODUCTION

1.1. Quartz transducers

Most modern engine research requires the use of various transducers. One such type is the quartz pick-up.

The Piezo-electric effect of quartz crystals was used as early as the 1930's. The crystals possess a property, whereby an electric charge is produced in the crystal if a force is applied to the crystal. The charge produced is proportional to the applied force. This property renders the crystal ideal for construction of various types of transducers, (see Chapter 3). In conjunction with the development of cathode-ray oscilloscopes, the use of quartz Piezo-electric transducers, provided an inertia-free instrument for recording the various physical quantities measured in the engine. This stimulated the rapid development of the crystal transducers and their use has now become widespread both in research and industry.

To achieve a comprehensive use of the crystal transducers, their calibration under static conditions, dynamic conditions and of temperature effect should be carefully investigated. All methods of transducer calibration involve the application of a known input to the transducers, followed by an accurate and precise measurement of the transducer output. For the static calibration

of pressure transducers, a digital voltmeter and a deadweight
tester were initially used in this work. It was observed that
the rate of application of the input pressure had an effect on
the transducer maximum output reading. This led one to suppose
that the crystal pressure transducers produce an output that
varies significantly with the rate of pressure changes. This
observation had also been made at Thornton Research Centre,
Shell U.K. Research Ltd., who kindly provided facilities for
investigation of this phenomenon, (see Chapter 4).

Since static calibration curves only. were supplied by the
transducer manufacturers for relating input pressure to output
charge, pressure measurements in running engines had to be cor-
rected for this effect and a satisfactory procedure for dynami-
cally calibrating pressure transducers was required.

Because there was no suitable standard to use for pressure
measuring systems, extreme care must be taken to test the
transducer in a manner that minimized the need for an absolute
standard.

During the dynamic calibration, several tests were carried
out at engine speeds between 500 and 2750 r.p.m. on both Kistler
and AVL crystal transducers. The temperature effect on the
static and dynamic outputs of those transducers was also

investigated, (see Chapter 4).

To assist in further investigation of engine measurements Quartz thermometers, Load Cells and Accelerometers are very accurate devices. Only brief account of the construction and function of these instruments is given since they were not used by the author, (see Chapter 3).

1.2. Engine Indicators

An engine indicator is an instrument designed to produce a Pressure-Volume diagram for a reciprocating engine.

Improvements in engine design may be achieved by the help they give in investigations of the varying pressures inside the engine cylinder during actual working conditions.

Early indicators were mechanical, consisting of links, springs, pen and paper automatically operated. The inertia of the moving parts of the mechanism, had an increasing effect on the accuracy of the P-V diagrams produced as engine speeds increased. Consequently these types of indicators are unsuitable for producing a reliable indicator diagram from a high-speed reciprocating engine.

The construction, operation, and validity of the main types of indicators are discussed in Chapter 6.

To overcome the limitations imposed by the use of mechanical indicators, an inertia free indicator for producing a P-V diagram on the CRO screen is preferred. The design, construction, and performance of such an indicator are discussed in Chapter 7.

The accuracy of an indicator of this design is not affected by temperature changes, inertia effects or engine vibration.

P-V records can be obtained from a pressure indicator system by making the vertical and horizontal motions of the cathode-ray spot follow the pressure changes and the piston movement respectively. One method of achieving this requirement is to:-

(a) Incorporate a Piezo-electric transducer for the pressure indication.

(b) Convert crank angle signal into piston swept volume.

The problem of conversion to swept volume is solved by using a pair of strain gauges bonded to the opposite sides of a spring steel strip which is fixed at one end, the other end resting on a cam mounted on the crankshaft. The cam lift induces a stress in the steel spring, hence the strain of the strain

gauges is proportional to the piston displacement. By this means,
the signal from the strain gauges is proportional and in phase
with the piston swept volume. To minimize the fatigue effects on
the steel spring, the cam was originally designed to give a very
small lift. The signal from the strain gauges being amplified
to have an appropriate amplitude for display on the CRO screen.
The small gauge signal was found to be of the same order as the
noise signal because the amplification of the small strain gauge
signal was so high as to introduce some distortion signals due
to:-

   (a) Friction between the spring and cam.

   (b) The natural frequency of vibration of the
        spring.

Elimination of the strain gauge signal distortion was
achieved by carrying out some modifications on the design which
are described in section 7.2.

After producing a display of a satisfactory P-V diagram on
the CRO screen, the validity of the signal is used by recording
on single frames. Photographic records could give a wide range
of information that is extracted from the engine running at certain
sets of operating conditions. From these records the engine
performance may be studied.

The M.R.E. 141 recording unit used, incorporating three modes of photographic recording. These were:-

(a) Drum recording.

(b) Continuous-Feed recording.

(c) Single-Frame recording.

Originally drum recording had been used for photographing P-T diagrams. For this purpose only the pressure is triggered, the time-base signal being represented by the rotation of the camera drum. This arrangement is not suitable for recording a P-V diagram because no direct relationship exists between the volume signal and the time-base signal. Thus a single-frame photographic unit is mounted for the P-V recording. Having obtained the required records, two difficulties prevented continuation of work with P-V diagrams. These were:-

(a) The record obtained was not large enough to be accurately calibrated, particularly when measuring the area under the P-V loop

(b) No dynamic pressure calibration curves were available from the manufacturer of the transducers and equipment for transducer dynamic pressure calibration was not immediately available in the department.

Because of these limitations, the study of engine behaviour was confined to the study of P-T diagrams.

Detection of the top-dead-centre position for synchronization on a P-T diagram is of great importance. It gives information about the combustion and fuel injection processes inside the engine cylinder.

Few sufficiently accurate instruments are used in detecting top-dead-centre on P-T records. Those instruments are expensive. A simple inexpensive method for detecting top-dead-centre on the P-T record is discussed in this work. The method gives a reasonable accuracy of about 0.2° to 0.5° of crank angle depending on engine speed. A disc calibrated in degrees by steel inserts, together with a magnetic pick-up, was used (see Chapter 6).

1.3. <u>Performance parameters</u>

In order that different types of engines or different engines of the same type could be compared, certain performance parameters were defined. Actual values of these for an engine may be obtained by measurements of the different variables during laboratory tests and calibration is by standard procedure. The results could be plotted graphically or recorded in the form of performance curves.

The procedure for engine testing is to:-

(a) Determine information that cannot be obtained by calculation.

(b) To confirm data used in design, the
validity of which is in doubt.

(c) To run commercial tests to satisfy the
customer on the performance of the engine.

In considering the performance of an engine, the following
four parameters are discussed in Chapter 5:-

1. Fuel consumption
2. Power
3. Motoring capability
4. Willan's line   (C.I. engines only)

To investigate the power losses for the Lister F.R.1 diesel
engine, Willan's line only was obtained for this work.

Consideration of the combustion of the fuel in the cylinder
of internal combustion engines, brings out many problems, the
solution of which is essential for the efficient running of the
engine. Some of the problems, such as diesel knock, delay and
rate of combustion are investigated in this work using information
in the form of P-T diagrams extracted from the variable compression
Lister F.R.1 diesel engine, (see Chapter 8).

For each set of engine working conditions, both the cylinder
and combustion chamber pressures were indicated on each P-T record.
Comparison of different sets of records is therefore possible.

To simplify and assist the discussion, variables such as
injection-period, injection-angle and delay-period are defined.

The experimental information available included:-

   1.   Effect of change of speed on diesel
        combustion.

   2.   Effect of change of compression ratio
        on diesel combustion.

Both these tests were carried out at:-

(i)   Full load.

(ii) No load.

Further investigations were carried out to study the
restriction effects of the shape of passages on pressure indication.
The amplitude of pressure signals indicated by a transducer, is
dependent on the geometric positioning of the transducer in the
engine cylinder and on the passage geometry. The effect of these
two aspects on passage indication is explained in Chapter 8.

An important problem concerning I.C. engines is the breathing
capacity and the most valuable parameter in an experimental
approach to this problem is the volumetric efficiency which is
rarely constant over the whole speed range. It is desirable to
be able to determine the volumetric efficiency at different
points on the power curve, which may provide further information
about engine performance.

In Chapter 9 an investigation is described using Piezo-electric pressure transducers in measurement of engine volumetric efficiency by measuring the compression pressure when the engine misfires. This technique is the most convenient one to employ during field investigation on high performance engines. To estimate the validity of this method, two other techniques were employed for measurement of volumetric efficiency. These involve:-

    (a)   direct measurement of air flow by Alcock viscous flowmeter.

    (b)   direct measurement of fuel flow together with infra-red exhaust gas analysis to determine air fuel ratio.

The results obtained by the three techniques were compared.

2. DESCRIPTION OF THE EXPERIMENTAL ENGINES AND ANCILLARY EQUIPMENT

2.1. The Lister F.R.1 Diesel Engine

A single cylinder variable compression diesel engine, Fig. 2.1-1, was used for investigating combustion phenomena, engine indication and engine testing. It produces a maximum of nine brake horse-power at 1800 r.p.m. and it incorporates a 'Ricardo' swirl type combustion chamber. The cylinder head is bored out to receive the variable compression unit (Fig. 2.1-2) which consists of a piston having an equal diameter to that of the spherical combustion chamber, and a hemi-spherically dished end.

Mounted in this piston is a water-cooled Piezo-electric pressure transducer which is directly exposed to the combustion chamber.

The compression ratio can be varied while the engine is ticking over, from approximately 11:1 up to 23.8:1. A second Piezo-electric pressure transducer is fitted in the cylinder wall for indicating the cylinder pressure. The engine is a vertical cylinder four-stroke, water cooled, having a 3.75 inches cylinder bore and 4.5 inches stroke. The speed range is from 250 to 1800 r.p.m.

FIG. 2.1-2. The variable compression unit dismantled

FIG. 2.1-1. The Lister F.R.1 variable compression diesel engine

-12-

The fuel injection system incorporates a C.A.V. Pintle nozzle and a cam-operated spring return plunger pump of the constant stroke.

A special 'Higgs' 220 volts D.C. shunt wound motor is used to start the engine; the motor can also be used as a generator to absorb the engine power.

Special starting and loading circuits are provided on the electrical instrument panel. This includes a heavy duty rotary switch for changing over from motoring to generating through the "off" position. The torque on the engine can be measured using the twelve inch radius torque arm which is mounted on the front of the motor casing. Load can be applied to the dynamometer by switching into the armature circuit 20 resistance mats arranged in parallel. This gives variations in the torque reaction in steps of up to 2 lb. ft. A rheostat is installed in the field circuit for making fine adjustments between successive steps of the armature load. Fig. 2.1-3 shows a view of the complete rig. An air box panel incorporating a one inch diameter B.S. sharp edge orifice is mounted for measuring the engine air consumption.

Water flowmeter, fuel meter, speedometer and thermometers for measuring inlet and outlet water temperature, exhaust temperature and atmospheric temperature are incorporated on the instrument panel.
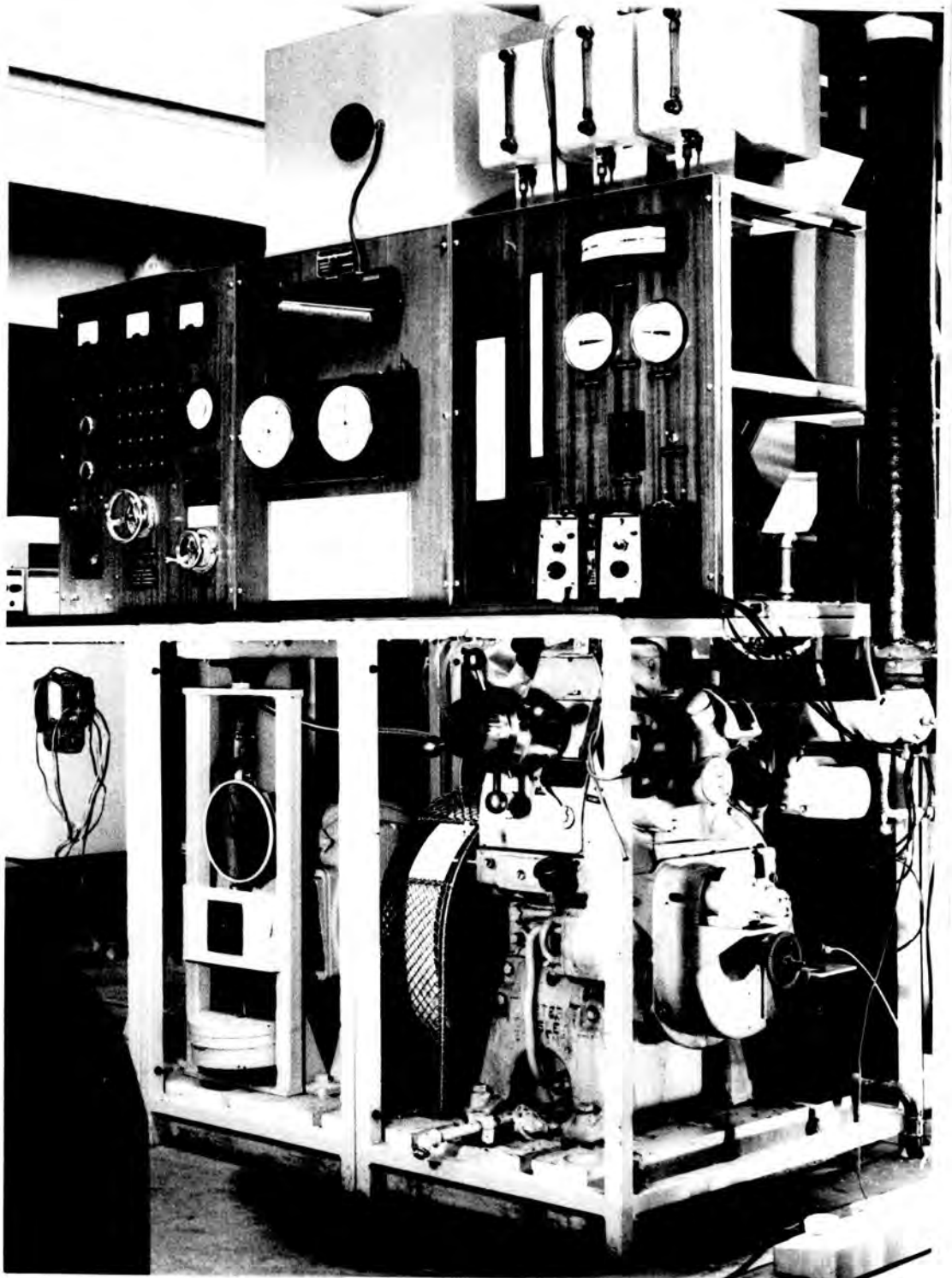
<u>FIG. 2.1-3.</u> The variable compression diesel engine test rig

2.2. <u>The Ricardo E6/S Variable compression petrol engine</u>

This is of the single cylinder poppet valve, four-stroke type, having a bore of three inches and a stroke of $4\frac{3}{8}$ inches. The engine incorporates a cylindrical combustion chamber, the ends being formed by the flat surfaces of the cylinder head and the piston. This ensures that the chamber retains the same form as the compression ratio is varied. The spark plug is situated at the side of the combustion chamber. A similar hole on the other side of the combustion chamber enables the pressure transducer to be fitted. An air heater is utilized for satisfactorily vaporizing the fuel before passing into the engine. An automatic electronic fuel timer is installed for measuring the fuel consumption.

Thermocouples were utilized for measuring the temperatures of inlet air, cooling water and of the Alcock-viscous flowmeter which was used for measuring air consumption. Fig. 2.2. shows the engine and driving motor which is similar to that of the Lister F.R.1 diesel engine.

Both the dynamic calibration of the crystal transducers (Chapter 4) and the volumetric efficiency investigations (Chapter 9) were carried out with this engine.
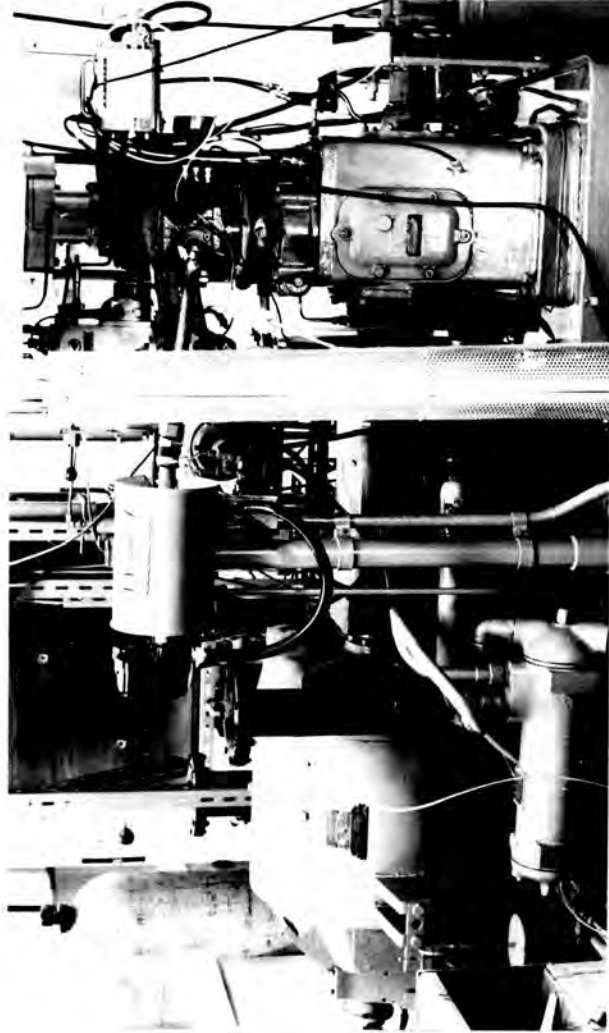
FIG. 2.2. The Ricardo E6/S Petrol engine and driving motor

2.3. The M.R.E. 141 Recording Unit (Fig. 2.3.)

This comprises a four beam oscilloscope situated in the centre section (M.R. 1938 panel).

The unit is supplied of the eight signals each of pre-set amplitude. A time-base amplifier (M.R. 1937 panel) is provided on the left hand section from which the output may be fed to the X-plates of the cathode-ray tube. The M.R. 525B marker amplifier is situated in the top centre section, this provides shaping of the poorly defined input pulses into well defined peaks of equal amplitude. This amplifier was used with the magnetic transducer and the degree marking disc that are stated in Chapter 6, it was also used for providing a suitable signal for triggering the camera shutter.

Two M.R. 1936 Double-Driver identical amplifiers are included in the unit, the output from which could be fed to either or both the Y or X plates of the cathode-ray tube.

Each of these amplifiers incorporating controls for beam, focus, gain and brightness.

The camera is situated on the top right hand section of the unit, and it incorporates drum, continuous feed and frame feed modes of recording.

For the drum recording the film speed may be varied from
0.4 to 100 inches per second.

In the single shot modes of operation, automatic frame
feed unit is fitted to the camera, which may be operated manually
or from an external signal source.
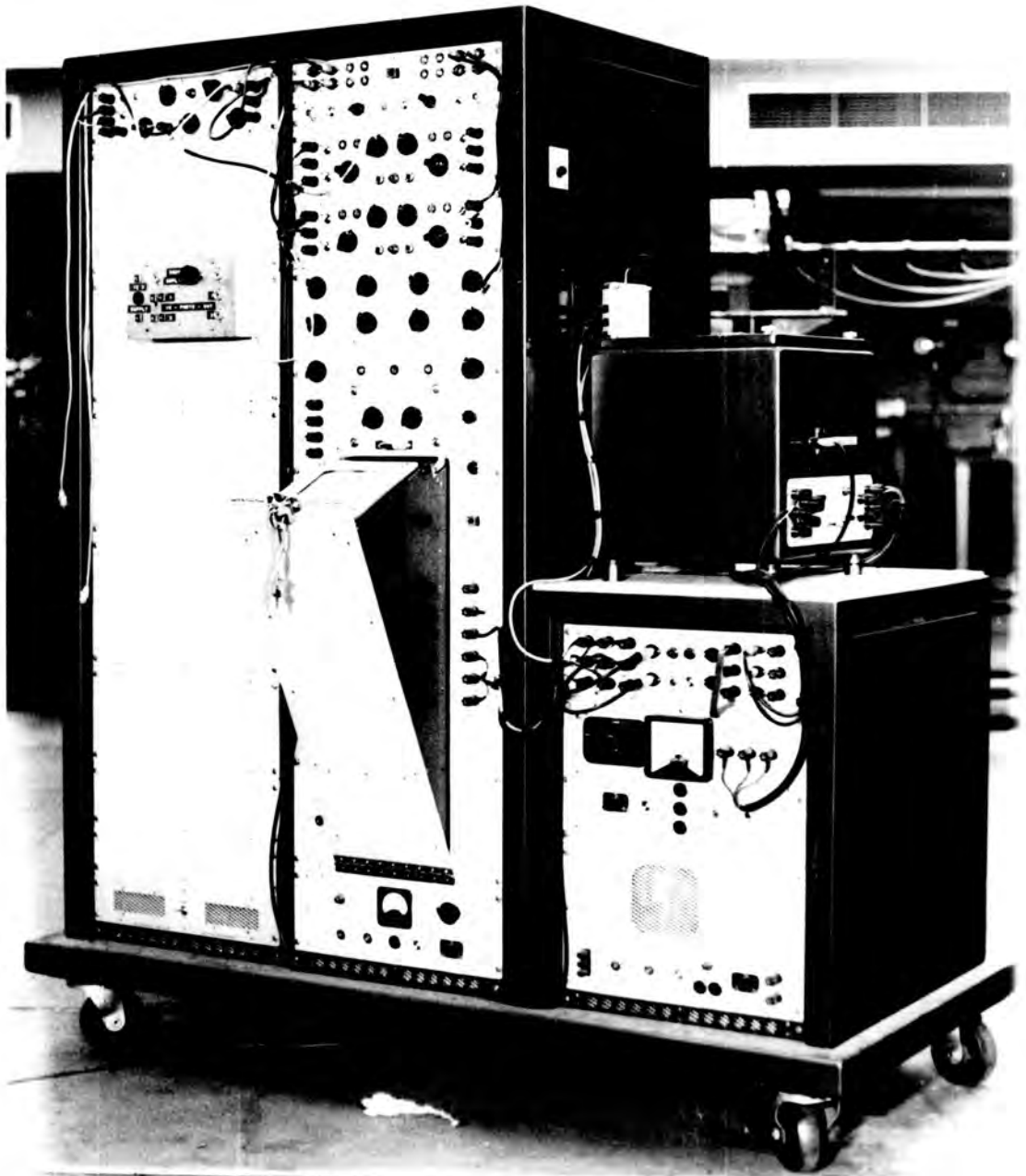
FIG. 2.3. The M.R.E. 141 Recording unit

3.   QUARTZ TRANSDUCERS AND THERMOMETERS

3.1.   General.   The Piezo-electric effect and the quartz properties

There are two types of Piezo-electric effects and they depend on the direction of the applied force relative to the crystal orientation, see Fig. 3.1.

The first is the transverse effect of the force on the Y planes of the crystal which produces an electrostatic effect at the X planes. The resultant charge depends on the acting force, the Piezo-electric constant, d_{11}, and a form factor which depends on the geometric configuration. The second effect is the longitudinal effect, a charge will be created at the X planes of the crystal when a force is applied in the direction of the X axis. The electrostatic effect is independent of all geometrical dimensions of the quartz crystal.

It is claimed that quartz crystals produce no charge due to temperature variations and their sensitivity is constant for practical purposes ($\pm$ 1%) in the temperature range $-200^{\circ}C$ to $450^{\circ}C$. (This is claimed by the transducer manufacturer).

When constructing a pressure transducer, the quartz crystals are housed in a sealed steel sleeve. The external pressure being applied to the crystals through a steel diaphragm. This

arrangement is thought to have an effect on the transducer calibration if compared with the calibration of an uncased Piezoelectric crystal.

The behaviour of the quartz pressure transducers under static, dynamic, cooled and uncooled conditions are investigated in Chapter 4.

The latest transducers possess a greater charge per unit pressure than the early type. This is obtained by bonding individual quartz discs in series by means of a welding process where the connecting zones are also utilized as electrodes.

3.2.   Quartz transducer construction

3.2.-1. Pressure transducer

This consists of the Piezo-electric element, hermetically sealed by a welded sleeve under tension.

A quartz disc is situated in front of the disc electrode. The schematic principle of a cooled quartz pressure transducer is illustrated in Fig. 3.2-1.

A drilled quartz disc being situated behind the electrode for the purpose of insulation against the body.
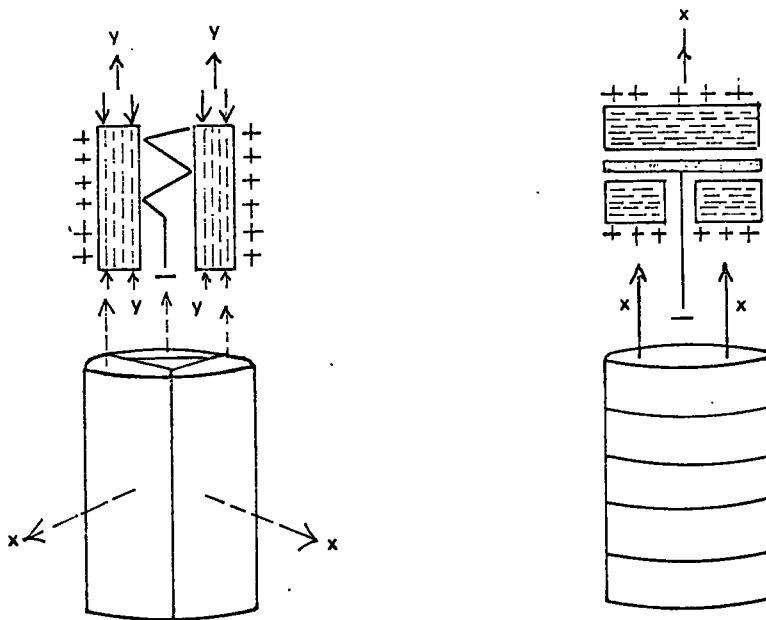
FIG. 3.1. The Piezo-electric effect of quartz crystals
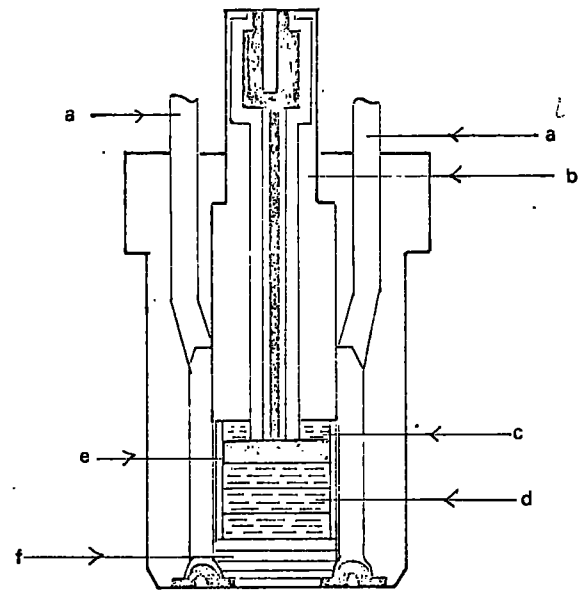
FIG. 3.2. Cooled quartz pressure transducer

Key:-

a	-	coolant	d	-	quartz layers
b	-	sealed sleeve	e	-	electrode
c	-	insulating disc	f	-	diaphragm

All components such as the base of the sleeve, the quartz discs, the electrode and the drilled quartz disc are bonded together by a welding process. The annular space between sleeve and transducer housing being in direct contact with the coolant.

3.2-2. Quartz Accelerometers

Fig. 3.2-2 illustrates the construction of such transducers. A seismic mass is composed of a material having a high specific gravity (such as tungsten), is attached and hermetically sealed in a sleeve together with a quartz-layer body.

The accelerometer illustrated possesses an electrode for discharging negative charges. Positive charges will be discharged through the body. Under the influence of acceleration, the seismic mass situated in front of the quartz will exert a force in the direction of the transducer axis.

3.2-3. Load Cell transducer

The quartz element is hermetically welded in a tensional sleeve. A force acting in the direction of the transducer axis will be measured.

Charge Amplifier

Transducer

Continuous Recording

Indicator

Frame Recording

FIG. 3.3. Typical measuring arrangement for quartz transducers

Seismic Mass

Quartz layers

Electrode
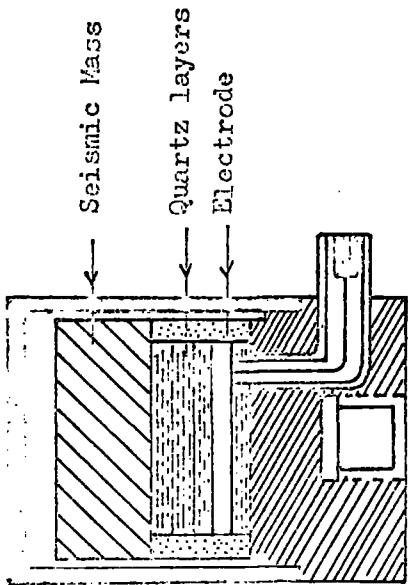
FIG. 3.2-2. Construction of quartz crystal Accelerometer
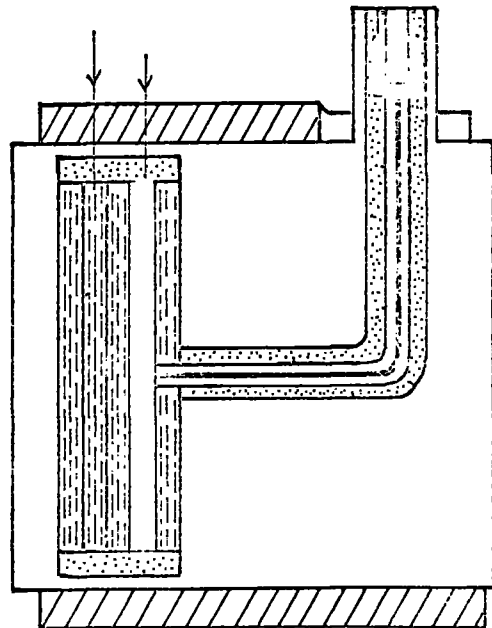
FIG. 3.2-3. Construction of quartz crystal Load Cell

Fig. 3.2-2 shows a simple type load transducer suitable for measuring mechanical forces.

The crystal transforms the force into an electrostatic charge.

3.3. Measuring arrangements for Piezo-electric transducers

The amplification of the transducer signal is established by a high impedance amplifier. The signal from the amplifier is fed into the indicating device to which a recording device of the standard type might be attached, Fig. 3.3. The recording of the signal may take place on single frame shots, drum recording or continuous feed recording.

3.4. Features of Piezo-electric transducers

The basic features of the Piezo-electric transducers can be outlined as follows:-

1. Since it is possible to manufacture transducers with very small dimensions, very high natural frequencies can be obtained.

2. The transducers possess a good linearity and can be arranged for high sensitivity.

3. The transducer may be used over a wide range of temperatures; there is also the facility for compensating the influence in construction and by calibration.

4. The disadvantage of the Piezo-electric
    measuring method is the high input impedance
    of the amplifier to which the transducer is
    connected. This makes static measuring
    difficult, particularly at high temperature.

5. The measurement of fast changing pressure for
    periodic and for non-recurring events is the
    main field of application of quartz pressure
    transducers provided that a satisfactory
    dynamic calibration is established.

The charge produced by the quartz crystal in its longi-tudinal mode is given by:-

$$Q = d_{11}.f \qquad \text{where;}$$

Q   -   induced charge in coulombs.

d_{11} -   Piezo-electric constant.

f   -   applied force in newtons.

The output voltage of the crystal is given by:-

$$E = g.\ t.\ P$$

t   -   crystal thickness in metres.

g   -   voltage sensitivity.

P   -   applied pressure in $newton/metre^2$.

3.5. Quartz thermometers

In the above section it was mentioned that the charge is found to be temperature independent but quartz crystals may be used for temperature measurement. The thermometer is based on the sensitivity of a given crystal orientation. The resonant frequency of the quartz crystal is extremely sensitive to a temperature change. (1000 cycles/sec per ^{o}C). These characteristics are used as means of accurate temperature measurements known as quartz crystal thermometry. Quartz thermometers which exhibit very linear and sensitive correspondence between resonant frequency and temperature have a crystal orientation known as the LC cut. The linearity of the quartz thermometer is superior to that of thermocouples and thermistors. The temperature sensing characteristic is read directly in a digital form without the use of bridge balance, reference to resistance, etc.

3.6. Construction of quartz thermometers

The thermometer consists of the probe which contains the quartz crystal, hermetically sealed in a cylindrical stainless steel case, in a helium atmosphere. The case is attached to a stainless steel tubular body which varies in length with the probe model, see Fig. 3.4. The only probe material in contact with the measurand is the stainless steel. For each temperature sensing probe, conversion from temperature to frequency is

performed by a sensor oscillator which is a transistorized device enclosed in an aluminium housing. The sensor oscillator is normally installed in the parent digital thermometer. The cable connecting the probe to the sensor oscillator forms part of the tuned circuit and cannot be altered in length.

3.7. Measuring arrangements for quartz thermometers

One principle of operation of quartz thermometer is shown on Fig. 3.5. The sensor oscillators operate at a nominal frequency of 28 MC/S. To obtain a frequency sensitivity of 1000 cycles/sec per ^{O}C, the sensor oscillator frequency is hetrodyned with a nominal frequency of 28 MC/S derived from a reference oscillator. The reference frequency is fed to decade counting unit of the counter portion of the instrument. The reference oscillator crystal is designed to have as nearly as possible a zero temperature coefficient.

3.8. Features of quartz thermometers

The main features of the thermometer are as follows:-

1. It is a complete measuring system, no other
    instrumentation is required.

2. It provides a linear digital readout in ^{O}C
    or ^{O}F.

- 28 -
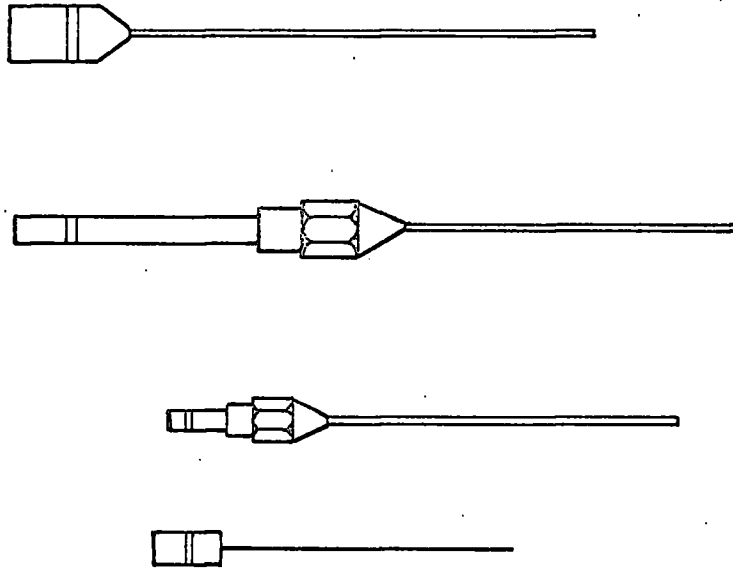
FIG. 3.4. Outline drawings of four different type models of temperature sensing probes

Sensing probe   sensor oscillator

≈ 28 M.C

Reference Oscillator
0°C or 32°F

≈ 2.8 M.C

× 10

Mixer

+ or −
indication

4 digit
counter

Dividers

Gate
Control
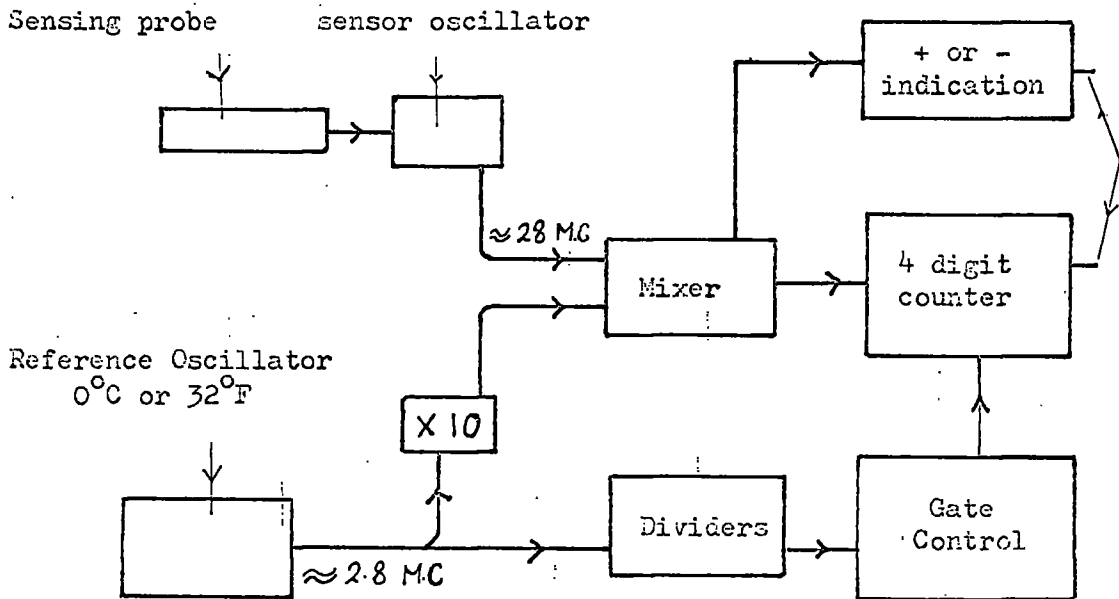
FIG. 3.5. Simple block diagram of a quartz thermometer

3. Resolution up to 0.0001°C or °F.

4. The output from the thermometer can be used for recording on digital recorder.

5. Temperature sensing probes can be up to 500 feet from the measuring equipment or 4500 feet with optional amplifier.

6. No cable resistance or noise problem.

7. The thermometer can also be used as frequency counter (up to 300 KC/S).

4. STATIC AND DYNAMIC CALIBRATION OF PIEZO-ELECTRIC PRESSURE TRANSDUCERS

4.1. General

It is essential to obtain an accurate method for calibrating pressure transducers in order to fully exploit their natural advantages. Until recently, it was assumed that the static calibration curves of crystal transducers were sufficiently accurate for the dynamic pressure measurements.

This was born out by the fact that the manufacturer supplies only a static calibration. In order to carry out a static calibration, a digital voltmeter (type Solartron No. LM 1420.2) was used in conjunction with a deadweight tester.

The output signal from the transducer was amplified by a Kistler charge amplifier (type Kistler 568) then measured by the digital voltmeter. It was observed that unless the input pressure is applied very slowly to the transducer, the rate of input pressure produces a varying reading on the digital voltmeter. Hence it was suspected that the rate of pressure input has an effect on the transducer output, so a dynamic method of calibration was carried out using a comparative method. This work was carried out at Thornton Research Centre in co-operation with Shell Research U.K. Ltd.

Previous work on balanced-disc transducers had been carried out by Brown[1].

The pressure transducer was mounted in the engine cylinder head with the diaphragm flush with the cylinder wall. The pressure signal was amplified and then, with a time-base signal, was displayed on the oscilloscope screen producing a pressure time diagram. A capacitance type Balanced-Disc Pick-up (Fig. 4.1-1) was also mounted in the engine cylinder head (Fig. 4.1-2) such that the engine cylinder pressure was acting on the lower face of the pick-up disc, while a regulated pressure from a compressed nitrogen gas cylinder was transmitted to the upper face of the diaphragm to act as a reference pressure. The reference pressure was accurately measured by a standard pressure gauge connected to the pressure line, which was accurate to $\pm$ 2 lbf/in^2.

The balanced-disc is part of a variable capacitor that was connected to a tuned oscillator. The output from the oscillator was fed to an F.M. unit (Southern Instrument No. 1860).

This output provides the reference pressure signal which is displayed vertically on the CRO screen, the horizontal signal acting as a time-base. Fig. 4.1-3 shows a diagrammatic arrangement of the rig.
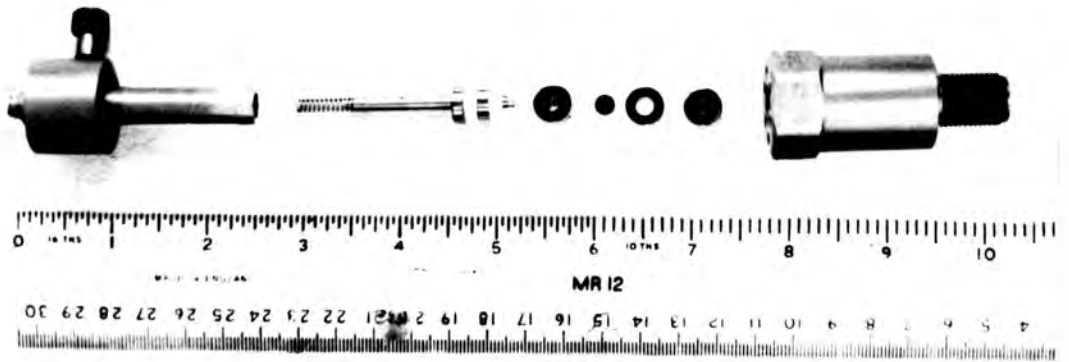
FIG. 4.1-1. Capacitance type balanced-disc pressure pick-up

FIG. 4.1-2. The balanced-disc pressure pick-up (centre)
shown mounted on the engine

Oscilloscope

Charge Amplifier

Pressure Transducer

Engine

F.M. Unit

Oscillator

Balanced Disc
Pressure Pick-up

Standard Pressure
Gauge

Compressed Nitrogen
Cylinder

Bleeding Valve

Regulating Valve
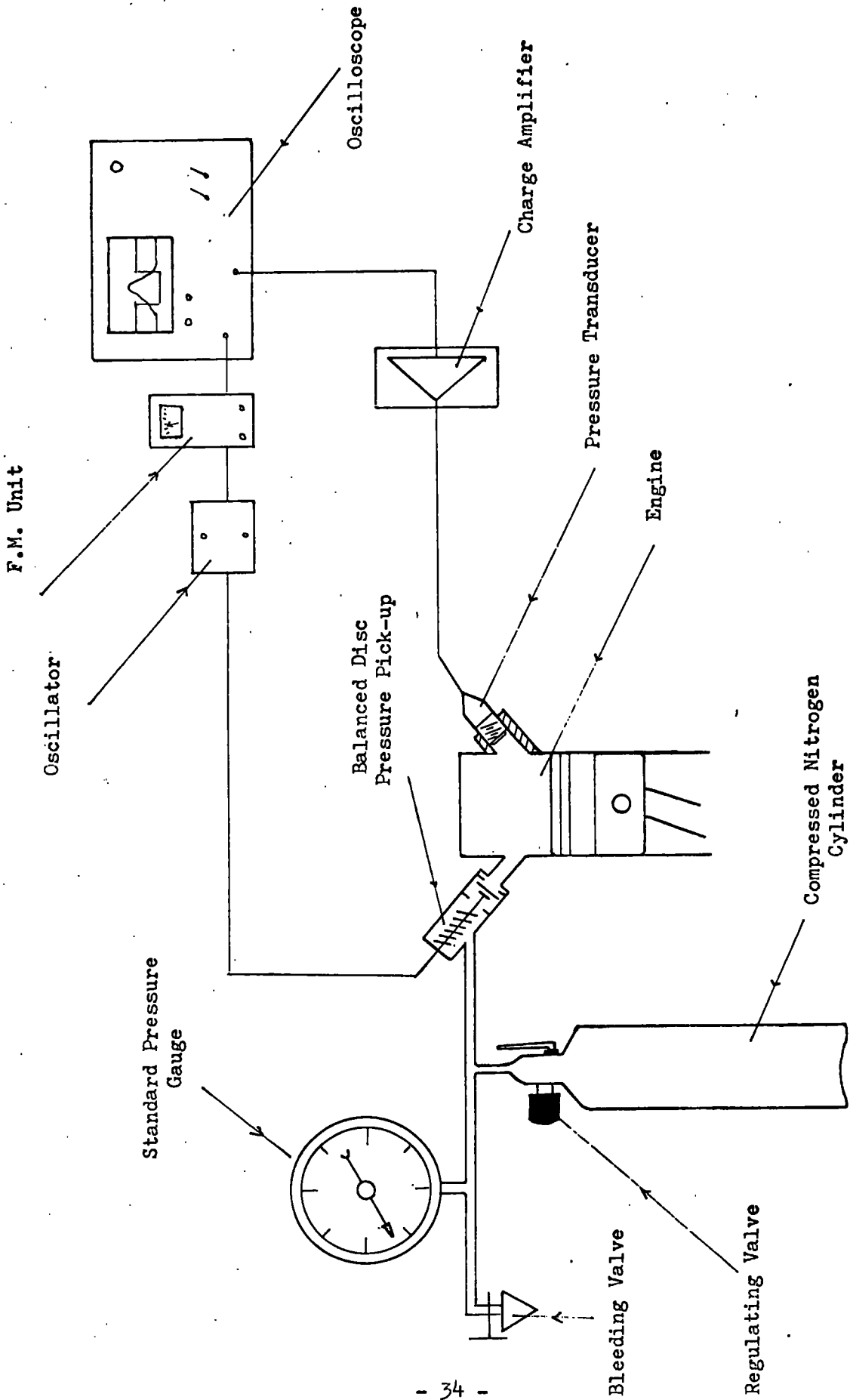
FIG. 4.1-3. Diagrammatic representation of the Dynamic Pressure
Calibration Rig

- 34 -

The movement of the disc can be recorded and used as a means of evaluating the dynamic pressure indicated by the transducer. This disc will start to move when the engine cylinder pressure is equal to the reference pressure which can be regulated by means of a valve connected to the upper end of the nitrogen gas cylinder. When the engine cylinder pressure exceeds the reference pressure, the disc moves up and stays up in this position until the engine cylinder pressure falls below the reference pressure when the disc returns back to its original position. By this means the capacitance balanced pressure pickup gives rise to a step signal that is displayed on the oscilloscope screen.

To find the corresponding beam deflection for a given dynamic pressure, the reference signal is moved vertically until the point indicating the start of the disc movement coincides with a point on the P-T diagram (see Figs. 4.1-4 and 4.1-5). The distance between the point of coincidence of the two beams and the atmospheric pressure line on the CRO screen represents the dynamic pressure value (in oscilloscope division units) corresponding to the pressure on the standard gauge. By altering the value of the reference pressure in increments of 50 p.s.i. from 420 to 70 p.s.i., the corresponding beam deflections are measured for comparison with the static readings.
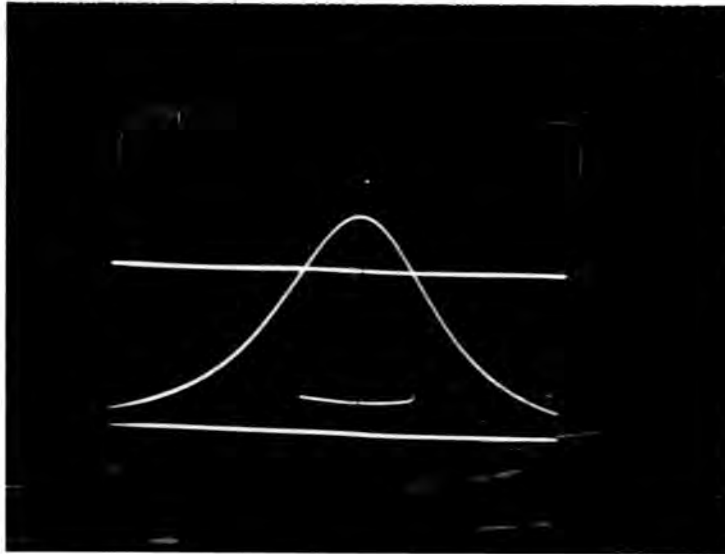
FIG. 4.1-4. P-T diagram and reference pressure signal. Calibration during upward movement of the disc. Reference pressure 270 p.s.i. Engine speed 1000 RPM
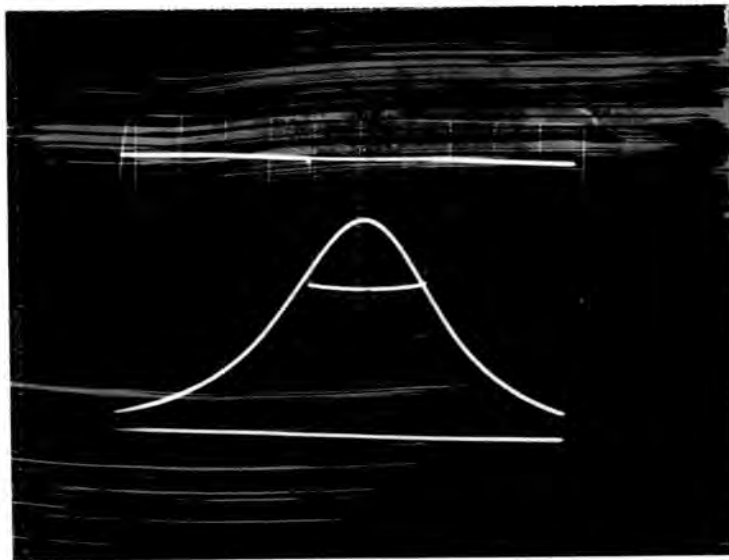
FIG. 4.1-5. P-T diagram and reference pressure signal. Calibration during downward movement of the disc

The results are given in greater detail in Appendix 1 (static measurements), Appendix 2 (dynamic measurements) and Appendix 3 (modified dynamic measurements).

4.2.   Results

The following transducers were statically tested (see Fig. 4.1-6).

    1 - Kistler   Type 601A   No. SN 30917.

    2 - AVL 10 mm Type 80P   No. 500C.

    3 - SLM   Type PZ14   No. 3815.

Only the Kistler and AVL transducers were tested dynamically.

4.2-1. Static Calibration

Fig. 4.1-7 shows the apparatus used to statically calibrate the transducers. The transducers were calibrated at room temperature and at $80^{\circ}C$ in order to see if there was any temperature effect variations. Graph 4.2-1 shows the static calibration of all three transducers; no variation of calibration could be detected due to the change in temperature.
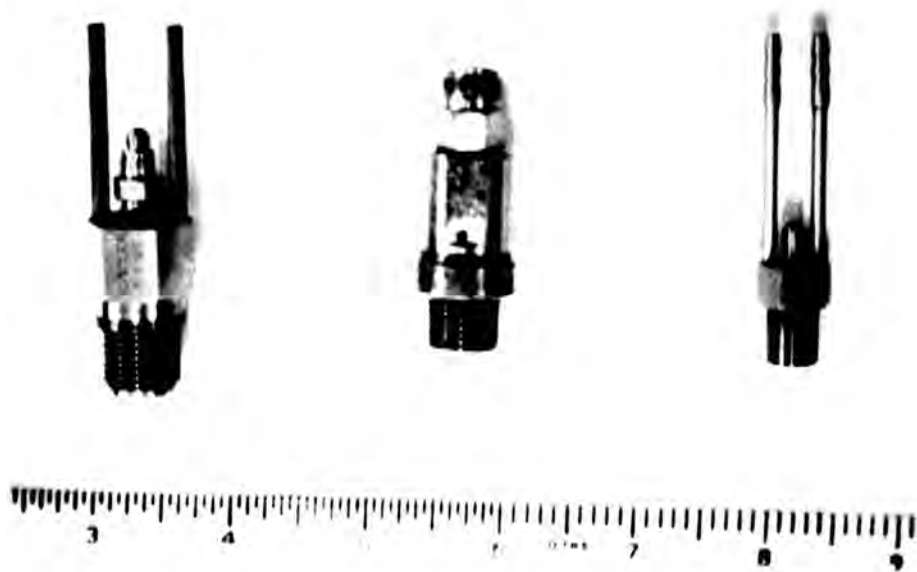
FIG. 4.1-6. Photograph showing the three transducers tested

1	-	Kistler	601A	(left)
2	-	SLM	PZ14	(centre)
3	-	AVL	10 mm	(right)
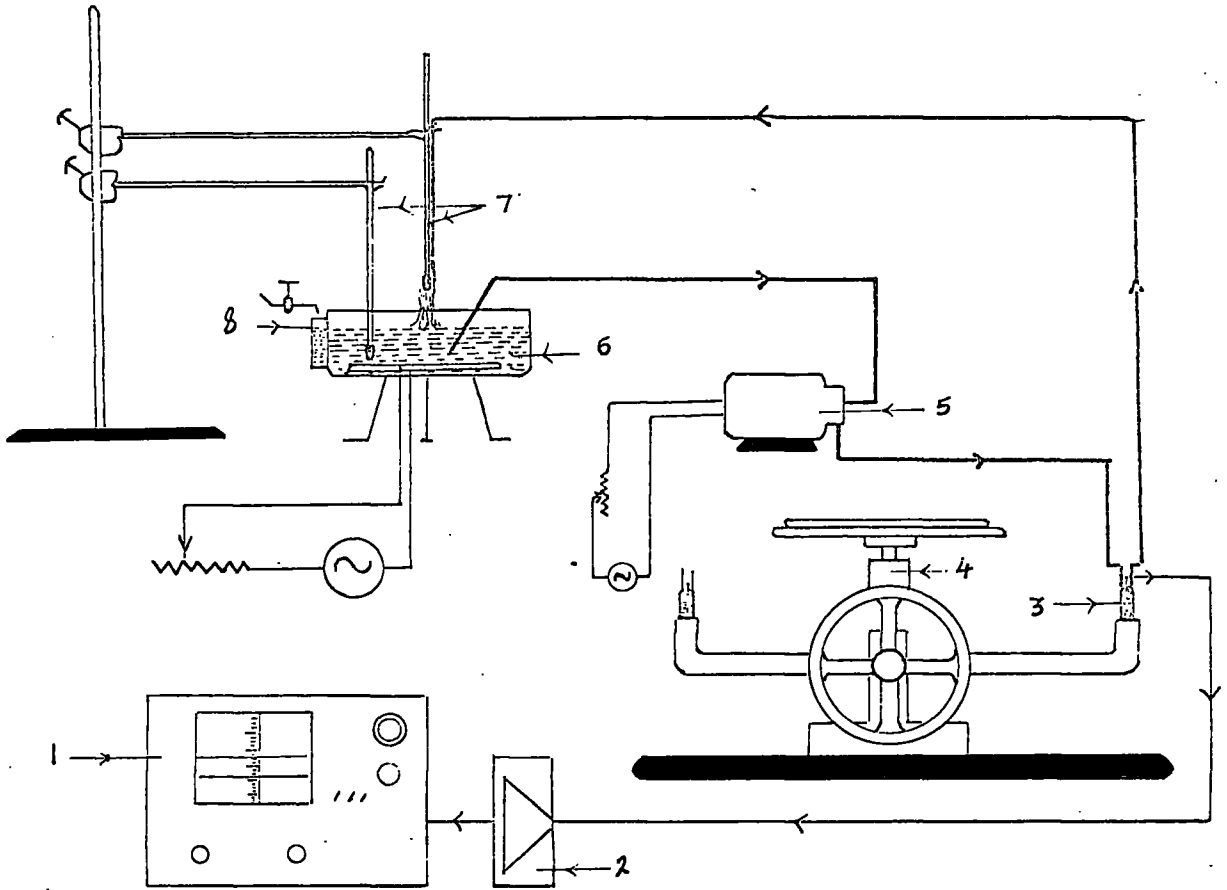
FIG. 4.1-7. Diagrammatic sketch of the rig used for the
hot static testing

KEY:

1. Oscilloscope   5. Water pump

2. Charge amplifier   6. Electric boiler

3. Transducer   7. Thermometers

4. Deadweight tester   8. Cooling water make up

- 39 -

Static calibration curves at room temperature and at 80°C

kistler
sLM
AvL

GRAPH 4.2 -1

Output deflection (oscilloscope division units)

Input pressure Lbf/in²

- 40 -
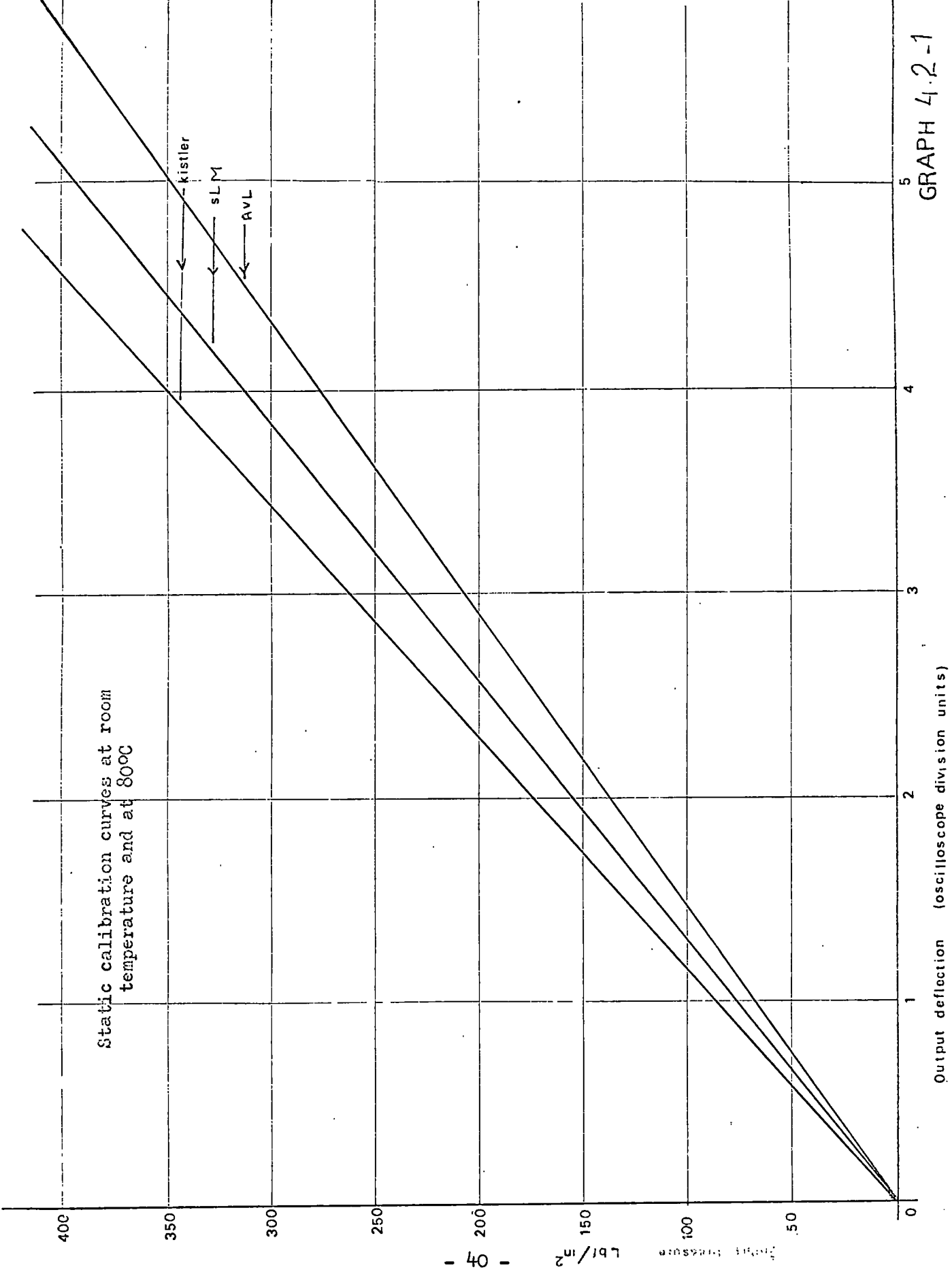
4.2.-2. Dynamic Calibration

The dynamic calibration of the Kistler and AVL transducers was carried out at engine speeds of 500 to 2750 r.p.m. For this the dynamic pressure readings were obtained for both the L.H.S. and R.H.S. of the P-T diagram using the technique described in Section 4.1. and during the reference signal indicating the upward and downward movements of the balanced-disc (see Figs. 4.1-4 and 4.1-5).

The signs ⟋ and ⟋ shown on graphs represent results for the L.H.S. and R.H.S. of the P-T diagram.

A difficulty of this technique of calibration can be seen in Fig. 4.1-8 which only occurred at speeds higher than 2000 r.p.m. and this shows a kink in the reference line, denoting the opening of the induction valve.

This difficulty was not so pronounced at lower speed, see Figs. 4.1-9 and 4.1-10, which represent two dynamic pressure calibration records taken at different reference pressure and speed of 1000 r.p.m.

Graph 4.2-2 shows a typical calibration curve for the Kistler transducer, obtained by both the upward and downward
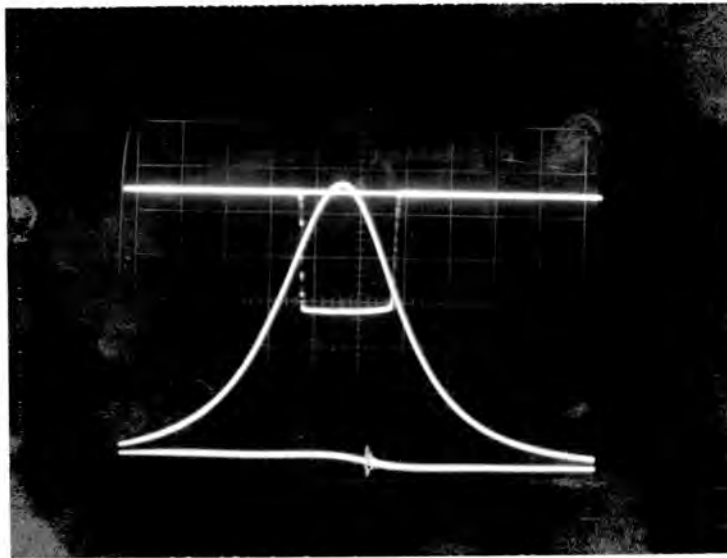
FIG. 4.1-8. Photograph showing the deviation of the atmospheric
pressure line
Engine speed 2750 RPM,   Kistler transducer
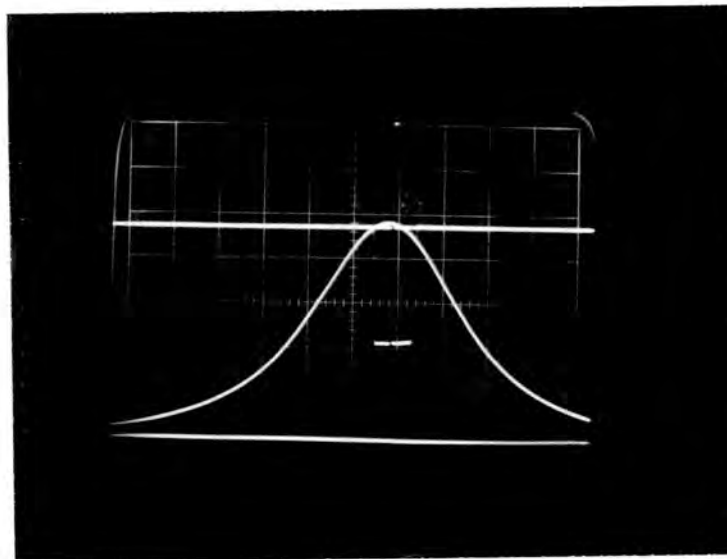
FIG. 4.1-9. Dynamic calibration at 400 p.s.i. reference pressure
Engine speed 1000 RPM
Transducer output, 4.78 oscilloscope division units

GRAPH 4.2-2

Output deflection (oscilloscope division units)

Input pressure lb f/in²

Kistler Transducer
Type 601A No. SN 30917
Engine Speed 1000 RPM
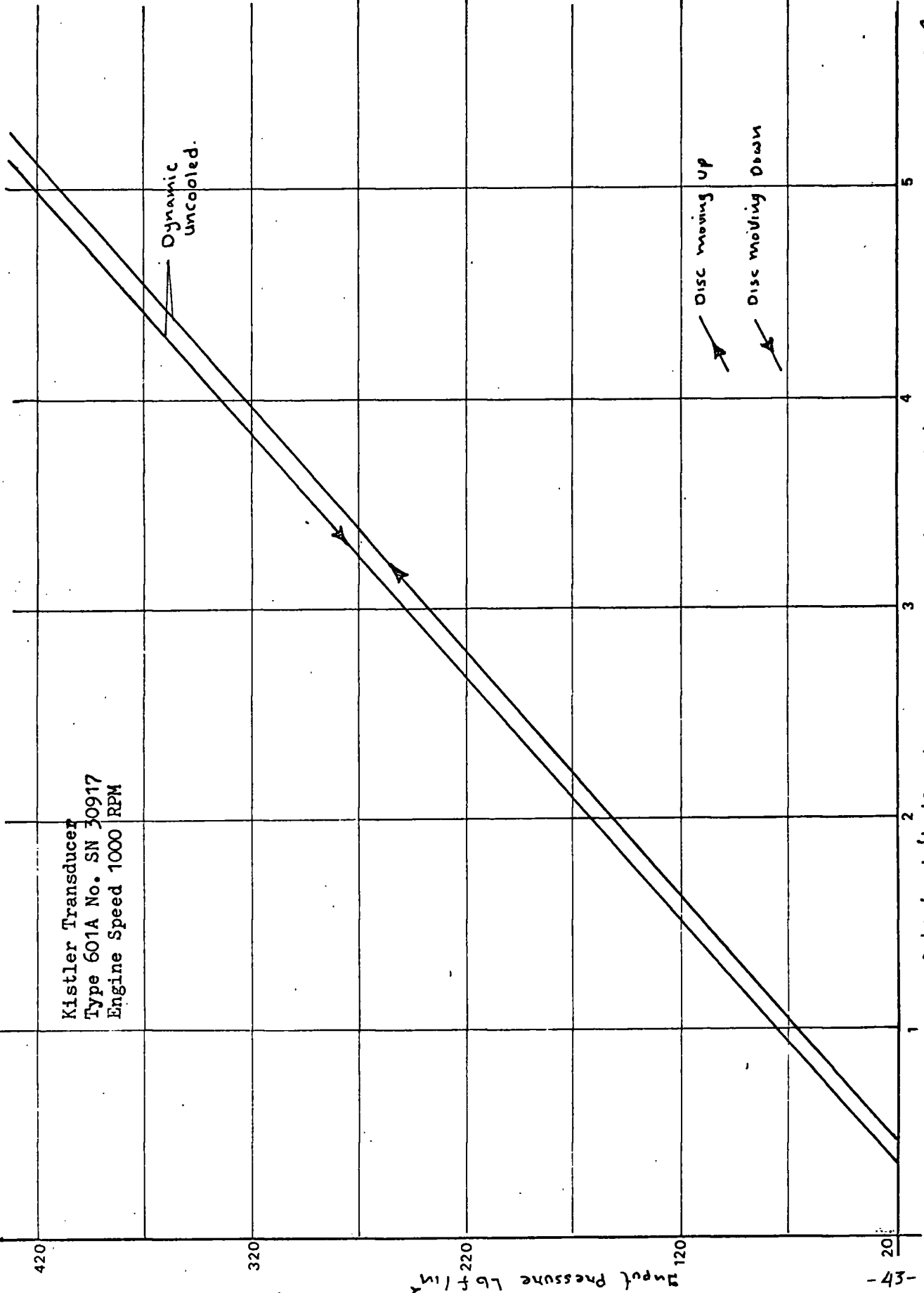
Dynamic
uncooled.

Disc moving up
Disc moving Down

-43-

movements of the balanced-disc with the engine running at 1000 r.p.m. The results are given comprehensively for the static calibration and the dynamic calibration in Appendix 1 and 2 for both the Kistler and AVL transducers. Those results showed significant delay indicated by the balanced-disc pick-up. The delay was more pronounced at the higher engine speed. Graph 4.2-3 shows the static calibration and the dynamic calibration curves for engine speeds ranging between 500 and 2750 r.p.m. The graph indicated an apparent deviation of the dynamic calibration curves from the static curve as the engine speed was increased. Because of the difficulty to assess the balanced-disc delay which might be caused by the disc's stiction and kinetic energy release during impact, the calibration technique was modified by calibrating the transducer during the floating performance of the balanced-disc (see Fig. 4.1-11). This involved the application of different known values of reference pressure and in each case the engine compression ratio was altered to give a compression pressure equal to the reference pressure, thus providing an equalizing pressure on both sides of the balanced-disc.

Graphs 4.2-4 and 4.2-5 show the dynamic calibration (using the modified technique) for the Kistler and AVL transducers at engine speeds ranging between 1000 to 2750 r.p.m.
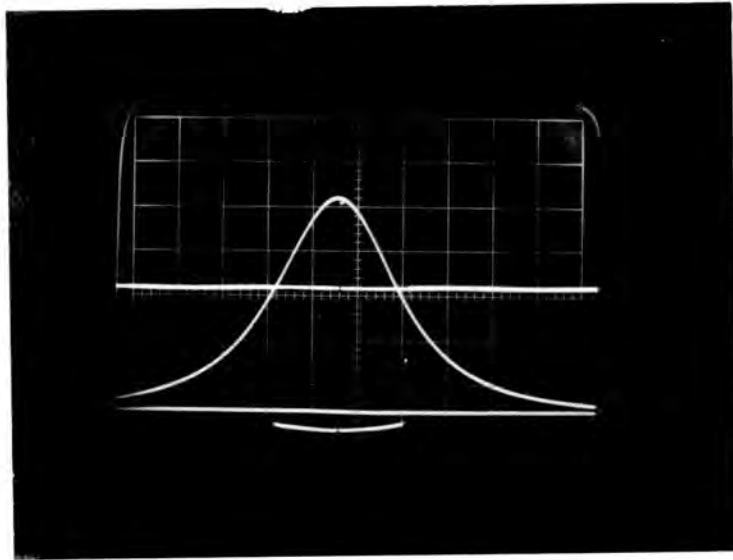
FIG. 4.1-10. Dynamic calibration at 218 p.s.i. reference pressure
Engine speed 1000 RPM
Output deflection   2.78 oscilloscope division units
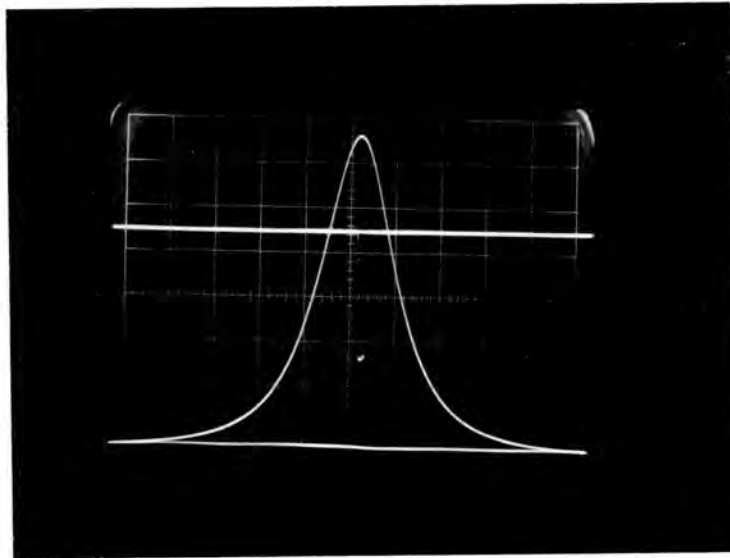
FIG. 4.1-11. P-T diagrams and reference signal showing the balanced-
disc during its floating performance

- 45 -

GRAPH: 4.2-3

Kistler Transducer
Type 601A
Cooled

static

500 r.p.m.

1000 r.p.m.
2000 r.p.m.
2750 r.p.m.

Disc moving UP

Output deflection (oscilloscope division units)

input pressure   lbf/in²
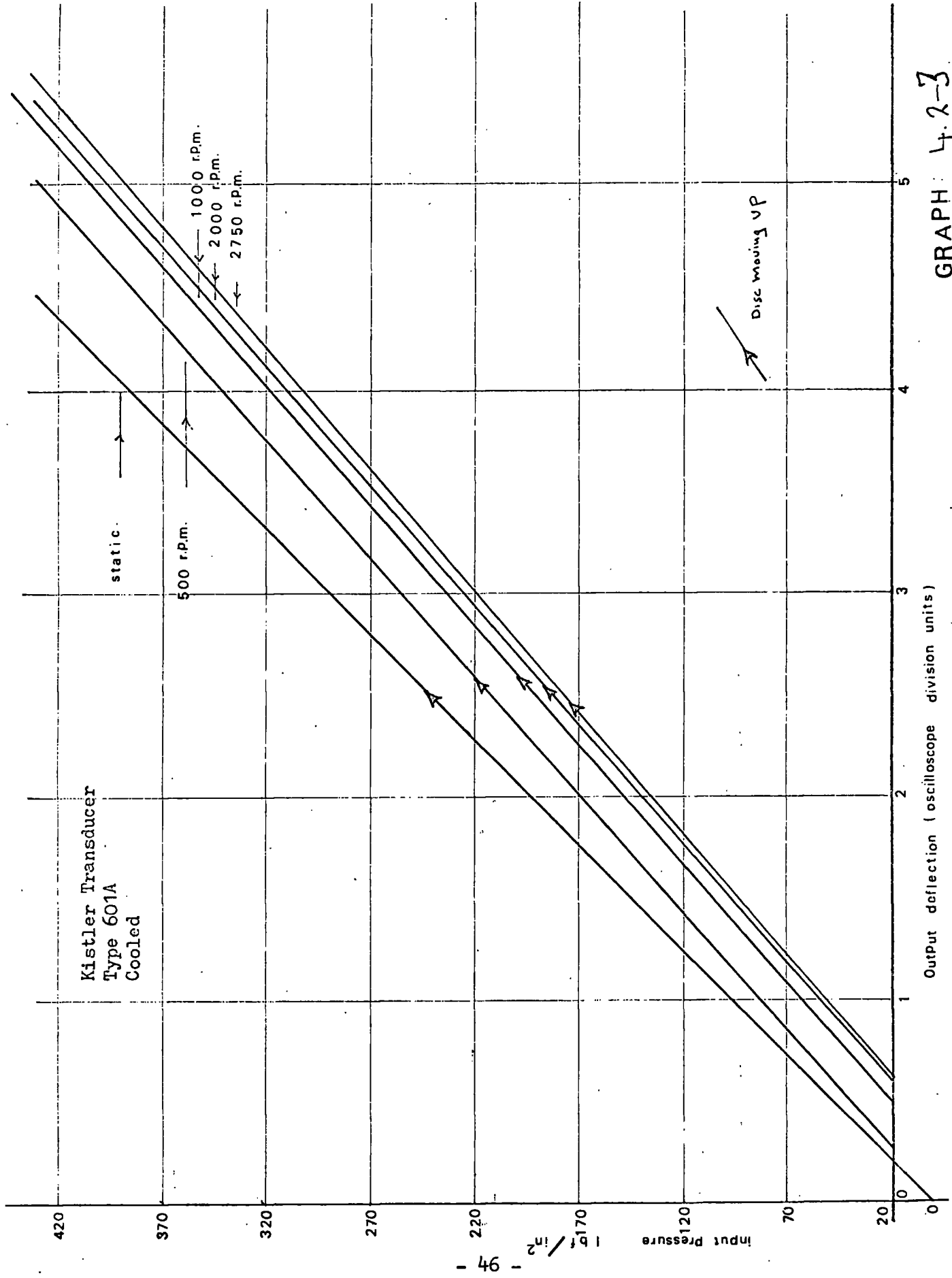
Up to the maximum speed used in the experiments, the balanced-disc pressure pick-up provided a reliable signal.

One limitation to the modified technique described is the difficulty of calibrating the transducers at pressures below 90 p.s.i., since this was the minimum compression pressure obtained from the E.6 engine.

The importance of this region of pressure indication is discussed later in this section.

4.3. Effect of engine speed

For the Kistler and AVL transducers examined, the effect of an increase in engine speed on output sensitivity is shown in Graphs 4.2-4 and 4.2-5 respectively.

To clarify the behaviour of the crystal pressure transducer under dynamic working conditions, Graphs 4.2-6 and 4.2-7 of transducer output against engine speed, were extracted from Graphs 4.2-4 and 4.2-5. This is proceeded by choosing a value of static input pressure, then finding the corresponding output beam deflection at the different engine speeds used during the test. In Graphs 4.2-4 and 4.2-6 it can be seen that for any input pressure, the Kistler transducer sensitivity has increased

Modified dynamic calibration
Kistler transducer, type 601A

static
1000 rpm
2000 rpm
2750 rpm

Input Pressure lbf/in²

Transducer output (oscilloscope division units)
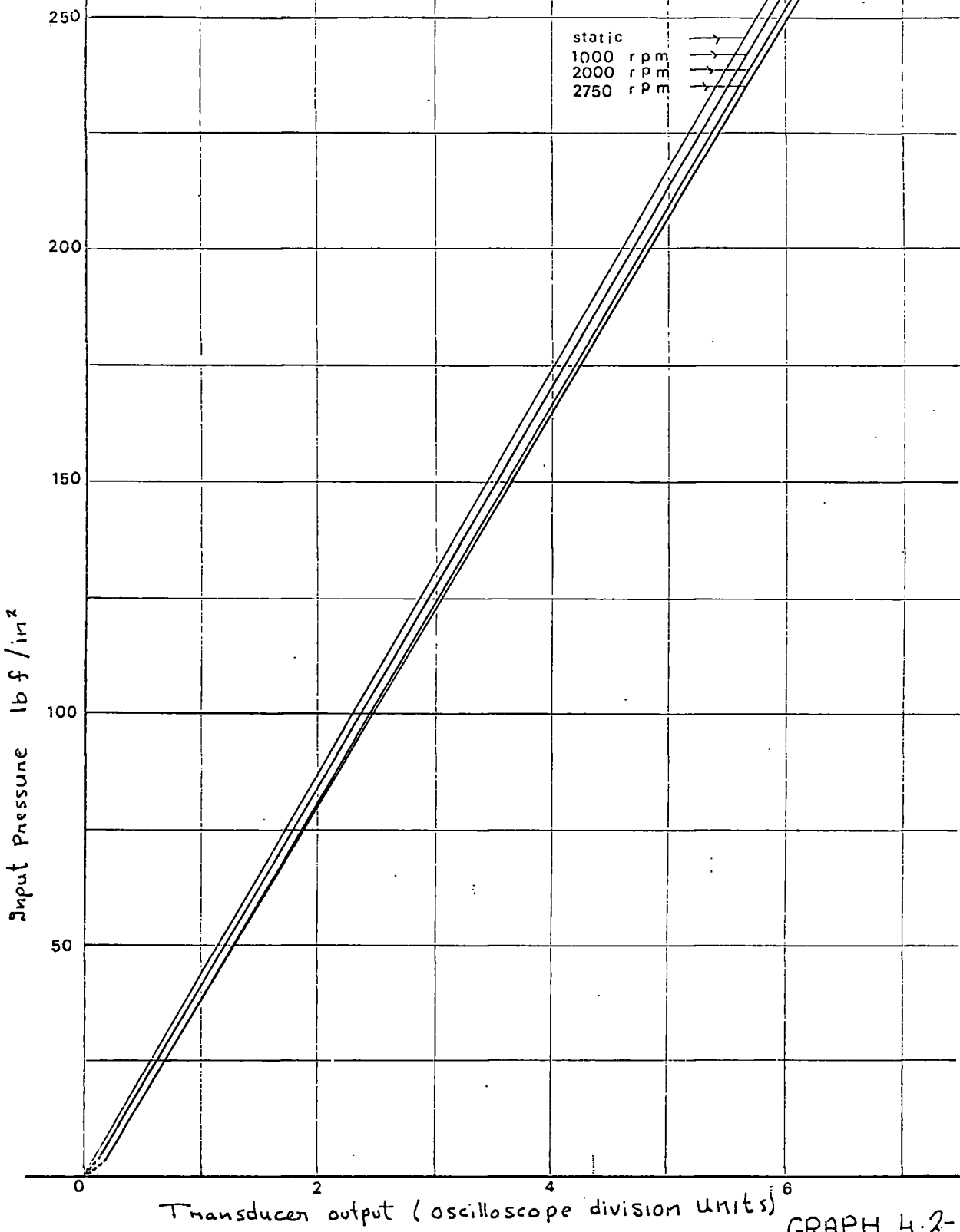
GRAPH 4.2-4

Modified dynamic calibration
AVL transducer type 80P
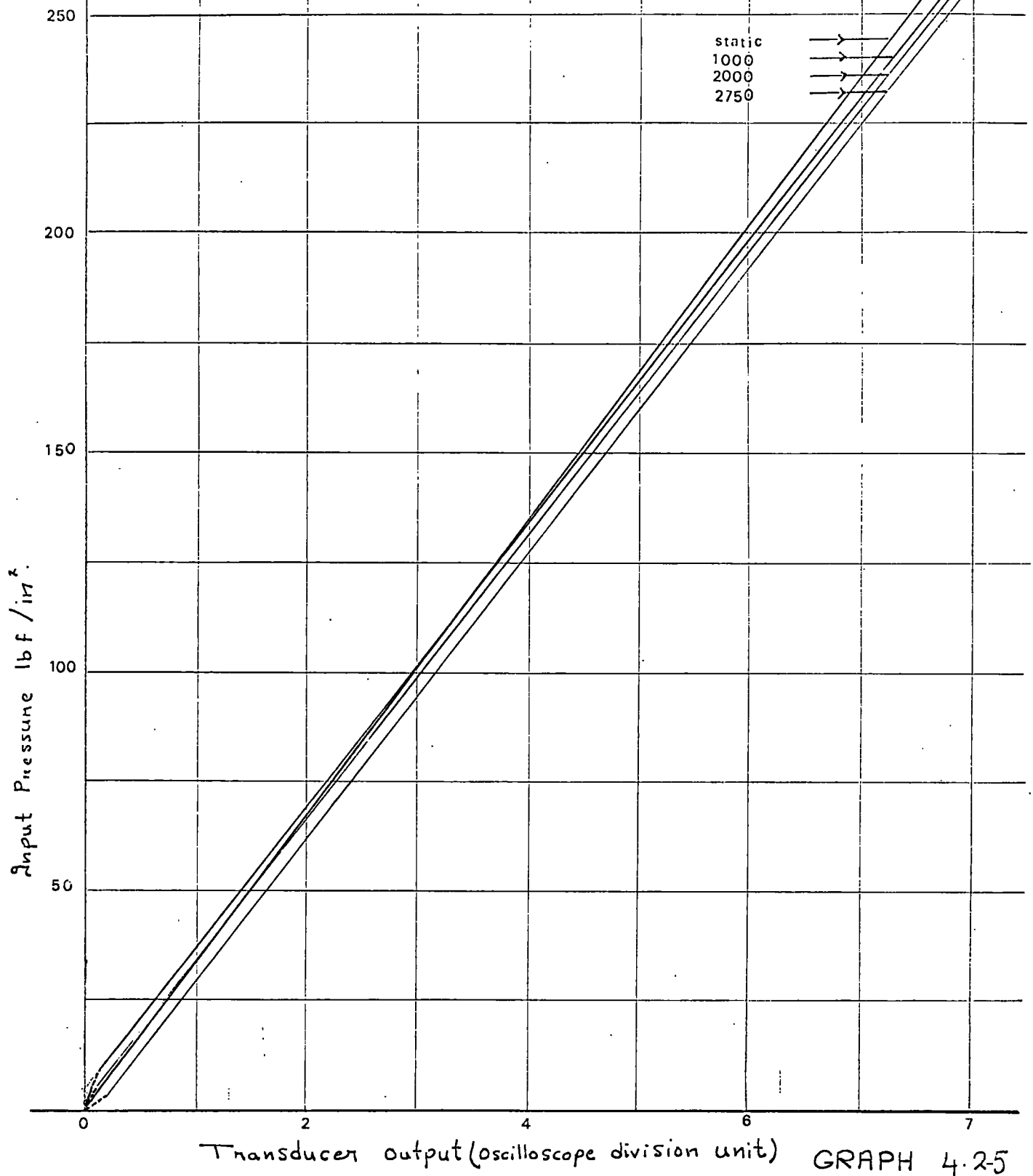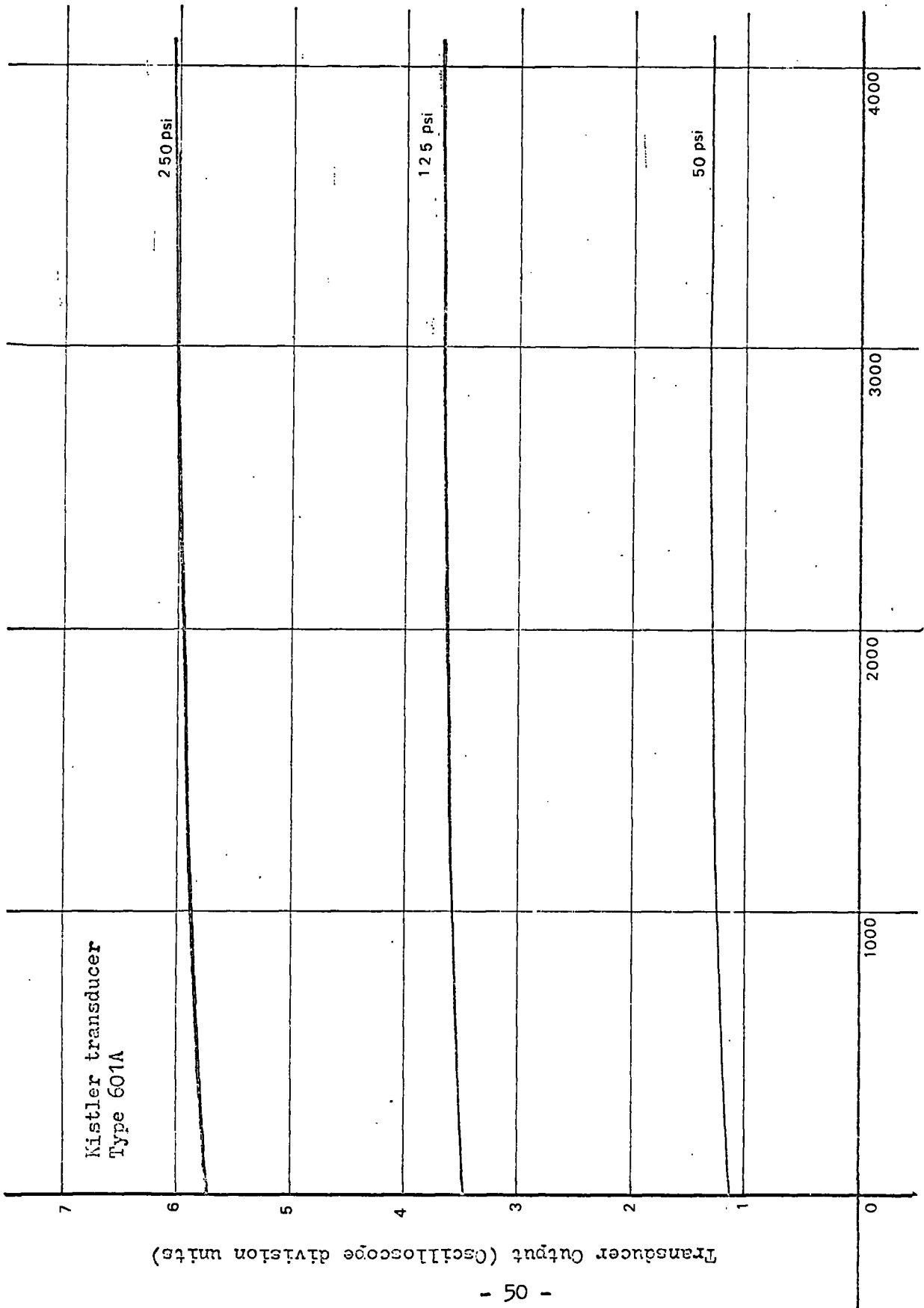
static
1000
2000
2750

Input Pressure lbf/in².

Transducer output (oscilloscope division unit)

GRAPH 4·2·5

Kistler transducer
Type 601A

250 psi

125 psi

50 psi

Transducer Output (Oscilloscope division units)

7 6 5 4 3 2 1 0

1000   2000   3000   4000

Engine Speed RPM

GRAPH 4.2-6

AVL transducer

250 psi

125 psi

25 psi

GRAPH 4.2-7

ENGINE SPEED RPM

Transducer Output (Oscilloscope division units)

1000   2000   3000   4000

0 1 2 3 4 5 6 7 8

- 51 -
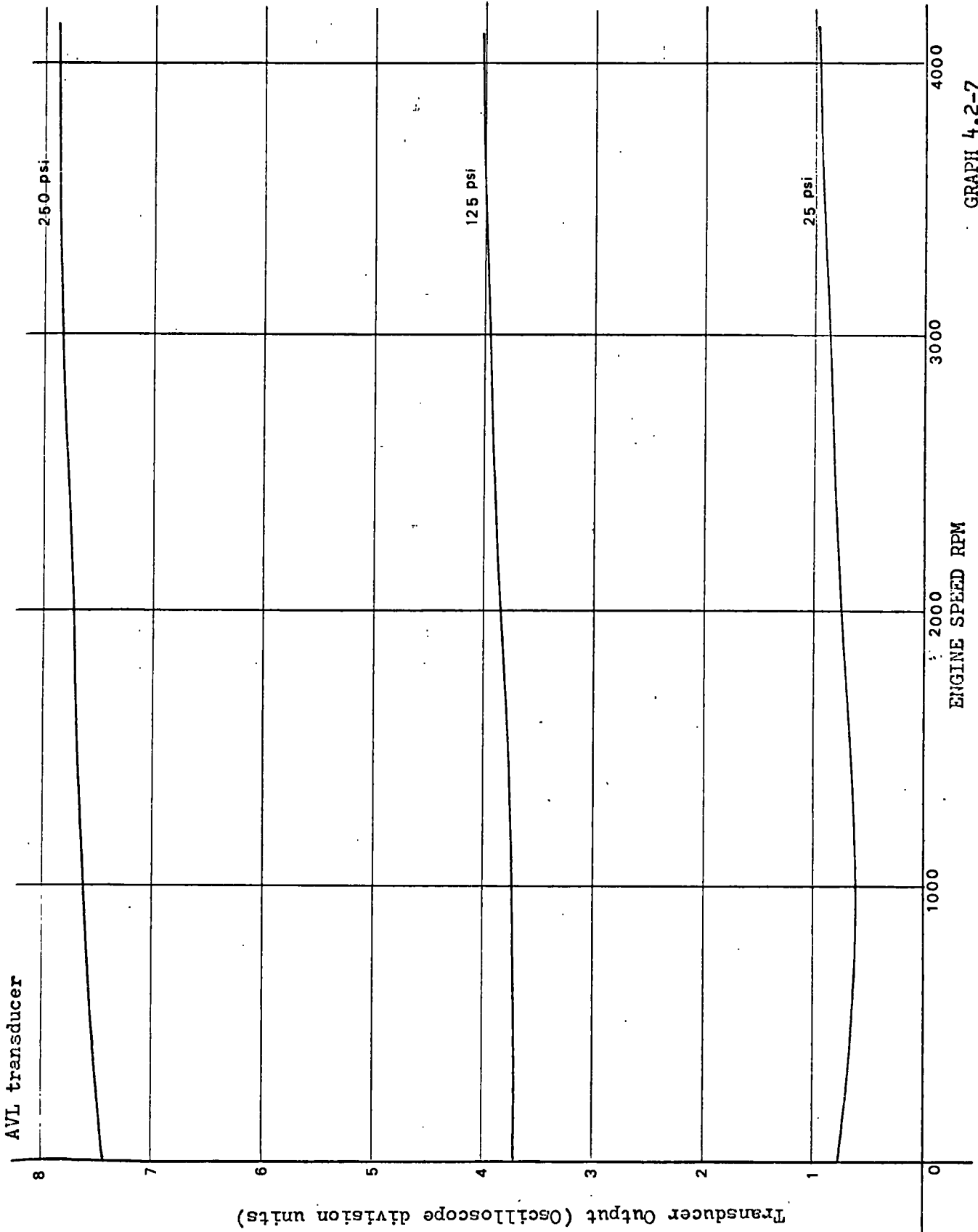
with increasing engine speed. Over 2000 r.p.m., the sensitivity increases less rapidly. Graphs 4.2-6 and 4.2-7 however show for the AVL transducer a different sensitivity response for different values of input pressure. At 250 p.s.i. static pressure (7.45 oscilloscope division units), the sensitivity continues to increase with increasing engine speed. At 125 p.s.i. static pressure (3.72 oscilloscope division units), the sensitivity remains constant up to an engine speed of 1000 r.p.m. then it increases with increasing speed and at 25 p.s.i. static pressure (0.75 oscilloscope division units), the sensitivity shows a minimum value at 1000 r.p.m. after which it increases with increasing engine speed. Because of these characteristics, the Kistler is likely to give more consistent results in engine tests.

Generally both transducers showed a satisfactory linearity response.

4.4. Effect of Temperature

The Kistler and AVL transducers were examined at two temperatures under dynamic conditions (see results in Appendices 1 and 2) in the case of the cooled transducer tests, the coolant water outlet was at a temperature of 27°C and in the case of the uncooled transducer tests, the transducer operated at the engine water jacket temperature of 78°C.

Under dynamic conditions an apparent anomoly exists whereby the sensitivity of both the Kistler and AVL transducers is decreased when operated at the temperature of 78°C. This effect is related to the dynamic operation of the transducer because Tables 4.2-1, 4.2-2 and 4.2-3 show conclusively for these different transducers that during the static calibration, the temperature of the transducer had no effect on the output. An explanation of this is difficult, but a possible cause could be that for a higher transducer operating temperature, the response of the crystal for a given load, is affected by the expansion of the steel sleeve enclosing the crystals. In the case of the AVL transducer, the effect of the higher temperature, was to increase the apparent pressure values indicated by the transducer by an average 3 p.s.i. over the cooled transducer output values. In the case of the Kistler transducer, this higher temperature caused the output to give an average increase of 4 p.s.i. over the cooled pick-up output.

4.5. Transducer response

In all cases for the AVL transducer dynamic calibration and at the higher engine speed for the Kistler dynamic calibration the curves do not pass through 0 p.s.i. at the intercept, this

- 53 -

effect is probably due to the physical response of the crystal transducer.

It was not possible to separate the response of the crystal only from the response of the crystal in its steel mounting. The magnitude of the error in this respect varies with engine speed. Brown[1] has observed this non-linearity of transducer output at low pressure and under dynamic working conditions.

5.   ENGINE TESTING

5.1.   General

Any engine is selected to suit a particular application, the main consideration being its torque/speed characteristics. Important additional factors are initial capital cost and running cost. To give an engine its performance specifications, the operation of the main variables relating to the working of the engine are considered, such as power and fuel consumption and also the different types of tests concerning the performance. Brief consideration of the evaluation of indicated horse-power, brake horse-power, friction horse-power and mechanical efficiency are given with information required for the principal measurements for I.C. engines.

5.1-1.   Types of engine tests

These are divided into four main groups which will convey a fairly complete picture of the engine performance:

        I   - Fuel consumption tests
       II   - Power tests
      III   - Motoring tests
       IV   - Willan's line (C.I. engines only)

I.   Fuel consumption tests

Since fuel consumption constitutes the major expense associated with an engine, special tests are usually made to determine the effect of the mixture strength on the specific fuel consumption, (s.f.c.) of the engine. These tests may take one of two forms:

I-1.   Constant speed, constant throttle opening

The mixture strength is varied by changing the jet opening, and the engine load is adjusted to keep the speed of the engine constant. By plotting the s.f.c. and the brake mean effective pressure (b.m.e.p.) against mixture strength, the b.m.e.p. and s.f.c. for a given mixture strength may be obtained from these curves and plotted against each other to give a fuel consumption loop.

I-2.   Constant power test

If the speed and torque are kept constant, the power will be constant, so that any change in mixture strength must be accompanied by a change in throttle opening. On plotting the s.f.c. and b.m.e.p. against mixture strength, the curves resemble those of constant speed and constant throttle opening.

II.   Power tests

The throttle opening is fixed and the brake load is varied
to give a complete range of speeds, the ignition advance (for
S.I. engines) being adjusted at each speed to give maximum power.

These tests are divided into three parts:

II-1.   Indicated horse-power (i.h.p.)

This is defined as the rate of work done by the gas on the
piston as evaluated from an indicator diagram obtained from the
engine.

An indicator diagram has the form shown in Fig. 7.8-2.
This shows the power loop only; the pumping loop could be obtained
by using a light spring.

The mean effective pressure (P_i) is defined as the height
of the rectangle having the same length and area as the cycle
plotted on a P-V diagram.

For mechanical indicators -

$$P_i = \frac{\text{net area of diagram in in}^2}{\text{length of diagram in inches}} \times \text{spring constant}$$

The spring constant unit is in Lb f/in.^{2} per vertical displacement of the indicator stylus.

For the indicator described in section 7, P_i is obtained from dynamic calibration curves for the pressure transducer used.

Considering one engine cylinder:

Work done per cycle $= P_i \times A \times L$ Ft lb f/cycle

$\quad$ A: area of piston in in^2.

$\quad$ L: length of stroke in ft.

Work done per min $=$ work done per cycle x cycles/min.

$$\text{i.h.p.} = \frac{P_i . A.L. \text{ (cycles per min)}}{33000}$$

For four-stroke engines, the number of cycles per minute $= \frac{N}{2}$ and for two-stroke engines $= N$ where N is the engine speed. If the number of engine cylinders equal n, then the i.h.p. of the engine is given by:

(a) Four-stroke engines - i.h.p. $= \dfrac{P_i \ A.L.N.n}{2 \times 33000}$

(b) Two-stroke engines - i.h.p. $= \dfrac{P_i \ A.L.N.n}{33000}$

The m.e.p. obtained from the Farnborough diagram is averaged over many engine cycles, whereas the one obtained from the

electronic indicator is given from an individual cycle.

II-2. Brake horse-power (b.h.p.)

This is the measured output of the engine. The engine is connected to a brake or dynamometer which can be loaded in such a way that the torque exerted by the engine can be measured.

The dynamometer may be of the absorption or transmission type. Absorption dynamometers are more common and can be classified as:

(a) Friction type for small power low speed engines.

(b) Hydraulic.

(c) Electrical.

(d) Air fan type.

With types (a), (b) and (c), the torque is obtained by reading off a net load, W Lb f at a known radius, R.H. from the axis of rotation.

The torque T Lb f/ft is given by:

$$T = W.R$$

The brake horse-power is given by:

$$b.h.p. = \frac{2.\pi.N.T}{33000}$$

In the transmission type dynamometer, T transmitted by the driving shaft is measured directly. With air fans, the torque is obtained from calibrated curves for the fan.

II-3. Friction horse-power and mechanical efficiency

The difference between the i.h.p. and the b.h.p. is the friction horse-power (f.h.p.) which is defined as that power required to overcome the friction resistance of the moving parts in the engine.

$$f.h.p. \ = \ i.h.p. \ - \ b.h.p.$$

The mechanical efficiency of the engine is defined as

$$\eta_m \ = \ \frac{b.h.p.}{i.h.p.}$$

η_m usually lies between 80% and 90%.

For graphs, the b.h.p., f.h.p., η_m and s.f.c. are plotted on a base of engine speed.

III. Motoring tests

High speed I.C. engines are not particularly easy to indicate owing to mechanical inertia, thermal and phasing difficulties of the indicator. Ricardo drove the engine immediately after a test by means of an electric motor, the torque on

which could be measured. Owing to the rapidity with which an engine cools down, a most refined technique is necessary to obtain reliable information. By noting the reduction in b.h.p. which attends the cutting out of each cylinder in turn, an approximate method of obtaining the i.h.p. of the cylinder is available. This is known as the Morse test which is only applicable to a multi-cylinder engine. The object of the test is to obtain the approximate i.h.p. of the engine without any elaborate equipment. The engine is run at the required speed until all conditions have stabilized and then the torque is measured. One cylinder is cut out by shorting the plug if an S.I. engine is under test, or by disconnecting the injector, if a C.I. engine is under test. The speed falls because the loss of power with one cylinder cut out but is restored by reducing the load. The torque is measured again when the speed has reached its original value.

If the values of i.h.p. of the cylinders are denoted by I_1, I_2, I_3 and I_4, considering a four cylinder engine, and the losses in each cylinder due to pumping out the exhaust gases and to the friction between cylinder and piston rings are denoted by L_1, L_2, L_3 and L_4, then the values of b.h.p., B, at the test speed with all cylinders firing, is given by:

$$B = (I_1 - L_1) + (I_2 - L_2) + (I_3 - L_3) + (I_4 - L_4)$$

If No. 1 cylinder is cut out, then the contribution to I_1 is lost, and if the losses due to that cylinder remain constant, then the b.h.p. B_1 now obtained at the same speed is:

$$B_1 = (0 - L_1) + (I_2 - L_2) + (I_3 - L_3) + (I_4 - L_4)$$

and subtracting:

$$B - B_1 = I_1$$

By cutting out each cylinder in turn, the values I_2, I_3 and I_4 can be found from equations similar to the above. Thus for an engine:

$$I = I_1 + I_2 + I_3 + I_4$$

IV. <u>Willan's Line</u>

This method is applicable to C.I. engines only. A graph of fuel consumption against b.h.p. is drawn as in Fig. 5.1-1. This is called Willan's line which is used for analysis of engine power losses. The line was obtained for the Lister F.R.1 diesel engine; the compression-head was adjusted to give a compression ratio of 16.55:1; load was applied to the dynamometer by switching in all the resistances on the control panel. A load of 30 lb was placed on the spring balance. The engine speed was set at 1000
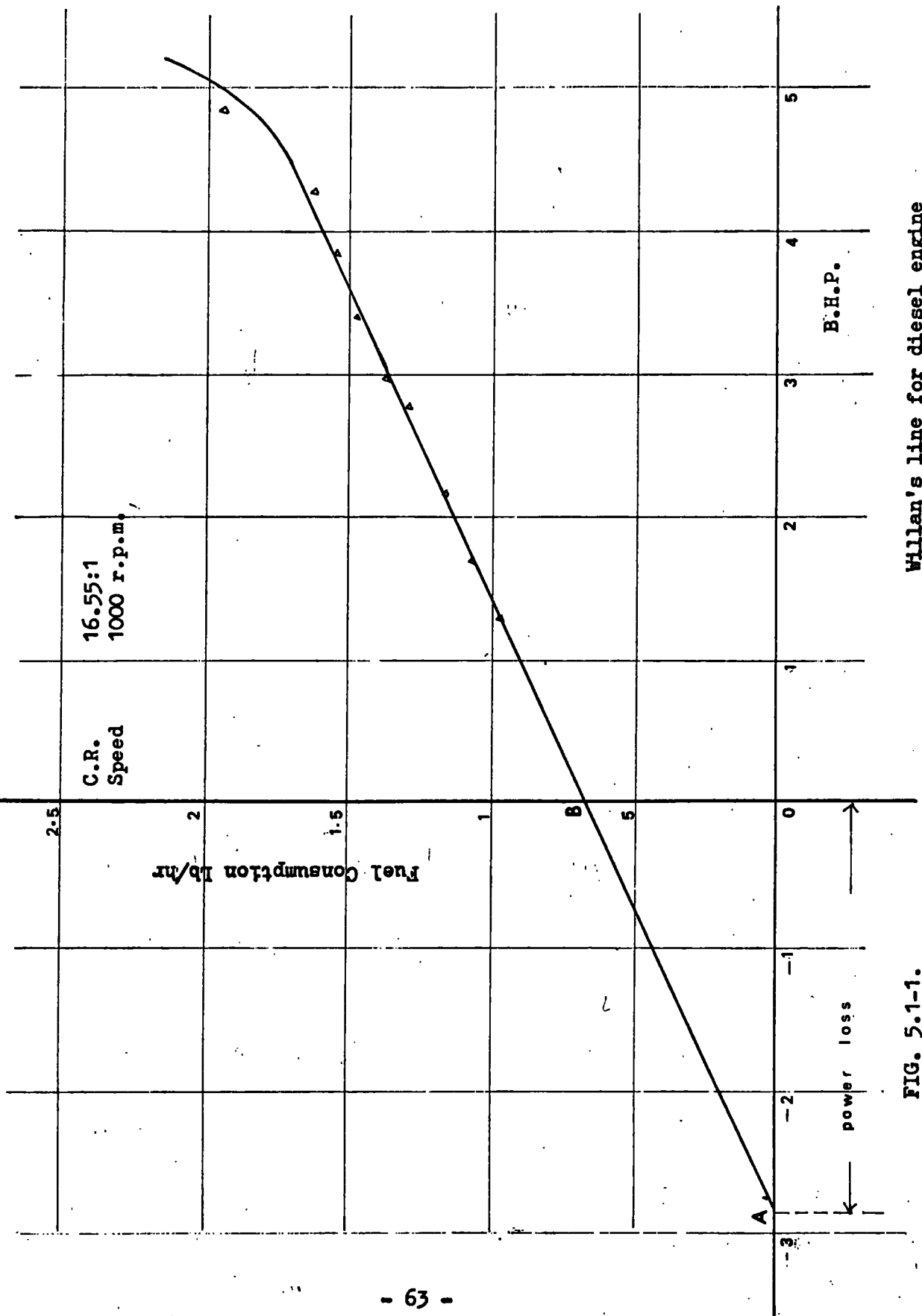
Willan's line for diesel engine

FIG. 5.1-1.

C.R.   16.55:1
Speed   1000 r.p.m.

Fuel Consumption lb/hr

B.H.P.

power loss

- 63 -

r.p.m. and kept constant by means of adjusting the throttle. After the engine had reached a steady state, the brake torque was recorded, and the time taken by the engine to consume one cubic inch of fuel was observed. Similar values were obtained successively after decreasing the load on the engine by switching out resistances on the control panel, and again allowing sufficient time for the engine to reach a steady state condition.

The torque on the dynamometer
> = [static load (1 lb) + added weights − spring balance
> reading] x Brake arm (1 ft)

Fuel consumption

$$= \frac{in^3}{sec} \times 16.387 \ \frac{cm^3}{in^3} \times \frac{S.G\ (.8)}{4.54} \times 60 \times 60 \ \ Lb/hr$$

Fig. 5.1-1 shows that for the Lister F.R.1 diesel engine the fuel consumption and b.h.p. follow a straight line, indicating a linear relation between the two variables up to a 4.8 b.h.p. This straight line was extrapolated back to cut the b.h.p. axis at point A. The reading OA (2.88 b.h.p.) is taken as the power loss of the engine running at 1000 r.p.m.

The fuel consumption at zero b.h.p. is given by OB (0.67 Lb/hr). If the relationship existing between fuel consumption and b.h.p. is assumed to be linear, then a fuel consumption of

0.67 Lb/hr is equivalent to a power loss of 2.88 b.h.p.

The deficiency of this method for engine testing is that Willan's line is not usually straight, particularly at the higher engine loads, and the validity of the extrapolation might not be very accurate.

5.1-2. Measurements for engine testing

The following are the principal measurements required for testing I.C. engines:

      1. Torque.

      2. Rotational speed.

      3. Fuel consumption.

      4. Air consumption.

      5. Various temperatures.

      6. Ignition advance (for S.I. engines only).

1.   Torque

In selecting a dynamometer, it is important that the engine torque at every speed should be exactly balanced, otherwise the engine will either stall or race away. Furthermore, the characteristics of the dynamometer should be the same as the anticipated service load on the engine, and, since in propulsion

work, this is mainly a question of overcoming a fluid resistance, then the froude hydraulic brake should meet most cases.

The electric dynamometer has the advantage that it can be used for motoring the engine as well as absorbing the power. When absorbing power from air-cooled aero-engines on test, the generated current may be used for driving the cooling fan.

2.   Rotational speed

This is measured by a centrifugal tachometer (similar to an engine governer) or by a chronometric type where the number of revolutions in a given interval of time are counted and recorded by the instrument, or by an electric tachometer where advantage is taken of the generated e.m.f. being proportional to the speed.

3.   Fuel consumption

This is most easily measured by noting the time taken by the engine to consume a given volume of fuel. Fig. 5.1-2a shows a common example where two spherical glass bulbs, one of (about) 100 c.c. capacity and the other of 200 c.c. capacity are connected by three-way cocks so that one may feed the engine whilst the other is being filled.

To convert the fuel consumption to a mass basis the specific gravity of the fuel should be taken at the ambient temperature during the time of trial.

Specific fuel consumption

$$= \frac{\text{Fuel in Lb/hr}}{\text{b.h.p.}} \quad \text{Lb m/b.h.p., hr.}$$

4. Air consumption

A sharp-edged orifice in conjunction with an anti-pulsating tank, having in the case of a single cylinder engine a volume about 500 times the swept volume of the engine, forms a simple and cheap method of estimating the air flowrate to an engine; Fig. 5.1-2b shows the type of tank employed in measuring air consumption.

Theory:

If the pressure difference over the orifice, by correct choice of orifice diameter, is limited to five inches of water, the coefficient of discharge C_d is sensibly constant at 0.596 and compressibility may be ignored; hence the internal energy of the air can be ignored and ρ_1 the initial air density would be equal to the final air density ρ_2:

Bornoulli's equation becomes:

Orifice

Manometer

Baffle

Anti-pulsating tank

To engine

FIG. 5.1-2b. Air consumption measurement

Petrol tank

200 c.c.

100 c.c.

Index

Index

Three way cock

To engine

FIG. 5.1-2a. Fuel consumption measurement

$$\frac{P_1}{\rho} + \frac{V_1^2}{2g} = \frac{P_2}{\rho} + \frac{V_2^2}{2g} \qquad\qquad (1)$$

Where V is the volume and P is the pressure.

From the continuity equation

$$A_1 V_1 \rho_1 = A_2 V_2 \rho_2$$

But ρ is assumed constant

$$\therefore \quad V_1 = \frac{A_2}{A_1} V_2 \qquad \text{let} \quad \frac{A_2}{A_1} = r$$

Hence

$$V_1 = r V_2$$

From equation (1) and substitute for V_1

$$\frac{V_2^2}{2g} - \frac{V_2^2 r}{2g} = \frac{P_1 - P_2}{\rho}$$

$$V_2^2 \left(\frac{1 - r^2}{2g}\right) = \frac{P_1 - P_2}{\rho}$$

$$V_2 = \frac{(P_1 - P_2)\, 2g}{\rho\,(1 - r^2)}$$

For air $\rho = \rho_a \qquad V_2 = V_a$

For the tank $A_1 = \alpha \qquad r = 0$

Hence $\quad V_a = \dfrac{(P_1 - P_2)\, 2g}{\rho_a}$

The pressure difference is usually expressed in inches of water h_w.

$$\therefore\ P_1 - P_2 = \frac{h_w}{12}\ \rho_w$$

Mass of air flow in Lb/sec $= C_d.A.V_a.\rho_a$

A: area of orifice in square feet.

$$\therefore\ \text{Mass flow} = C_d.A.\ \sqrt{2g.\rho_w\ \frac{h_w}{12}}\ \text{Lb m/sec.}$$

Its excellent damping qualities and low vapour pressure commend castor oil for use in the manometer.

5. <u>Temperature measurements</u>

The temperature rise of the circulating water is most conveniently obtained by mercury-in-glass thermometers which can be inserted directly into the rubber hose so that their bulbs are in the stream of circulating water. For exhaust and cylinder head temperature copper-constantan thermocouples should be used after calibration in oil against a high-temperature mercury thermometer.

6.   Ignition advance

The majority of car engines use an electric spark to ignite
the fuel/air mixture in the cylinder, and this spark requires
exact timing. Because combustion occurs in a fraction of a second,
the spark needs to be induced just before the piston reaches its
'T.D.C.' position. For best results, the spark timing needs to
be advanced further at the higher engine speeds to allow for the
combustion delay.

The basic ignition timing can be accurately set with the
aid of a test lamp connected between the distribution low-tension
terminal and an earth point. The lamp lights as the contact
points open, thus indicating T.D.C. of one of the engine pistons.
Advancing or retarding the ignition timing is possible by turning
the distributor in its mounting after slackening off its clamping
bolts.

6. ENGINE INDICATORS AND INDICATION

6.1. Types of indicators

There are three main groups of engine indicators:

1. Mechanical indicators.

2. Partial-electrical mechanical indicators (Farnborough).

3. Electrical indicators (cathode ray oscilloscope).

6.2. Construction and operation

6.2-1. Mechanical indicator

The essential features are shown in Fig. 6.2.1-1. The cylinder of the indicator is connected to the engine cylinder by means of a valve. The movement of the indicator piston is controlled by a helical spring of known stiffness; it is recorded on an indicator card attached to the drum and can be magnified by a mechanical linkage.

The movement of the engine piston is transmitted to the indicator drum by means of a linkage and connecting cord.

The record may be made by:

(a) Brass stylus on special paper.

(b) Stylus on a waxed paper.

FIG. 6.2.1-2. Working cycle for diesel engine

FIG. 6.2.1-1. Simple mechanical indicator

The action of the stylus in type (b) is to remove a thin trace of wax as it moves. Using this indicator, several types of diagram can be produced, each quite useful in assessing engine performance. The normal working cycle for a diesel engine is shown in Fig. 6.2.1-2.

To investigate the compression process in the cylinder, the fuel pump is cut out and the indicator drive is disconnected. The drum is rotated by drawing the cord slowly by hand and the recording stylus is held on to the drum for a number of cycles. This is called a draw cord; it may also be taken from the engine when it is firing.

The results are shown in Fig. 6.2.1-3.

6.2-2. Farnborough indicator

This is a mechanical device employing a partial electrical recording. A simple diagrammatic view of this indicator is shown in Fig. 6.2-2.

The device consists of a drum driven by the engine crank-shaft or camshaft.

High pressure from the air bottle is applied to a distri-bution box and is used as a reference pressure. The engine
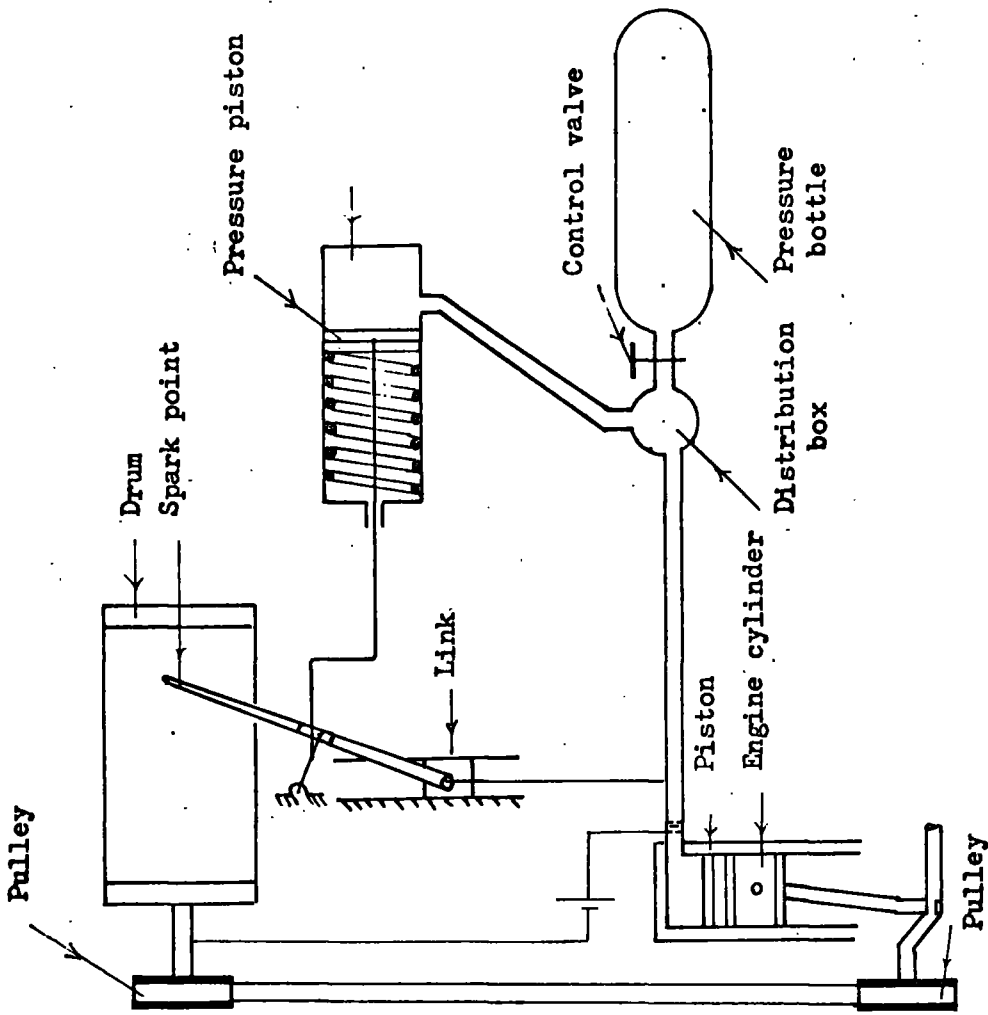
FIG. 6.2-2. Simple diagrammatic representation of Farnborough indicator
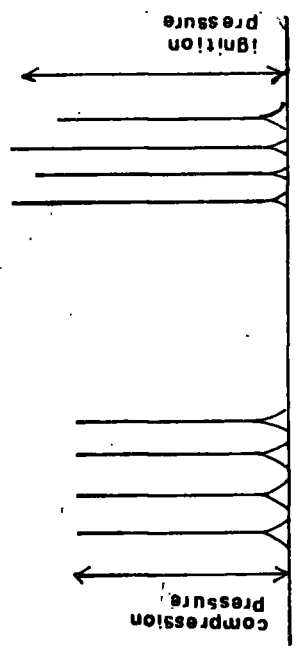
FIG. 6.2.1-3. Compression and ignition pressures for a diesel engine
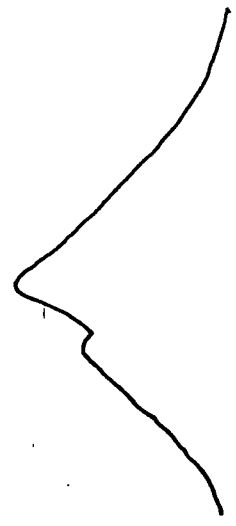
FIG. 6.2.1-4. Hand drawn indicator for a diesel engine

combustion chamber is connected to the distribution box and the resultant pressure of the engine and bottle is fed to the pressure cylinder. A high-tension battery is so wired that when the combustion chamber pressure exceeds the reference pressure an electric spark passes through the spark point on the probe; this makes a perforation on the recording paper which is fixed around the drum. The pressure from the air bottle is raised gradually causing a relatively slow movement of the probe, each consecutive cycle registering its point at slightly higher pressure than the preceding cycle until the probe has completed its full stroke.

Since the drum is connected directly to the engine camshaft or crankshaft, the perforations trace a P-T diagram made during a large number of consecutive cycles.

6.2-3. Cathode-Ray oscilloscope engine indicator

This consists of a typical cathode-ray tube of the hot cathode gas. Fig. 6.2.3-1 is a simple diagrammatic illustration of the tube.

Electrons emitted from a small oxide coated filament f, are drawn through a gun s, at a convenient positive potential. The electron beam passes between two pairs of deflecting plates b and d, which are mutually perpendicular, and finally, after a relatively
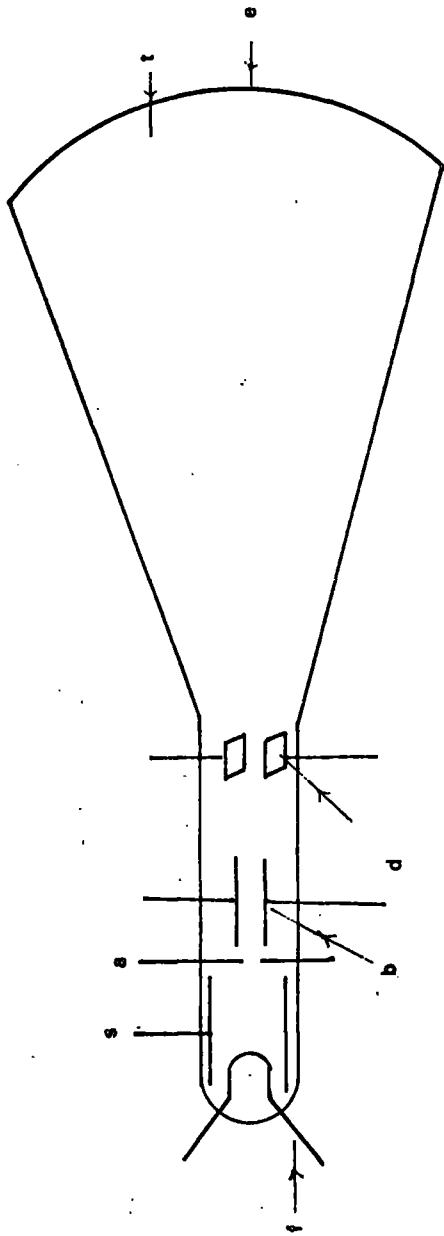
FIG. 6.2.3-1. Cathode Ray Tube

Key:

a: anode
b: horizontal deflecting plates
d: vertical deflecting plates
e: screen
f: filament
s: shield
t: tube

long travel, impinges on a fluorescent screen e. The tube is filled with inert gas at low pressure which allows the beam to be brought to a sharp focus on the screen. The focussing is carried out by adjustment of the filament current and of the negative bias on a focussing shield S which surrounds the filament.

The operation is based on the principle that a cathode ray can be deflected:

(a) By means of electro-magnet; the movement of the ray is proportional to the strength of the electro-magnet.

(b) By an electrostatic effect; the movement of the ray is proportional to the potential difference between the two plates. The ray can be made to trace a P-T or a P-V diagram on the screen. When the engine is running under steady state conditions the continuous tracing of the diagrams on the screen at the high speeds of the engine produces the appearance of a single diagram. This diagram can be observed directly by the eye, or a permanent record may be obtained by throwing the image on a photographic film. The ray is deflected in the vertical direction by means of

electric current which is proportional to gas

pressure in the engine cylinder. At the same

time the ray is deflected in a horizontal

direction in proportion to rotation of the

engine crankshaft. The combination of the two

perpendicular deflections produce the P-T

diagram. A P-V diagram can be obtained by

making the horizontal deflection follow the

piston displacement. Fig. 6.2.3-2 shows a

brief arrangement for controlling the vertical

movement of the ray. The initial position of

the ray is set on the screen by varying the

value of R. The pressure element D, such as a

Piezo-electric transducer, causes a difference

of voltage between the deflecting plates b_1 b_1

proportional to the cylinder pressure, the

difference governing the vertical deflection of

the ray.

Fig. 6.2.3-3 is an arrangement of controlling the horizontal

movement of the ray. The condenser c continually charges through

a variable resistance r; this produces a voltage across the

horizontally deflecting plates b_2 b_2. The ray will consequently
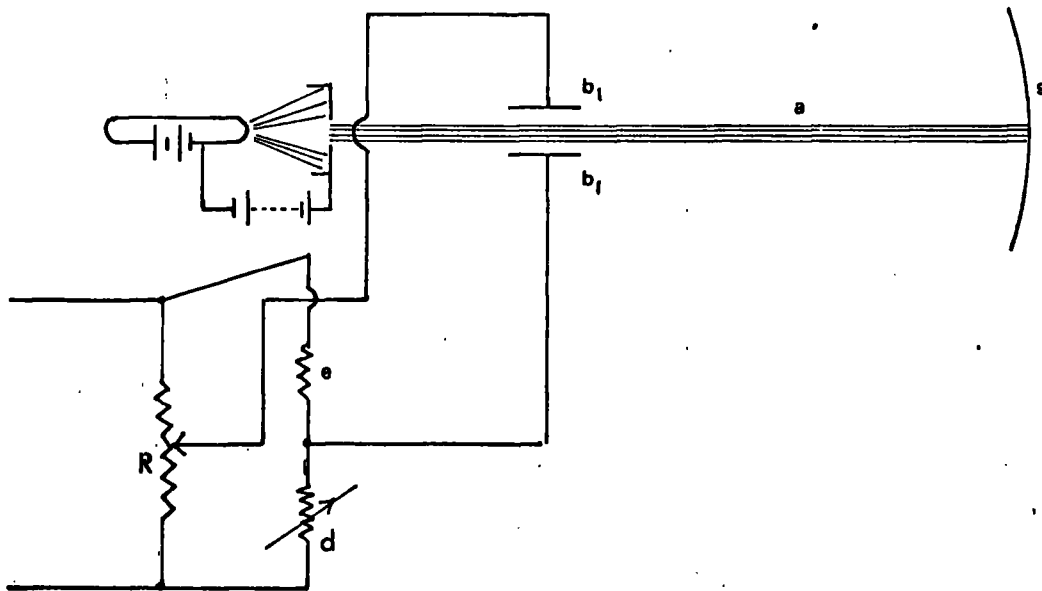
FIG. 6.2.3-2. Arrangement for controlling the vertical
movement of the ray
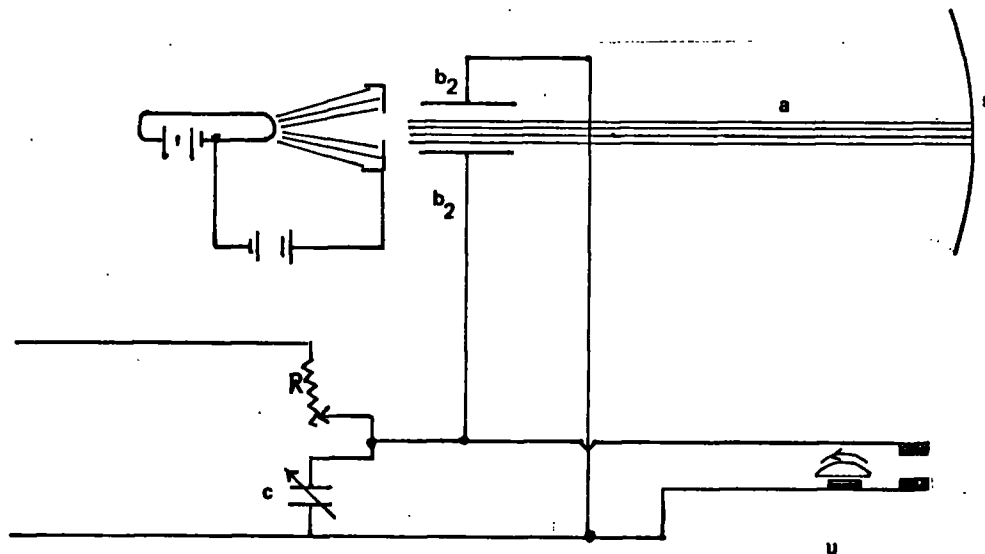
FIG. 6.2.3-3. Arrangement for controlling the horizontal
movement of the ray

Key:

a	:	Cathode-Ray	e	:	High resistors
b_1 b_1	:	Vertical deflecting plates	s	:	Screen
R	:	Variable resistance	c	:	Condenser
d	:	Pressure element	u	:	Commutator
			b_2 b_2	:	Horizontal deflecting plates

- 80 -

move at constant rate in the horizontal plane as the condenser

c charges.

A commutator．ʊ⸱ situated on the engine crankshaft breaks

the circuit at each revolution (or any other required interval)

causing the condenser to discharge which brings the ray back to

its original position.

6.3.   Top-Dead-Centre Detection

In engine testing, it is important to relate events on the

pressure trace to crank-angle position. To provide timing of

the crankshaft rotation, a Tufnol disc having sixty steel inserts

fitted round its circumference at equal intervals is mounted on

the crankshaft.

A magnetic transducer is placed radially with respect to

the disc axis such that the gap between the rim of the disc and

the magnetic pick-up is about 0.005 inch. Fig. 6.3-1. As the

crankshaft rotates, an electric pulse is generated, each time a

steel insert passes the magnetic pick-up. When these pulses are

amplified and fed to the vertical deflection plates of one

oscilloscope beam, a trace having equal spaces is displayed on

the screen together with the P-T diagram. For synchronising the
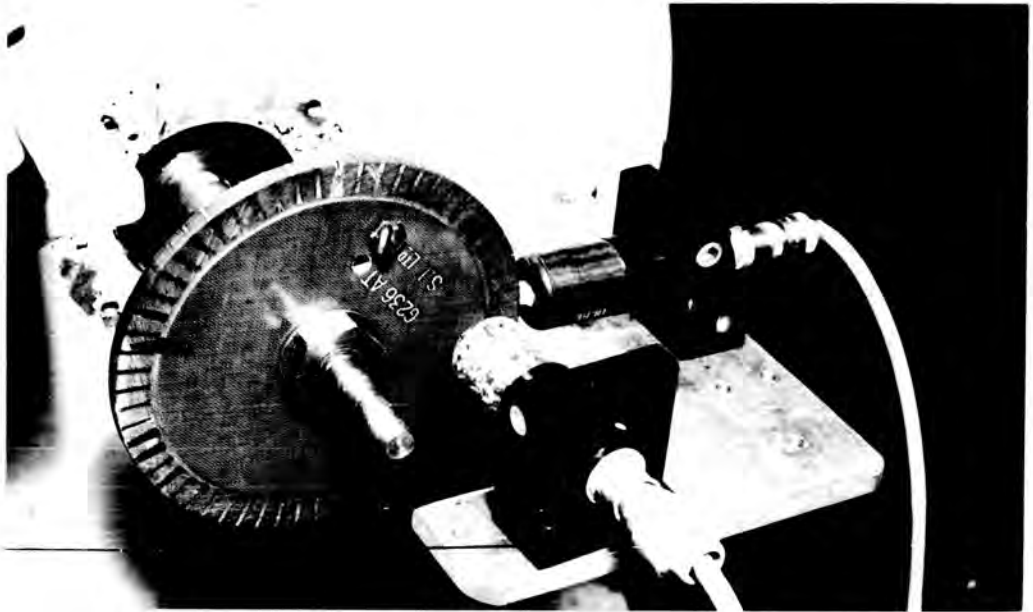
FIG. 6.3-1. The timing disc and magnetic pick-ups
shown mounted on the engine

horizontal movement of the beam with the engine rotation the beam is 'triggered off' from another pick-up which produces its signal when a steel projection on the side of the timing disc passes the pick-up.

To detect the T.D.C. the flywheel is rotated to bring the piston to T.D.C. This is indicated by a pointer and the degree marks on the flywheel.

One steel insert is removed from the timing disc which is then rotated until the empty slot faces the magnetic pick-up. The disc is then firmly clamped to the crankshaft. By this means the pulse from the magnetic pick-up which is judged to be coincident with T.D.C. is omitted from the timing trace; consequently, two of the adjacent spaces on the trace are linked together. A vertical line bisecting this interval is assumed to pass through T.D.C. on the P-T diagram.

During indicating tests, only the motoring pressure diagrams were photographed in order that the T.D.C. point (which is coincident with the highest point on the P-T trace) could be detected and compared with that detected by the magnetic transducer. Using this technique P-T diagrams were recorded at an engine speed of 1000 r.p.m. These indicated a delay of 3.4^o crank angle in

detecting T.D.C. This delay could either be introduced by the magnetic pick-up response or a misalignment of the flywheel with the crankshaft.

P-T diagrams were then recorded at a range of engine speeds between 600 to 1400 r.p.m. From these it was observed that the delay in indicating T.D.C. was reasonably constant with different engine speeds (see Figs. 6.3-2, 6.3-3 and 6.3-4). To render the method more valuable for T.D.C. detection, the timing disc was advanced in its angular rotation by a magnitude of 3.4° and re-secured to the crankshaft. Then P-T records were obtained at a range of engine speeds between 400 to 1400 r.p.m. (see Figs. 6.3-5, 6.3-6 and 6.3-7). These records show for the engine speeds used that no significant delay is present in detecting T.D.C. by this technique. The average accuracy obtained is about 0.3° of crank angle.

6.4. Recommendations

The types of mechanical indicator used depend on engine speed and the rate of pressure changes in the cylinder. It is constructive to consider a range of indicators; to those manufactured by Maihak of Hamburg, a range of springs is available, and, to cover as wide a range of requirements as possible,

Speed   600 r.p.m.
Delay   3.5°
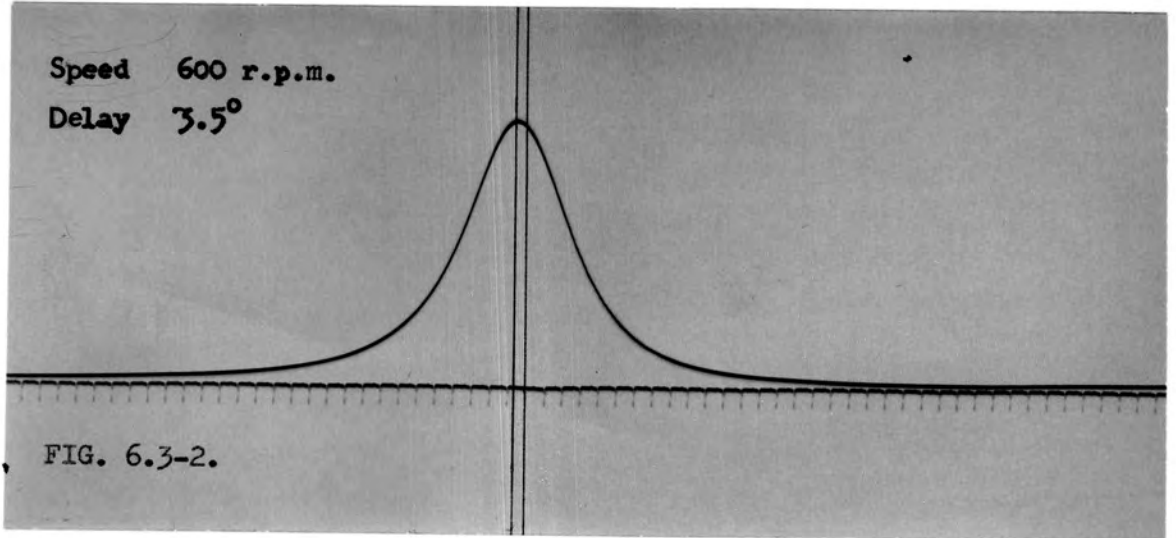
FIG. 6.3-2.

Speed   1000 r.p.m.
Delay   3.2°
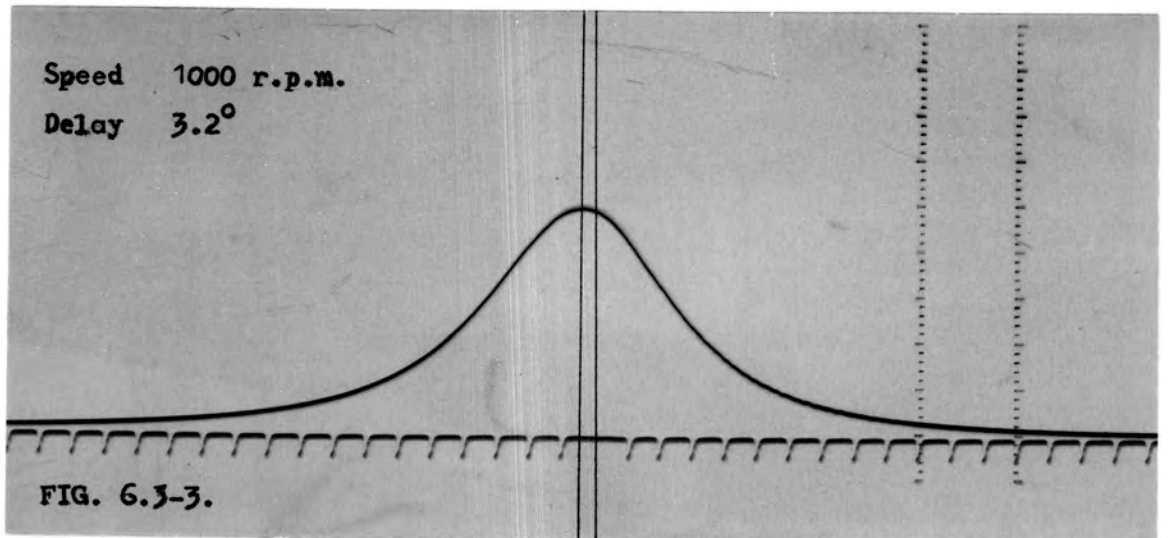
FIG. 6.3-3.

Speed   1400 r.p.m.
Delay   3.3°

FIG. 6.3-4.

Speed   400 r.p.m.

FIG. 6.3-5.

Speed   1000 r.p.m.

FIG. 6.3-6.

Speed   1400 r.p.m.
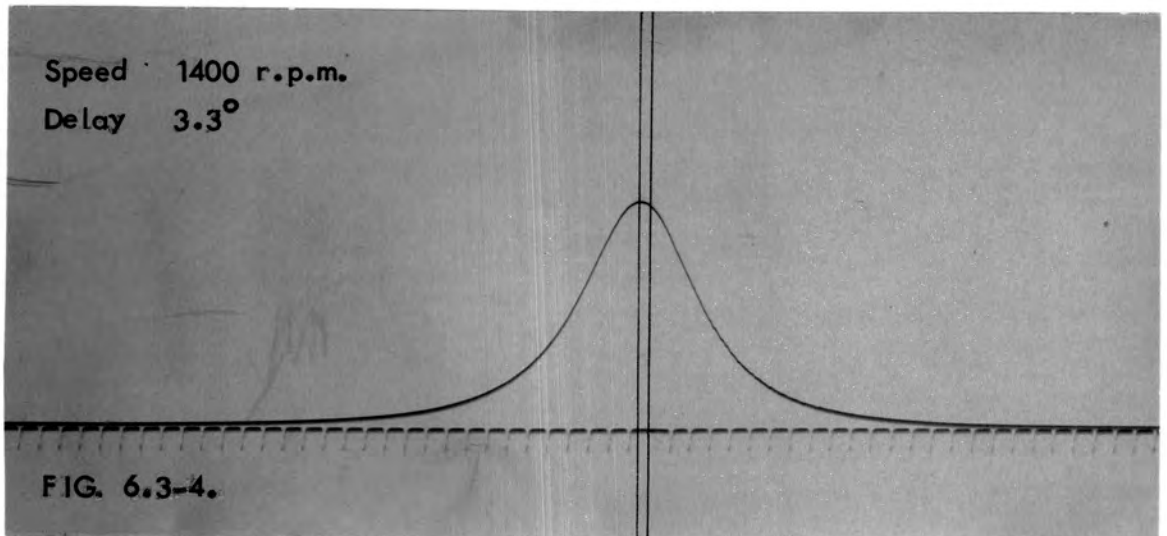
FIG. 6.3-7.
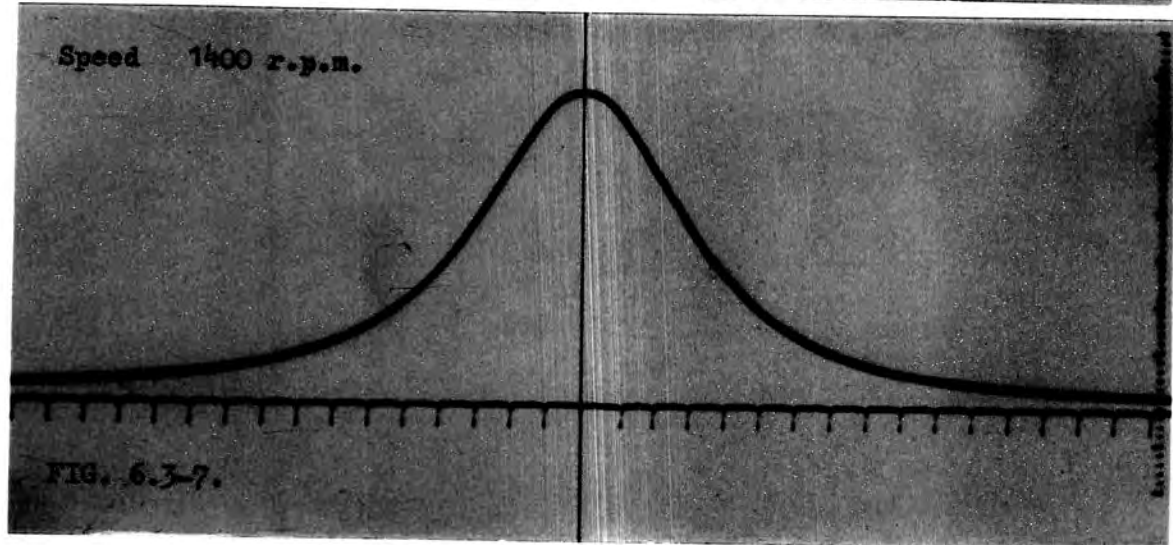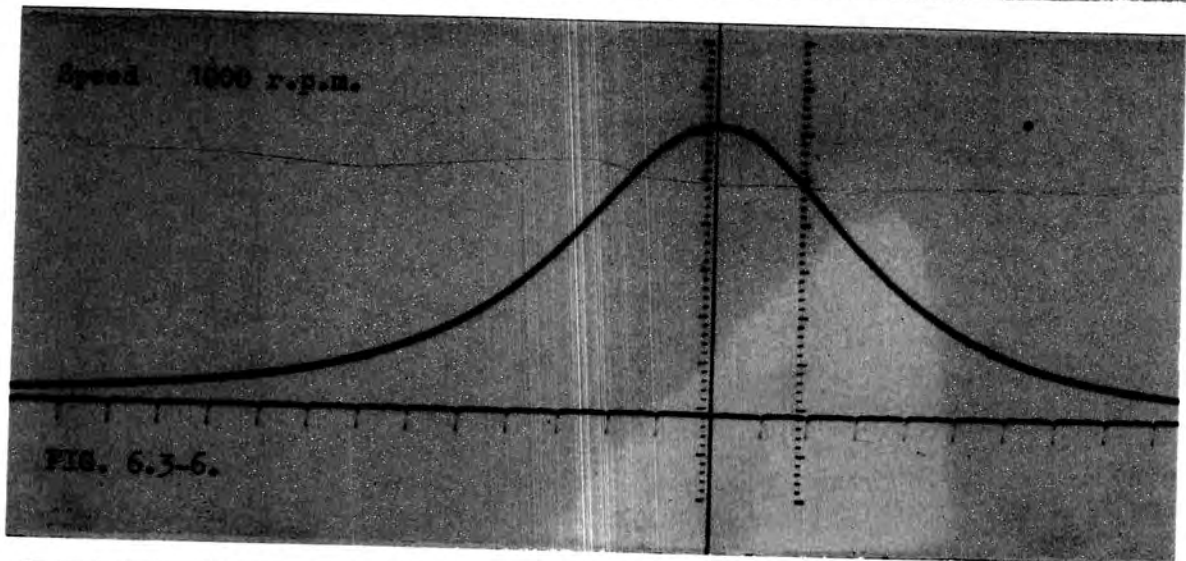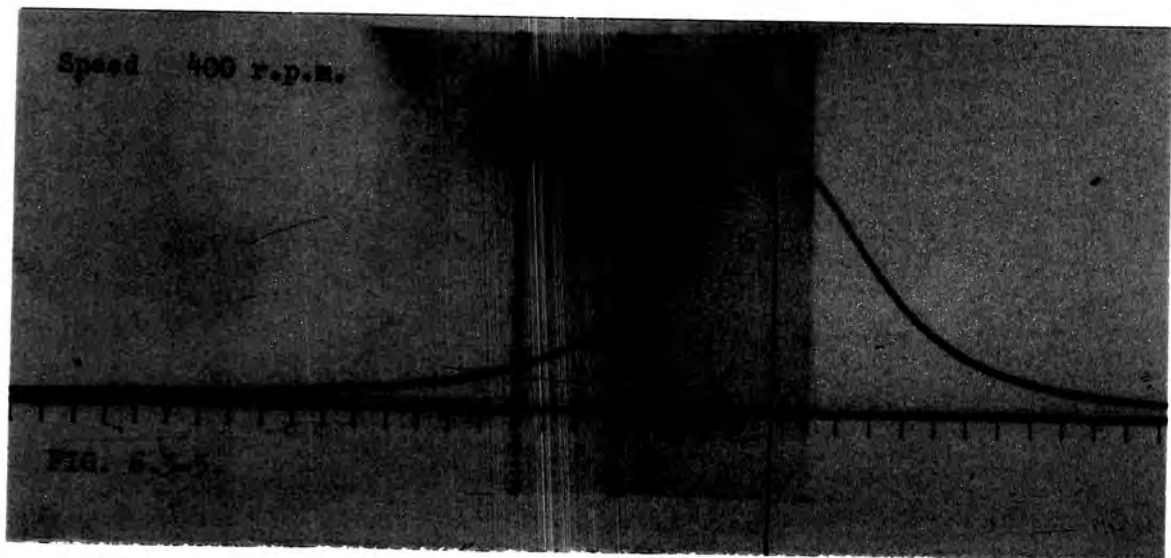
different size pistons and cylinders may be fitted with each
spring.

The Maihak type 50 Z indicator is used for speeds up to
400 r.p.m. and/or maximum rate of pressure change, dP/df of
2.5 x 10^5 Lbf/in^2 per sec. The type 30 has a smaller drum and
stronger springs to reduce the indicator piston movement; it
is used for speeds up to 1000 r.p.m. and values of dP/dt up to
3.4 x 10^5 Lbf/in^2 per sec. For higher speeds up to 2400 r.p.m.
type S has been devloped and is of a different design from those
described. A helical spring is not used but a cantilever-type
spring is fitted instead. This spring is much stiffer than the
helical type and, together with light reciprocating parts, form
a system having a high natural frequency of vibration.

The Farnborough indicator has a great advantage over the
mechanical indicator in that the P-T diagrams obtained are not
affected by the inertia of moving parts so that the indicator
may be used over wide ranges of engine speeds. Recent models of
this indicator include a vernier screw between the shaft of the
indicator drum and the engine shaft which enables more accurate
settings to be obtained. One disadvantage of this indicator is
that it has to be sited close to the engine which is inconvenient
for the operator

7. PRESSURE-VOLUME DIAGRAM

7.1. General

For speeds at which most internal combustion engines run
the mechanical indicator is unsatisfactory because of the consid-
erable inertia of its moving parts. The construction of a high
speed indicator is described; an eccentric cam mounted on the
crankshaft of the engine and a cam follower were used to obtain
a signal proportional to the swept volume of the piston. The
cam follower was made from spring steel strip, five inches in
length and one half-inch wide.

The spring was fixed at one end while the other end acted
as a cam follower (see Fig. 7.1). Two strain gauges were mounted
on the spring, one on each side at an equal distance from each
end of the spring. These gauges form two active arms in a
Wheatstone bridge (see Drawing 7.3-1). The cam lift varies with
the rotation of the crankshaft which in turn produces continuously
varying strains in the strain gauges. The strain induced is
directly proportional to the cam lift; hence the electrical signal
output from the strain gauges is proportional to and in phase with
the piston swept volume. A pressure-volume record is produced when
the strain gauge signal is applied to the horizontal deflection
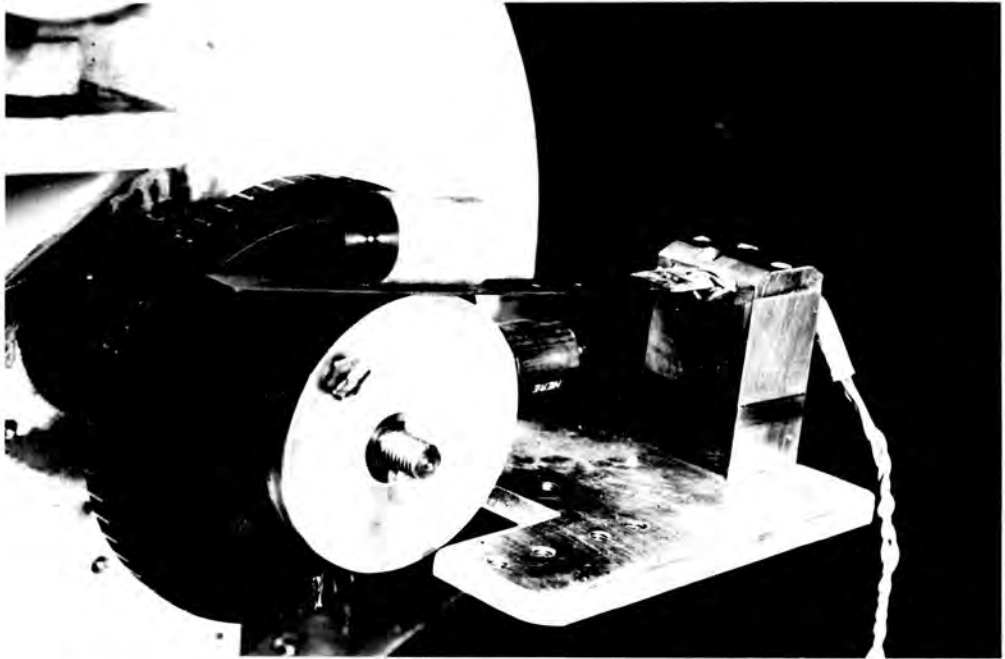
FIG. 7.1. The cam and spring mounted on the engine
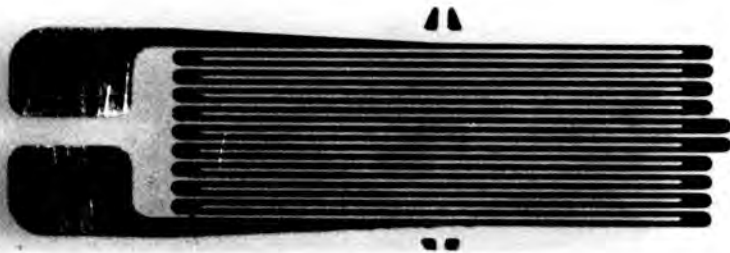
FIG. 7.5-2. A half inch long linear strain gauge

CRANK ANGLE

DISPLACEMENT

ECCENTRIC CAM LIFT

PISTON DISPLACEMENT

DRAWING 73-1

CAM
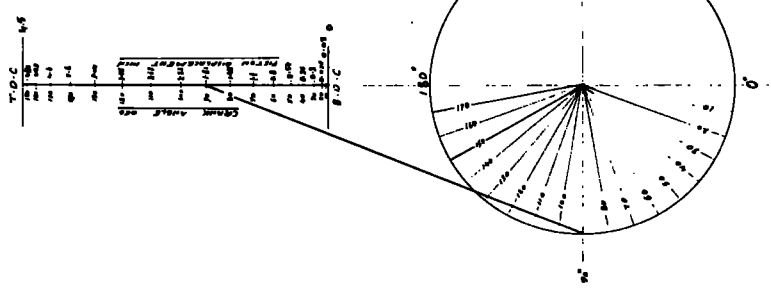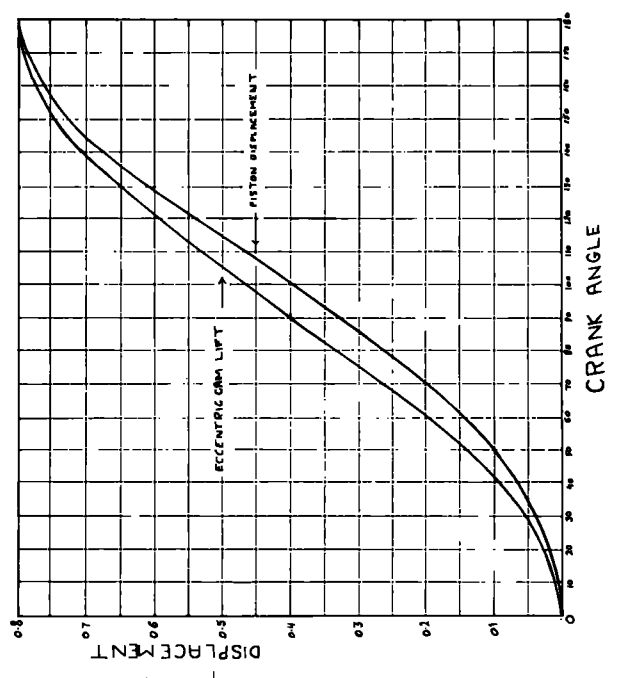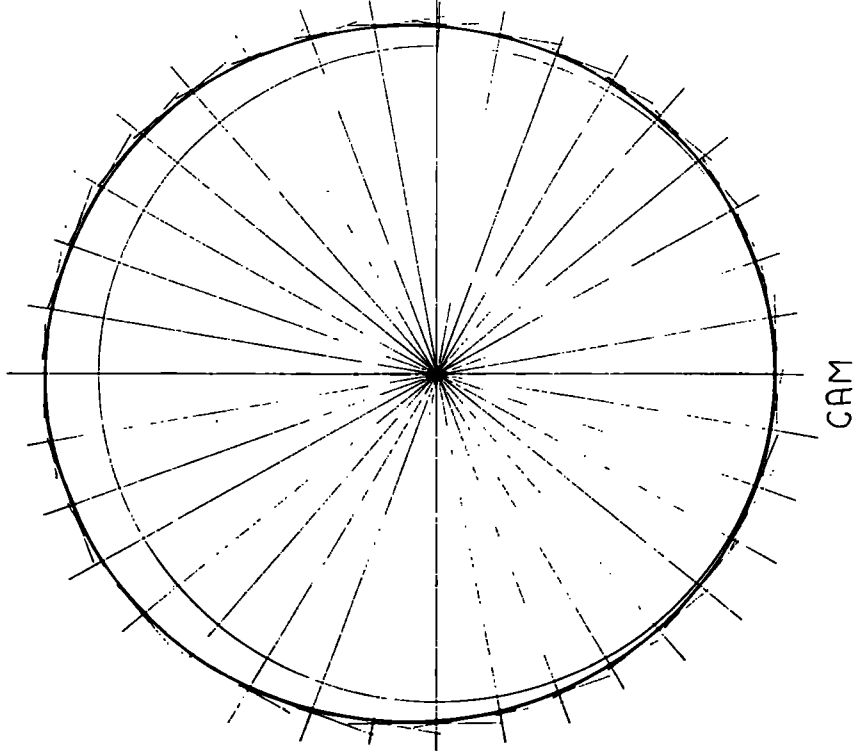
plates of the cathode-ray oscilloscope; the vertical deflection
plates are connected to a pressure transducer.

7.2. The design and dimensions

The device was designed so that it could be mounted on the
engine together with the 'Tufnol' degree-marking disc and the
magnetic pick-ups (Southern Instruments Ltd. No. G308) which had
been previously mounted on the engine (see Fig. 7.1). By using
this arrangement, the magnetic pick-ups and the degree-marking disc
could supply information of the engine position for the P-V diagram.

7.3. The cam

It was initially assumed that the piston motion was simple
harmonic. Making this assumption, a simple eccentric cam could
provide a signal proportional to the swept volume.

To establish the real relationship between piston stroke
and eccentric cam lift with respect to crank angle, the eccentric
cam lifts were calculated theoretically for each 10° crank angle
(see Appendix 4). The corresponding piston strokes were found
graphically (see Drawing 7.3-1). Graphs of cam lift and piston
stroke against crank angle were plotted (see Table 7.3-1 and

Appendix 4). From these it was found that the piston motion was not simple harmonic; the error involved varies with crank-angle, increasing from 0% of piston stroke at crank-angles of 0° and 180° up to a maximum error of 9.7% at crank-angles of 90° and 270° respectively. Hence, to produce an accurate P-V diagram, a special cam was required whose profile was drawn using the practical values of piston displacement with respect to crank-angles (see Drawing 7.3-2). First, a simple eccentric cam was machined from 'Tufnol' to give a maximum lift of 0.02 inch. This small lift was chosen in order to reduce fatigue effects that could be induced in the spring due to the stress cycles. However, after displaying the strain gauge signal on the C.R.O. screen, it was found that the friction between the cam and spring caused a considerable amount of distortion of the signal.

To reduce the friction a strip of 'P.T.F.E.' material was taped onto the spring at the position in contact with the cam. Although this improved the electrical signal obtained, it did not produce the required accuracy; also because of the soft structure of 'P.T.F.E.', this material suffered a fast rate of wear.

To obviate the former problem the cam lift was increased 10 times which produced a greater change in strain gauge resistance because of the greater stress induced in the spring. This meant

that the amplification of the strain gauge signal could be
reduced 10 times (... being 10 times larger than before) and
hence the signal distortion due to friction was reduced consid-
erably. For further improvement, the cam was machined from brass
which possesses a lower coefficient of friction than 'Tufnol'
when in contact with spring steel.

7.4. Spring holder

This was made of two parts (see Drawing 7.3-2).

1. The Base: This forms the lower part of a mild
   steel holder. It was secured to the top of an
   aluminium table that was previously mounted on
   the engine below the crankshaft. The base
   dimensions are: $1\frac{1}{2}$ inch in length, 1 inch width
   and $1\frac{3}{4}$ inch in height.

2. The Cap: This incorporated two slots, one being
   half inch long to support the spring and hold it
   firmly to the base, the other being $\frac{1}{8}$ inch wide
   and incorporating a rubber insert to support the
   strain gauge wires and prevent damage to the
   strain gauges due to accidental snatch. The cap
   was secured to the base by means of two half-inch
   diameter Allen screws.

CAM

SLEEVE

FLANGE

PLAN VIEW

STEEL SPRING

ACTIVE GAUGE

ACTIVE GAUGE

B ACTIVE GAUGE

A

B

G

80 Ω

80 Ω

12V
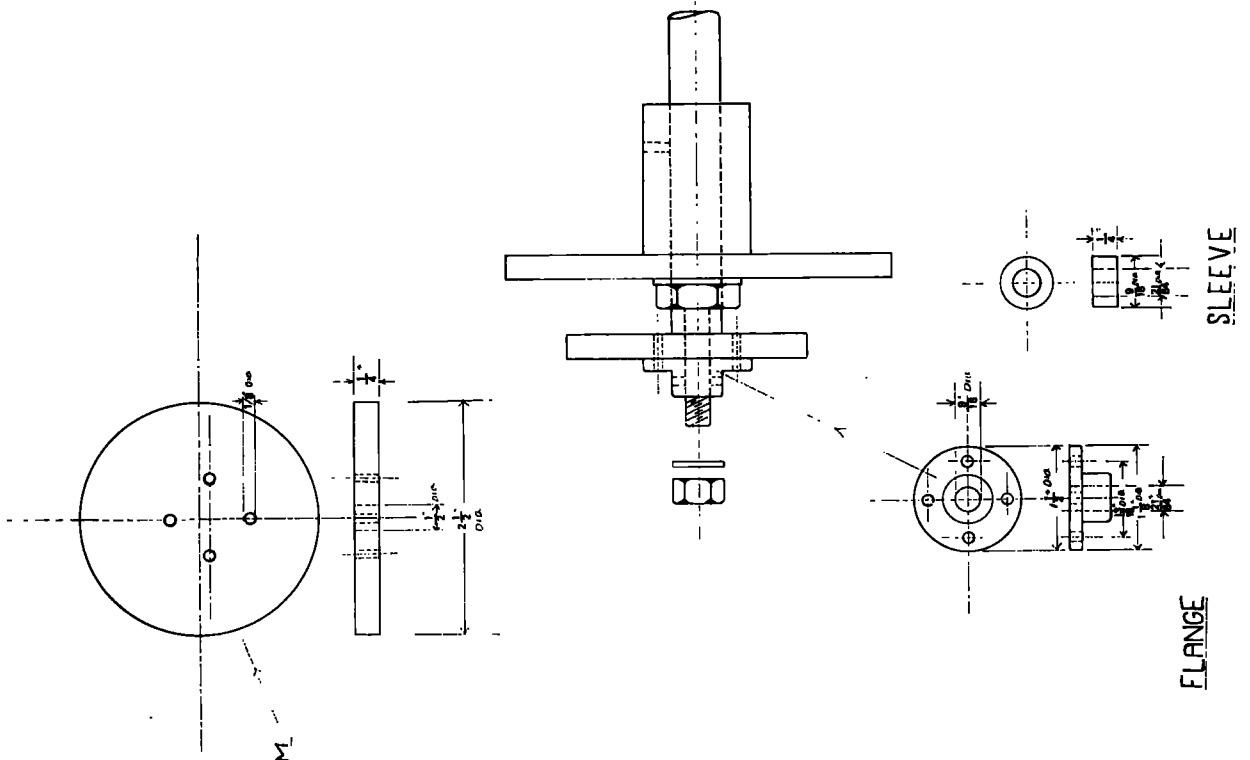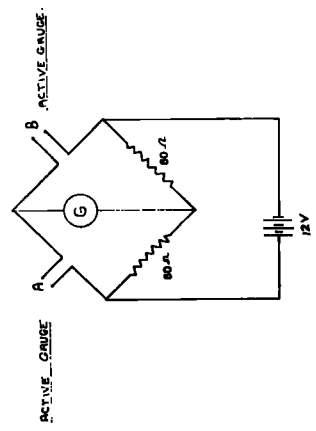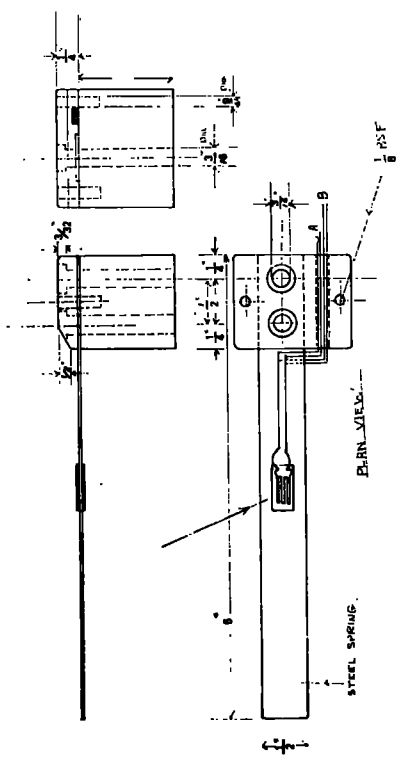
WHEATSTONE BRIDGE CIRCUIT

DRAWING 73-2

- 93 -

7.5. The strain gauges and circuit

7.5-1. Principle of operation

A strain gauge works on the principle that when an electrical conductor is stretched its resistance increases. Therefore, if a strain gauge is mounted onto the surface of the specimen, then any subsequent strain in the specimen is also experienced by the gauge resulting in a change of its electrical resistance. Each of the two strain gauges used form an active arm of a Wheatstone bridge network (see Drawing 7.3-1). The strain gauges were mounted at an equal distance from the spring ends thus experiencing the same degree of strain during the spring movement. By this means, the combination of each strain gauge signal provided a larger signal that was suitable for amplification and display on the C.R.O. screen; also this method is an accurate compensation for any errors that may arise due to temperature effects.

Appendix 5 shows the calculation for the Wheatstone bridge signal output.

7.5-2. Choice of strain gauge

The following points concerning the strain gauge were considered.

i - Linearity
        ii - Size
       iii - Temperature range suitability
        iv - Sensitivity

i. <u>Linearity</u>

In detecting the piston position by means
of a strain gauge, the electrical signal
produced must vary linearly with the
impressed strain so that the electrical
signal is proportional to the displaced
volume (see Appendix 4).

ii. <u>Size</u>

The size of the gauge was chosen to suit the
spring size so that it could be mounted
accurately on the spring, taking into account
that it should not touch the cam profile when
the device is under operation.

iii. <u>Temperature range suitability</u>

The continuous energy generation by friction
between the cam and spring made it necessary
to consider the temperature coefficient of the
gauge.

iv. Sensitivity

The gauge sensitivity should be sufficient

to pick up a signal that can be amplified

to a practical value.

To satisfy the above requirements, a half inch long linear
copper-nickel strain gauge (Saunders-Roe No. 720, 325) was chosen.

The gauge can be used under a temperature up to 100°C and
is claimed to be suitable for use with ferrous materials (see
Fig. 7.5-2).

7.5-3. Application of the strain gauge

The preparation of gauge and specimen for mounting and the
correct use of proper adhesive, have considerable bearing on the
accuracy governing the signal from the strain gauges. The strain
in the specimen is transmitted through the adhesive to the strain
gauge and to the associated measuring instruments. Araldite
strain gauge cement was used for bonding. After complete curing
of the cement, the tags of each strain gauge were cleaned and
joined to one arm of a Wheatstone bridge.

A 60Ω resistance was joined to each remaining arm of the bridge (see Appendix 5 for the bridge output signal calculations).

7.6. <u>Mounting and operation of the swept volume pick-up</u>

The spring and the strain gauge wires were fixed in the holder which was secured to the aluminium table.

The cam was mounted on the crankshaft under the spring (see Fig. 7.1), and the flywheel turned until the piston was on T.D.C.; then the cam was adjusted to give maximum spring lift which was indicated by a dial gauge. The cam was secured to the crankshaft at this position.

The formula for the balanced Wheatstone bridge is:

$$\frac{R_2}{R_1} = \frac{R_3}{R_4} \quad \text{(see Fig. 7.6)}$$

When the cam lift is zero (at B.D.C.), R_2 equals R_3; hence the bridge is balanced giving zero output.

As the crankshaft (and hence the cam) are rotated, the spring starts to deflect upwards causing positive strain and increasing resistance of the lower gauge, but an equally negative strain and

To horizontal deflection Plates

CRO Screen

Bridge output E_g

WHEATSTONE BRIDGE

B_1

R_3

i_2 i_1

$60\,\Omega$ R_4

A

B

R_2

$60\,\Omega$ R_1

i_2 i_1

A_1

C

E_b

$12V$

Double - Driver amplifier

To vertical deflection Plates

Charge amplifier

Pressure Transducer

Engine
Steel spring
Strain gauge

A_1 ? To
B_1 ?
Wheatstone bridge arms

Cam
Crankshaft.
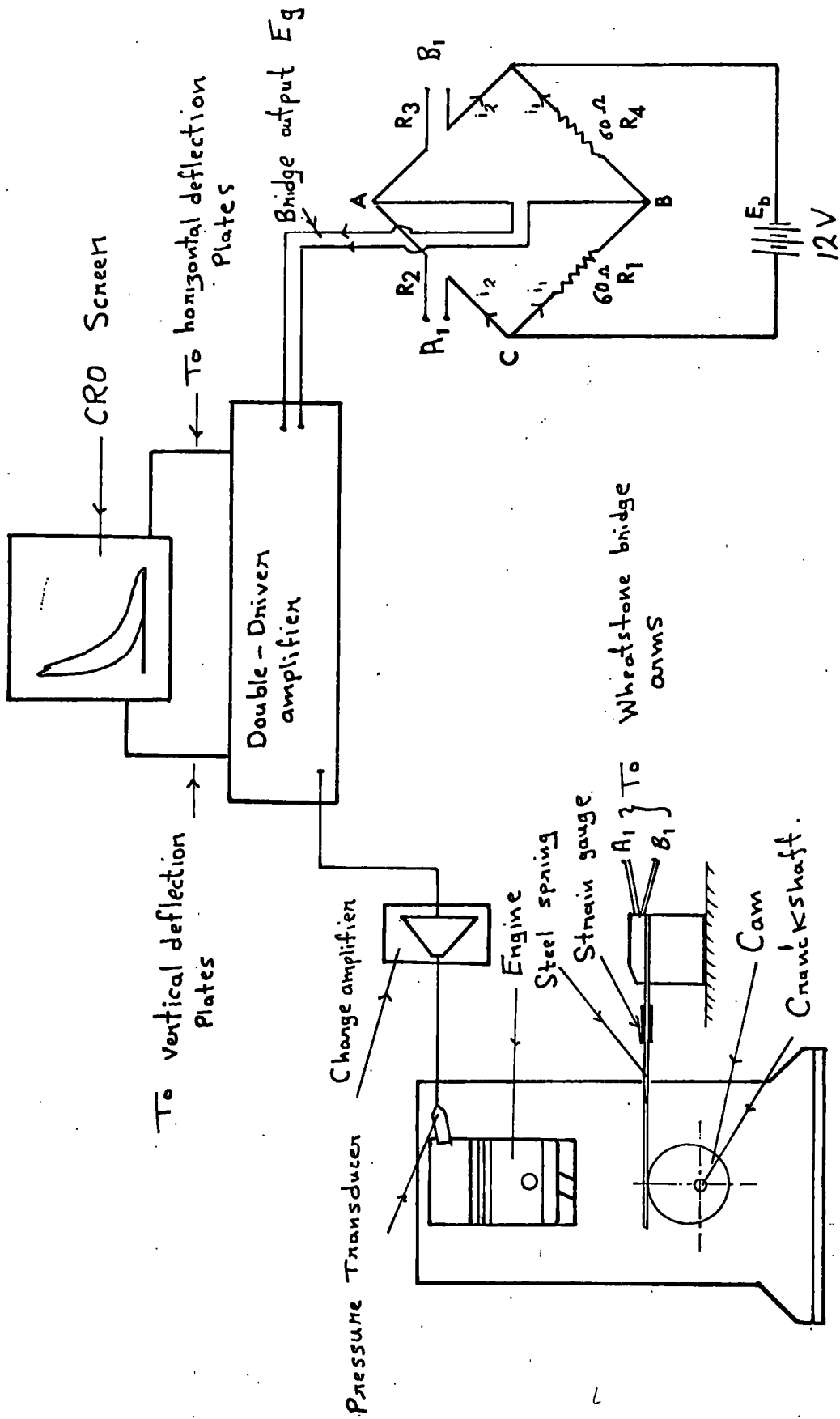
FIG 7.6

Diagrammatic representation of the principle used to produce a P-V diagram

decreasing resistance of the upper gauge. This upsets the bridge balance giving an output signal between the terminals AB. This signal is proportional to the cam lift and, consequently, to the engine swept volume. The output from the Wheatstone bridge was amplified one hundred times by a fixed gain 12 volt amplifier.

The signal from this amplifier was fed to one channel of the M.R.E. 141 recording unit; and thus the pressure and volume signal combined to move one beam of the oscilloscope to produce a P-V diagram on the screen (see Fig. 7.7-2).

As stated previously (7.3), some modification had to be made to improve the strain gauge signal. Although a great improvement was achieved, there still remained some source of signal distortion caused by the natural oscillations of the spring. A brass cylinder was mounted on the spring, above the crankshaft (Fig. 7.3).

This provided satisfactory results for damping out the spring vibration, thus providing a better signal and this modification gave very satisfactory results.

7.7. Single frame photgraphy

To make use of the P-V diagram, a permanent record of the signal was required. Photographs record a wide range of information that can be obtained from the engine running under varying sets of conditions. The individual sets may be used for comparison and calculation of engine output. The M.R.E. 141 recording unit incorporates three modes of photgraphic recording which are:

(i)   Drum recording

(ii) Continuous feed recording

(iii) Single frame recording

Originally drum recording had been in use for photographing P-T diagrams where only the pressure signal was triggered and the time-base signal was substituted . · . by the rotation of the drum.

This arrangement is not suitable for recording a P-V diagram where the volume signal cannot be so substituted. Single frame photography was employed for the purpose. The camera drum was removed, and a frame feed unit (Fig. 7.8-1) was assembled in its place.

To trigger the signal electronically, the cam was provided with a steel insert which passes a magnetic pick-up when the

piston is at B.D.C. This induced a pulse which was fed to the
M.R. 525B marker amplifier. This sharply defines and shapes the
pulse so that it can be used for external triggering. The signal
was fed to the Synch. 1 Terminal of the Record Control Panel and
used to switch off the oscilloscope beam. Photographs were taken
at different engine speeds, and these showed that the exposure
timing was not enough to trigger the complete diagram; also the
beam trigger was not provided with a 'duration' control that could
extinguish the beam for a predetermined time. Using manual
triggering the beam duration time was controlled directly by the
beam switch. The duration and brilliancy setting of the beam
for providing a sharp record was found by trial and error. This
method provided better results and a complete P-V diagram was
triggered (Fig. 7.7-2).

Although the P-V indicator discussed gave reasonable results,
the photographic record was not large enough for accurate cali-
bration particularly when measuring the area under the P-V loop
for the indicated-horse-power calculations. No dynamic pressure
calibration curves were provided for the pressure transducers used
with the indicator, and thus the use of the device was confined
with observation on the C.R.O. screen. Consequently combustion
investigations were restricted to P-T diagrams (Chapter 8).
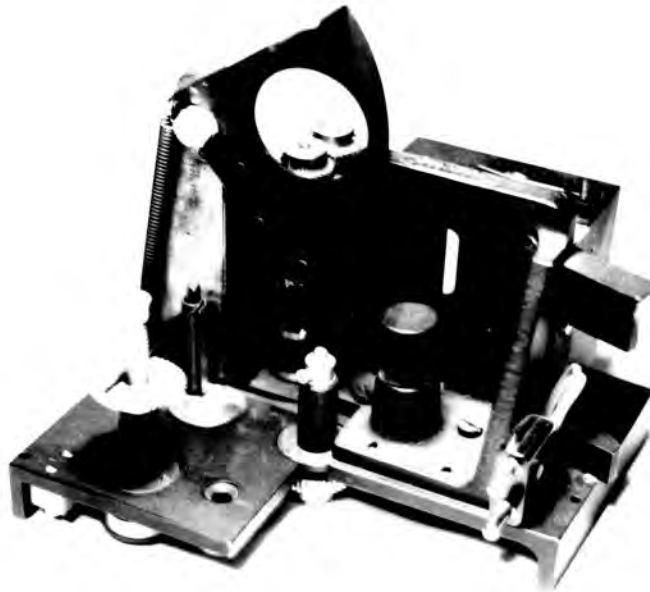
FIG. 7.7-1. Frame feed attachment of the M.R.E. 141 Recording unit

FIG. 7.7-2. Pressure-Volume diagram

8. THE USE OF PIEZO-ELECTRIC PRESSURE TRANSDUCERS IN DIESEL
    COMBUSTION INVESTIGATIONS

8.1. General

Pressure-Time diagrams may be used for examining the
combustion processes in reciprocating combustion engines. The
important part of the cycle is that around top-dead-centre and
can be produced to a larger scale on a P-T diagram than on a P-V
diagram. If the angular velocity of the crank is assumed to be
uniform, then the base of the P-T diagram may represent crank
angle.

In order to assist the discussion, the following terms
which are illustrated in Fig. 8.1-1 are defined.

1. Injection period

    The time elapsed between the start and stop
    of the fuel spray into the combustion chamber.

2. Delay period

    The time between the start of injection and
    first appearance of $\wedge$ increase in pressure
    in the combustion chamber.

3. Delay angle

    Crank angle corresponding to the delay period.
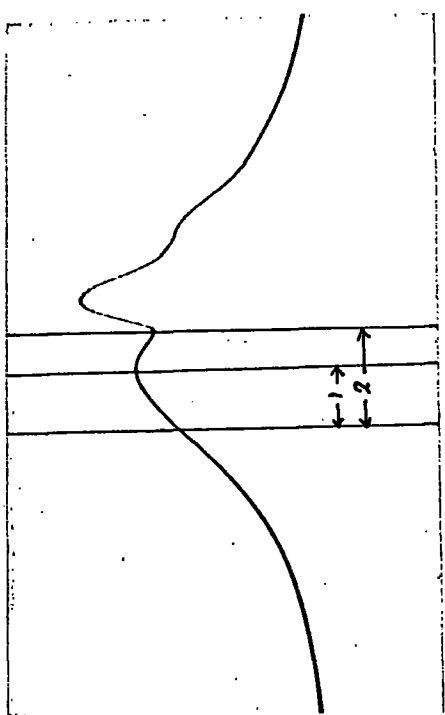
FIG. 8.1-1.
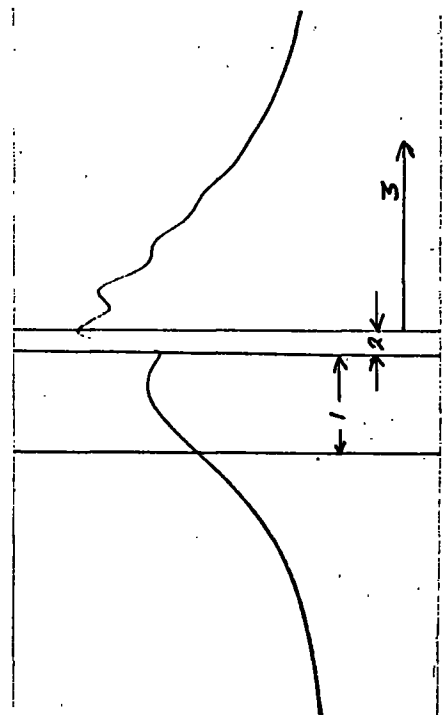
FIG. 8.1-2.
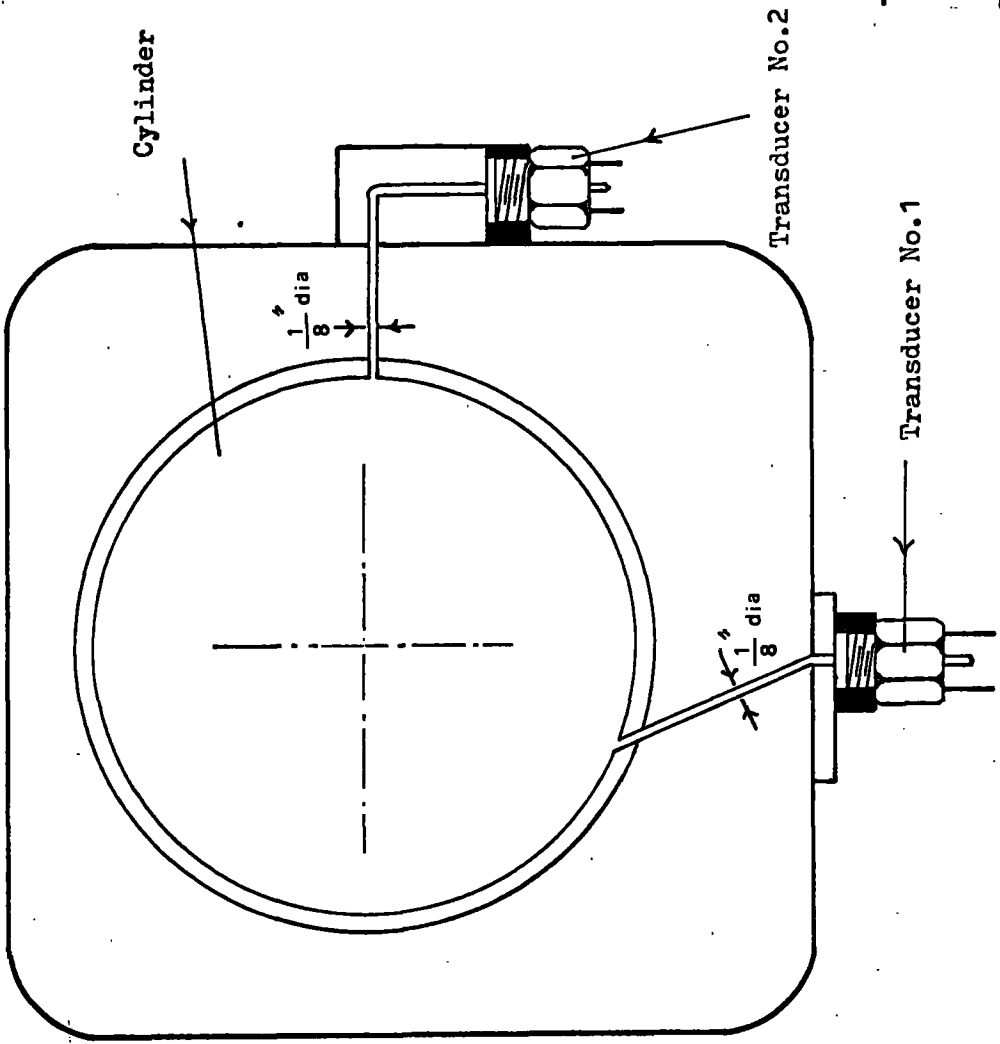
FIG. 8.5. Diagrammatic illustration of the two transducer positions in the engine cylinder.

-104-

Only the variations of the delay angle and the delay period could be observed on the P-T records; no physical values for these two variables or the injection period could be obtained from the engine as the fuel injector was not fitted with a transducer.

The combustion process is divided into three main stages:

1. Delay period (first stage).

2. Period of Rapid Combustion (second stage).

3. Third stage of combustion.

During the delay period, some of the evaporated and finally divided fuel mixes with air. There is then a short time period when chemical reactions take place with no rise in pressure, but once ignition has occurred, the fuel tends to burn very rapidly owing to the high temperature of the compressed gases (about $1500^{\circ}R$) in the combustion chamber. This is termed the period of rapid combustion. After this period, the fuel which has not yet burnt, together with any other subsequently injected fuel, burns at a rate controlled principally by the diffusion processes between the fuel and oxidant.

Two Kistler transducers No. 44991 and No. 17300 were employed to measure the cylinder and combustion chamber pressures.

The signal from each transducer was amplified by a Kistler charge amplifier.

In order to avoid overlapping of the P-T diagrams but to use the full range of the recording apparatus on a common record, different recording sensitivities were used for amplifying the signals (see Fig. 8.2.1-1). The upper trace represents the cylinder pressure on each record.

8.2. Effect of speed on diesel combustion

8.2-1. No Load, variable speed

Figures 8.2.1-1, 8.2.1-2 and 8.2.1-3 show the engine running with no load applied, at speeds of 500, 1000 and 1500 r.p.m. respectively and a constant compression ratio of 19.1:1. A fall of maximum pressure had occurred in the cylinder and combustion chamber as the speed was increased. At the time of fuel injection, since the temperature and pressure of the cylinder are both high, some chemical reactions occur so slowly that the actual combustion, normally appearing first as a visible flame or as a measurable pressure rise, occurs only after a delay; this includes a period when the temperature of the fuel droplets increases before any chemical reaction takes place.

Each droplet is surrounded by vapour immediately after entering the combustion chamber. The combustion flame starts in the vapour arround the drop surfaces after a delay. The combustion rate of fuel droplets in air is limited by their rate of evaporation. The delay time seems to be independent of engine speed, which means that for the above observations to be true the delay angle should vary with speed; hence the speed has a large effect on diesel combustion.

When the delay angle is too large, the period of rapid combustion occurs during the later stage of the expansion process (see Fig. 8.2.1-3); this decreases the peak pressure of the cycle. The shortest delay angle was obtained at a speed of 1000 r.p.m. (see Fig. 8.2.1-2) where the period of rapid combustion occurred approximately at T.D.C., however the P-T record shows that the rapid pressure-rise in the combustion chamber due to the second stage of combustion is comparatively low, showing a relatively poor rate of reaction. The combustion of the remaining fuel in the cylinder appears to have occurred in two stages; this might be due to the distribution of oxygen that is mixed with the products of the initial combustion, or due to the effect of transducer passage.

C.R.   19.1:1
Speed   600 r.p.m.
No Load
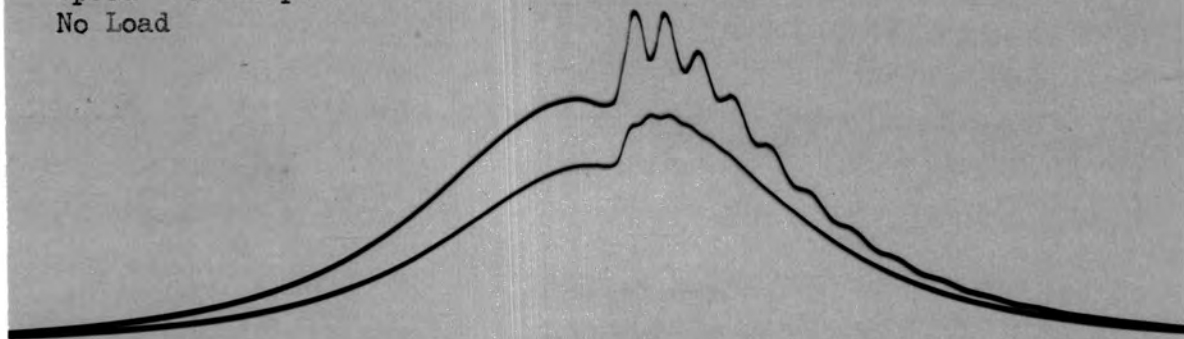
FIG. 8.2.1-1

C.R.   19.1:1
Speed   1000 r.p.m.
No Load
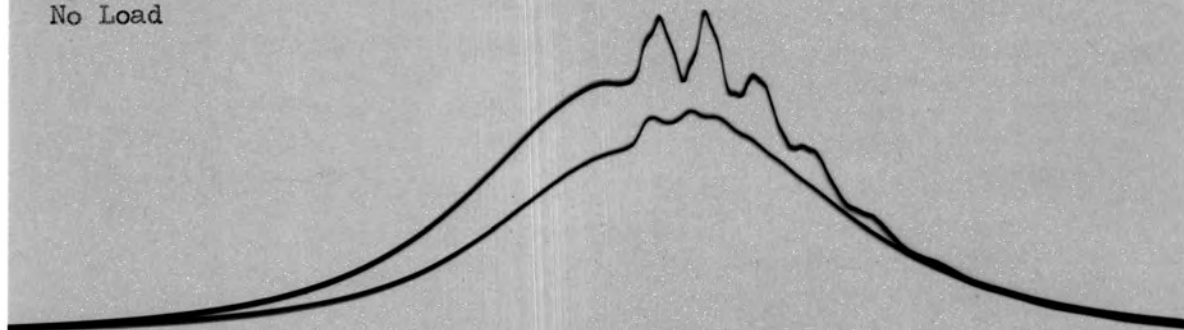
FIG. 8.2.1-2

C.R.   19.1:1
Speed   1500 r.p.m.
No Load
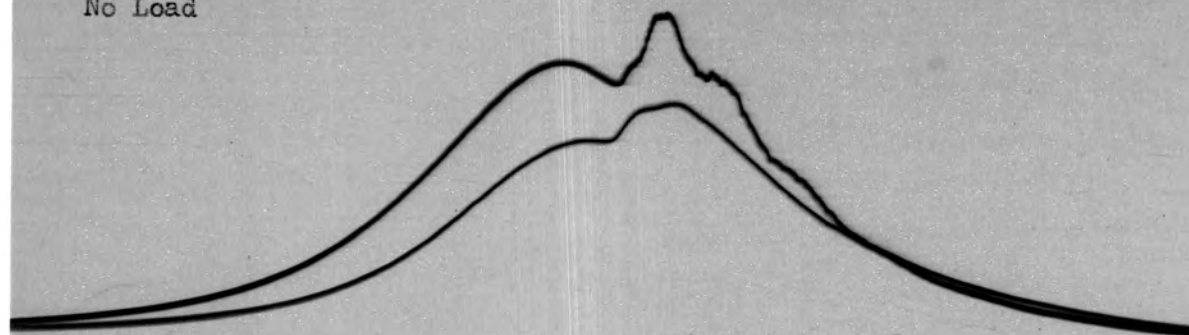
FIG. 8.2.1-3

At the three engine speeds, the records show that the
delay period for the combustion in the chamber is smaller than
the corresponding delay period for the combustion in the cylinder.
This is mainly caused by the narrow passage linking the combustion
chamber to the cylinder, which delays the rapid transmission of
pressure-rise from the chamber to the cylinder and also prevents
the introduction of the required amount of fuel to the cylinder
during injection; thus before the start of any combustion, the
mixture in the cylinder is weaker than the mixture in the combustion
chamber. This presents relatively better conditions for the
combustion in the chamber than for the combustion in the cylinder.

8.2.2. Full load, variable speed

P-T records obtained from the engine running at speeds of
600, 1000 and 1300 r.p.m., are represented by Figures 8.2.2-1,
8.2.2-2 and 8.2.2-3 respectively;   showing significantly
different characteristics from the corresponding records for
no load. The records show that for full load the peak pressure
of the cycle in both the cylinder and combustion chamber increased
with rising speed; also the delay periods were shorter than
the corresponding periods obtained for the no load condition.

C.R.　　19.1:1
Speed　600 r.p.m.
Full Load

FIG. 8.2.2-1

C.R.　　19.1:1
Speed　1000 r.p.m.
Full Load

FIG. 8.2.2-2

C.R.　　19.1:1
Speed　1300 r.p.m.
Full Load

FIG. 8.2.2-3
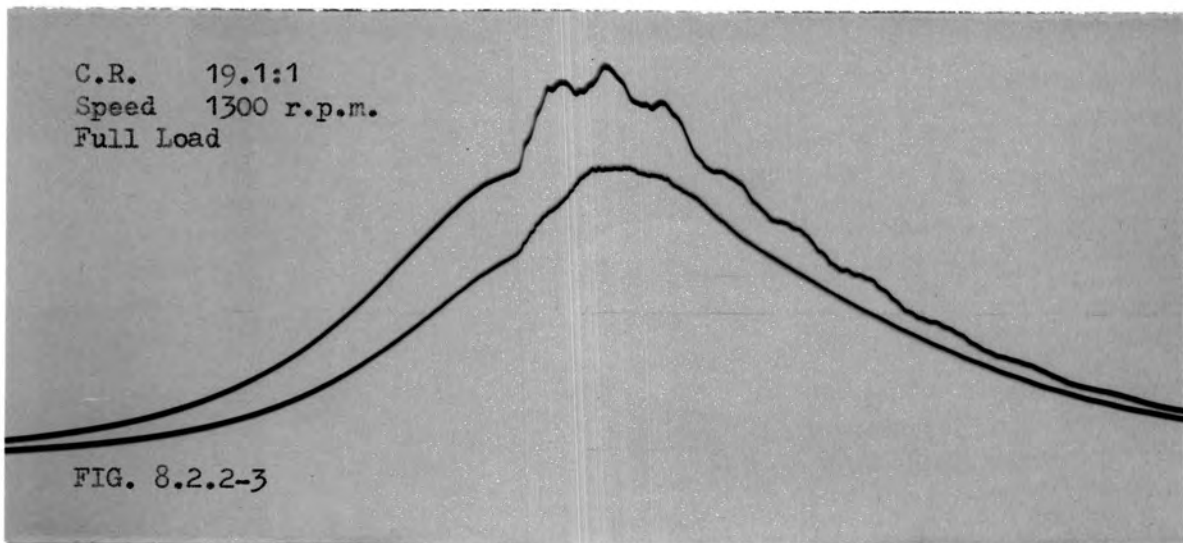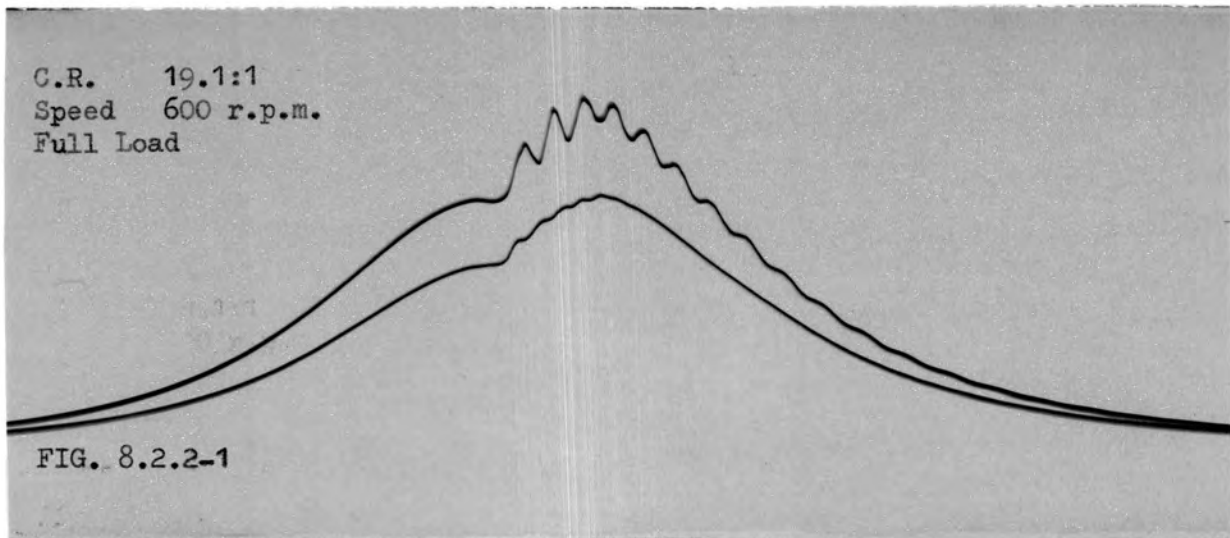
This phenomenon is mainly related to the greater quantity of fuel injected which results in a higher temperature inside the cylinder and combustion chamber at full load which in turn speeds the mixture reaction and increases the evaporation rate of fuel droplets.

As the engine speed is increased, the heat transfer from the charge to the walls of the camber, passage and cylinder during each individual cycle is decreased, consequently higher charge temperature is obtained. The turbulence of the charge is increased with increasing engine speed, thus improving fuel evaporation and oxygen distribution.

8.3. Effect of Compression Ratio on diesel combustion

8.3-1. No load, variable compression ratio

Figures 8.3.1-1, 8.3.1-2 and 8.3.1-3 represent P-T diagrams for the engine running at compression ratios of 15.9:1, 17.8:1 and 20.3:1 respectively; engine speed was kept constant at 1000 r.p.m.

The diagrams show for no load condition that the peak pressure of the cycle is increased with increase in compression ratio; this is because for a constant speed the mixture turbulence is little affected by varying the compression ratio. However, the temperature of the compressed charge is higher at the higher compression ratio,

C.R. 15.9:1
Speed 1000 r.p.m.
No Load
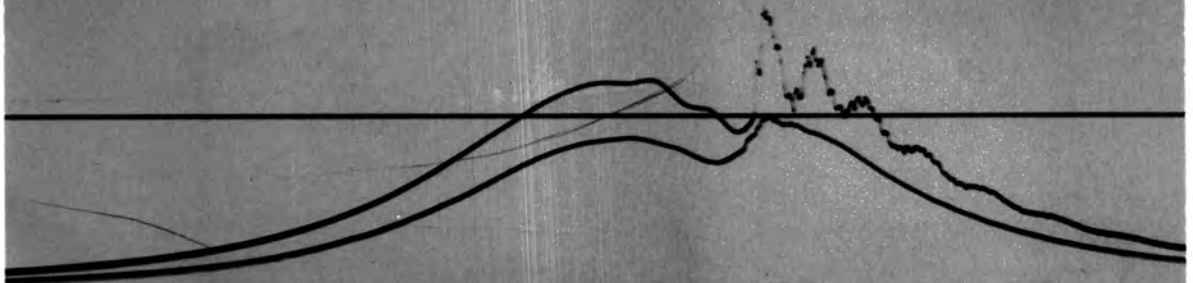
FIG. 8.3.1-1

C.R. 17.8:1
Speed 1000 r.p.m.
No Load
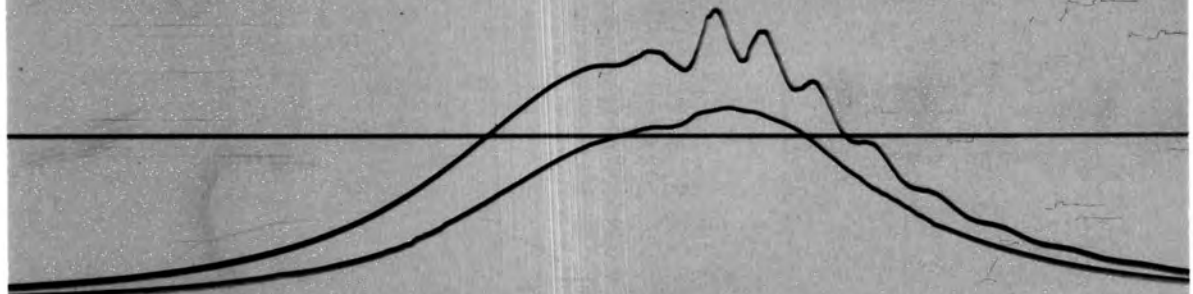
FIG. 8.3.1-2

C.R. 20.3:1
Speed 1000 r.p.m.
No Load

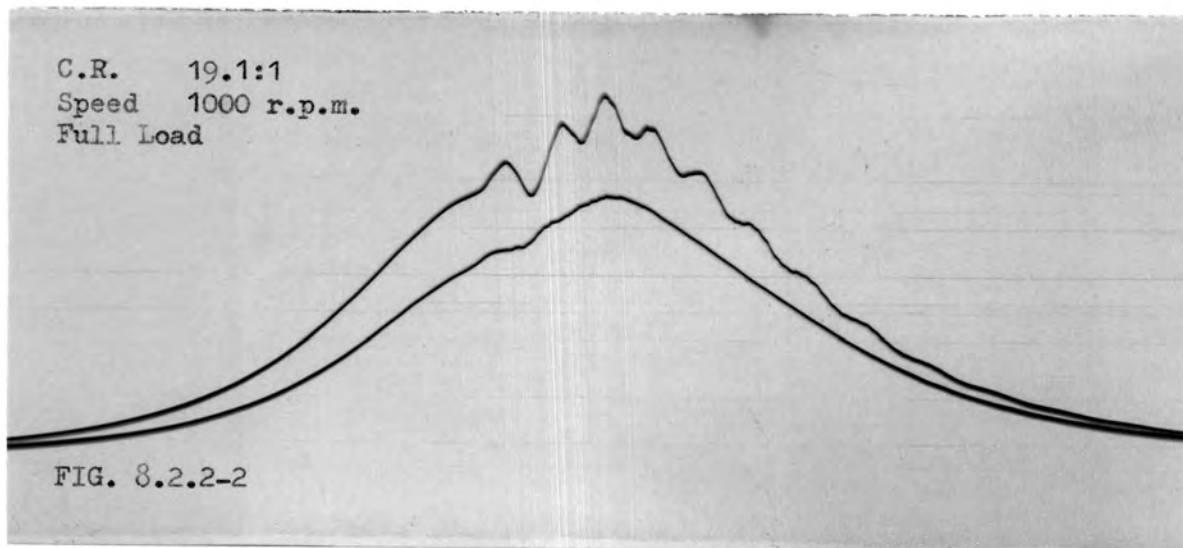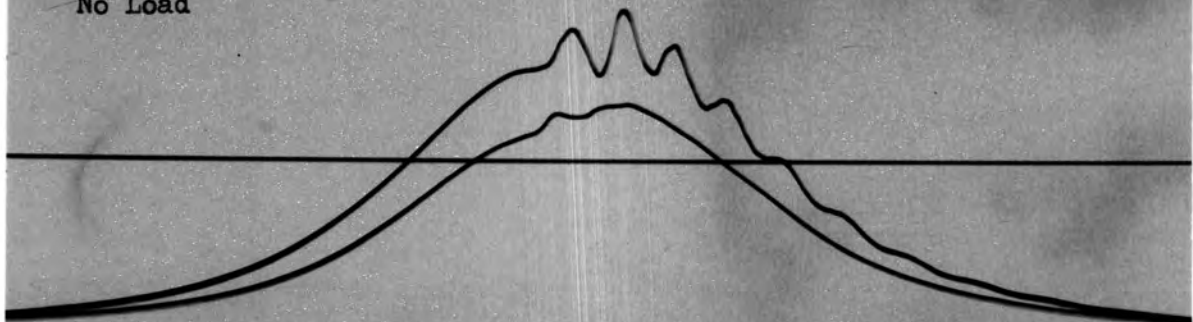FIG. 8.3.1-3

providing more rapid evaporation and combustion of the fuel drop-
lets injected into the combustion chamber. This is indicated on
the diagrams by the decrease in the delay period at the higher
values of compression ratios. The diagrams also show that the
decrease in compression ratio increases the tendency for diesel
knock which was observed at a compression ratio of 15.9 (see
Fig. 8.3.1-1) as an intense reaction and pressure rise produced
well away from T.D.C. This is indicated by the pressure traces
for the combustion chamber and cylinder. The effect of this was
to produce intense vibration in the cylinder walls.

Miller[2] has observed the injection and combustion of fuel
in diesel engines, recorded through glass windows mounted in the
cylinder head. For detonating conditions, the reaction time of
the unburnt mixture must be shorter than the time for a normal
flame to travel through the mixture. Draper[3] has investigated the
energy associated with pressure waves due to detonation and their
effect on the engine.

8.3-2. Full load, variable compression ratio

P-T records were obtained at constant engine speed of 1000
r.p.m. and compression ratios of 14.4:1, 17.8:1 and 20.3:1. These
are shown in Figures 8.3.2-1, 8.3.2-2 and 8.3.3-3 respectively.

C.R.   14.4:1
Speed   1000 r.p.m.
Full Load
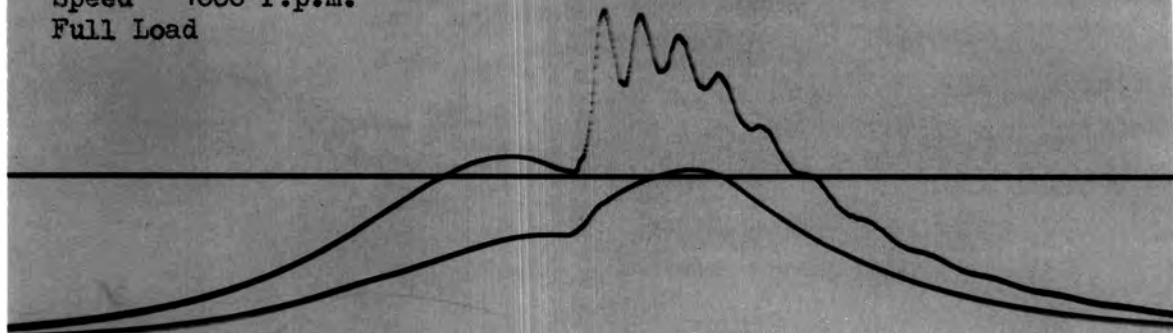
FIG. 8.3.2-1

C.R.   17.8:1
Speed   1000 r.p.m.
Full Load
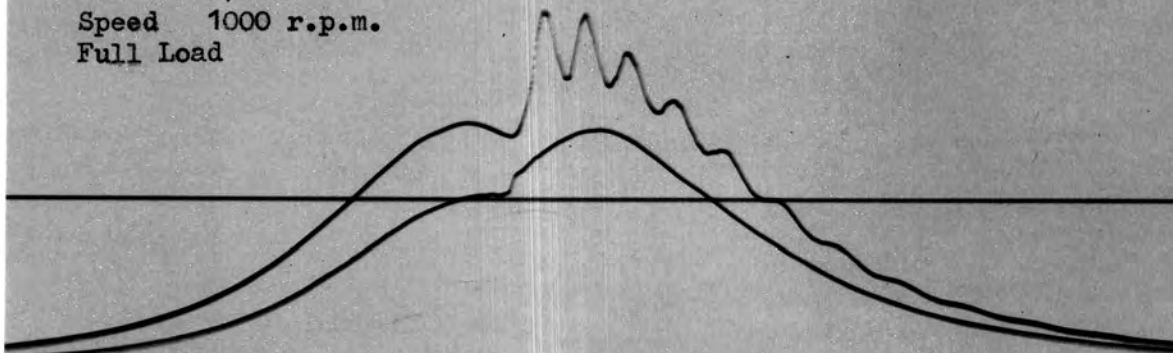
FIG. 8.3.2-2

C.R.   20.3:1
Speed   1000 r.p.m.
Full Load
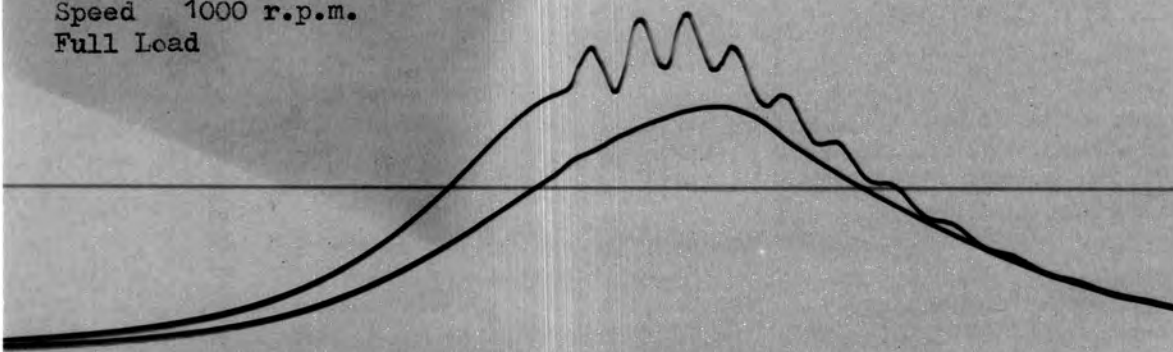
FIG. 8.3.2-3

The records show that the delay angles are smaller than corresponding angles for no load condition, but similar delay period characteristics with respect to varying compression ratio were obtained in both cases.

The records also indicate for a given compression ratio that increasing load decreases tendency for diesel knock. No signs of knocking were observed down to a compression ratio of 14.4:1; increase in load increases the charge temperature which improves the evaporation process; this allows the engine to work at a lower compression-ratio without introducing detonation.

8.4. Pressure fluctuations on the cylinder P-T diagrams

All the P-T traces recorded from the engine cylinder show fluctuations immediately following the stage of rapid pressure-rise. It is suspected that this effect is due to passage effects between the transducer and the charge in the cylinder (see Fig. 8.5). In diesel engines, the rate of pressure rise is very high and this could shock-excite the indicator passage into a damped vibration at its resonant frequency.

For very high rates of pressure rise, the gases in the combustion chamber might be set into vibration; however the flush-

mounted transducer in the combustion chamber showed no such
effect, consequently it is suspected that the pressure fluctua-
tions were effectively related to the indicator passage of the
cylinder.

Nagao[4] has investigated the frequency response of
connecting passages, concluding that in order to minimize the
fluctuating characteristics of pressure indicated through a
passage, the cross-sectional area of this connecting passage must
be made as large as possible so that its resonant frequency is
higher. Withers[5] has studied the effects of indicator passage
resonance on the accuracy of maximum pressure indication and
suggested that the shortest length of the smallest permissible
passage diameter should be used when passage resonance is likely.
This is also to minimize the effect of the passage volume on the
compression ratio.

8.5. Effects of transducer positioning and restriction on cylinder pressure indication

To investigate these effects, two transducers were mounted
at different positions in the engine cylinder (see Fig. 8.5).
Transducer No. 1 was mounted in a radial position to the cylinder,
the pressure to this transducer being transmitted through an $\frac{1}{8}$
inch diameter and 3 inch long passage leading from the transducer

mounting to the cylinder and inclined at an angle of $30°$ to the transducer axis. Transducer No. 2 was mounted in a tangential position to the cylinder; pressure is transmitted to this transducer through an $\frac{1}{8}$ inch diameter and 4.2 inch long passage directed to the centre of the cylinder.

At a compression ratio of 20.3:1, P-T diagrams were recorded at engine speeds of 600, 1000 and 1500 r.p.m., which are represented by Figures 8.5-1, 8.5-2 and 8.5-3 respectively. Further records were obtained at engine speeds of 1000 r.p.m. and compression ratios of 17.8:1 and 15.9:1, which are represented by Figures 8.5-4 and 8.5-5 respectively. These diagrams show the transducer No. 1 trace on the left while transducer No. 2 is shown on the right.

Generally all records show that transducer No. 2 indicated a comparatively larger delay angle than transducer No. 1. This may be caused by the further distance that a cylinder pressure wave has to travel in order to reach the diaphragm of transducer No. 2.

Considering the period of rapid combustion, the records show that transducer No. 2 indicated a higher pressure rise than transducer No. 1 for all engine speeds and compression ratios. This effect may be related to the passage resonance; the records

C.R. 20.3:1
Speed 600 r.p.m.
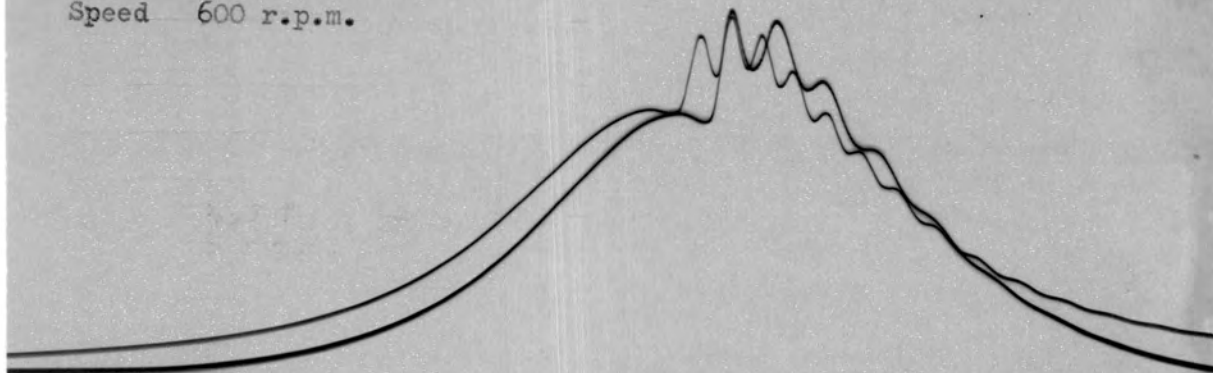
FIG. 8.5-1

C.R. 20.3:1
Speed 1000 r.p.m.
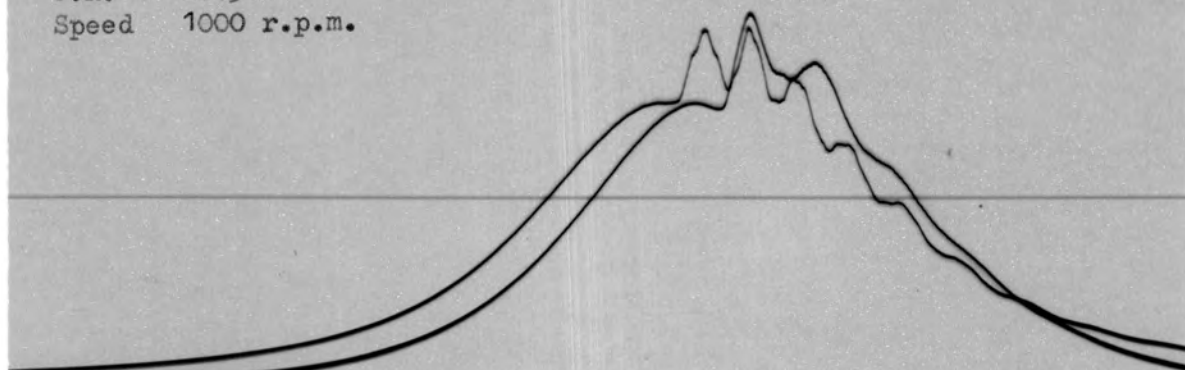
FIG. 8.5-2

C.R. 20.3:1
Speed 1500 r.p.m.
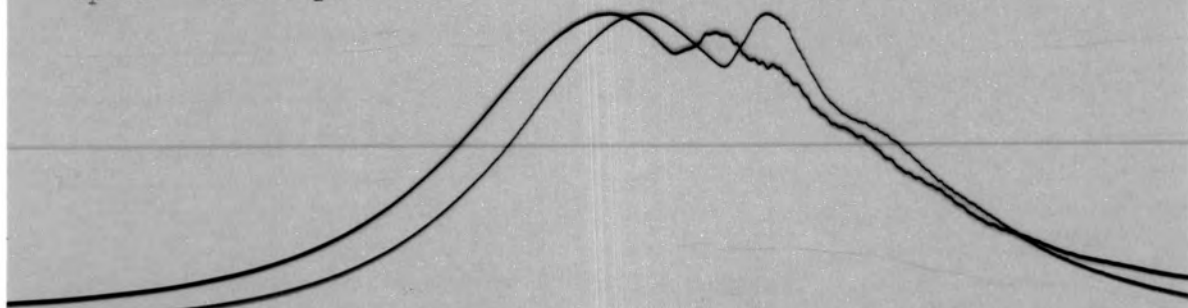
FIG. 8.5-3

C.R.   17.8:1
Speed   1000 r.p.m.
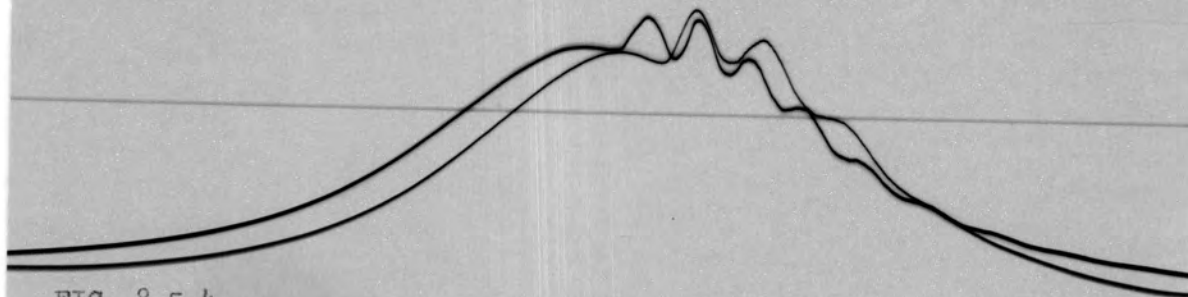
FIG. 8.5-4

C.R.   15.9:1
Speed   1000 r.p.m.
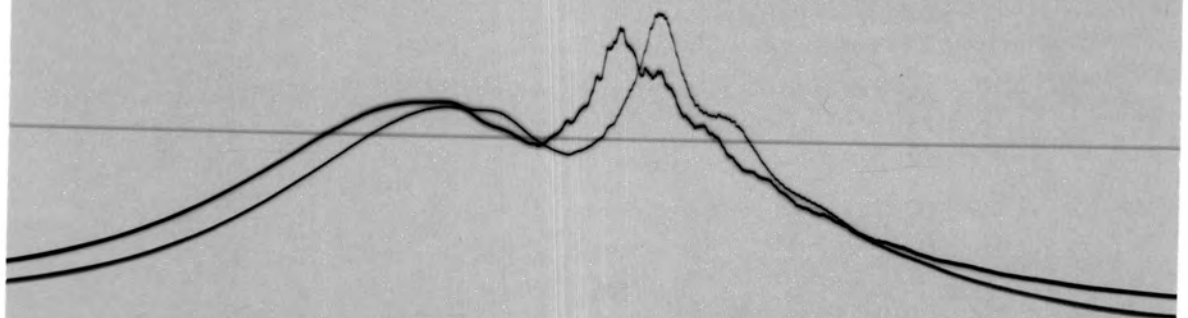
FIG. 8.5-5

indicated that the shorter passage of transducer No. 1 was resonating at a higher frequency than the second passage and it seems that the higher passage frequency has a greater effect on damping the pressure transmission through the passage.

At a compression ratio of 15.9:1, Fig. 8.5-5 shows diesel knock characteristics. The small pressure waves accompanying the rapid pressure rise are not clearly indicated by transducer No. 2 owing to complete damping of such waves before reaching the transducer diaphragm.

8.6. Conclusions about the combustion process

Considering the combustion process inside the swirl-type combustion chamber, generally better combustion is observed on the P-T records as the compression ratio is increased.

In order to obtain rapid and complete combustion, a high relative velocity between the air and fuel droplets is necessary. When the engine is working at the maximum compression ratio, the shape of the combustion chamber is spherical, providing a good efficiency of swirl during the compression process and, together with the higher compression temperature at this compression ratio, good distribution and atomization of the fuel during injection, all of which amount to satisfactory combustion. However, decreasing

the compression-ratio decreases the compression temperature and also changes the shape of the combustion chamber (see Section 2.1) thus reducing the efficiency of swirl.

Although the operation of Pintle nozzles is very satisfactory for swirl type combustion chambers, the Pintle nozzle is not likely to provide a uniform fuel distribution throughout the elongated combustion chamber (for this particular engine when working at low compression ratio). A Conical-End, Multi-Hole nozzle might give better results.

At full load and constant compression ratio, the peak pressure of the cycle increases with increasing engine speed. This phenomenon limits the design for constructing high speed compression-ignition engines.

The work described in section 8.5 shows that, at the higher rate of pressure rise, the passage frequency has serious effects on indication of the maximum cylinder pressure. Under resonating conditions, the maximum cylinder pressure is underestimated with using the shorter passage whereas the delay period of the combustion of fuel is overestimated with the longer passage used. Regarding the limitation of using the two transducer passages for pressure indication, it may be concluded that transducer No. 1 (see Fig. 8.5) is more suitable for studying the combustion

behaviour in the engine cylinder, while transducer No. 2 is more accurate in indicating the peak pressure of the cycle. The passages of both transducers were working at such high pressure (about 800 p.s.i.) that they were shock-excited, giving a false pressure indication during the power stroke.

9. COMPARISON OF ENGINE VOLUMETRIC EFFICIENCY DETERMINED BY THREE DIFFERENT TECHNIQUES

9.1. General

The volumetric efficiency of an engine is defined as the ratio of the mass of air supplied to the engine during one cycle to the mass of air which would just fill the piston swept volume, at the density in the inlet system.

The volumetric efficiency of the E.6 engine is determined at full throttle by three techniques at engine speeds starting from 1000 r.p.m. and raised in increments of 500 r.p.m. by means of the electric motor driving the engine. This procedure was followed for five different values of engine compression ratio ranging between 5:1 to 7.95:1. These three techniques involved the use of a Kistler transducer (to measure the compression pressure), an Alcock viscous flowmeter (to measure air consumption), and an infra-red gas analyser (to determine the composition of the exhaust gas).

The engine speed was accurately measured by a digital counter.

9.2.   Methods of measurement of volumetric efficiency

9.2.1.   Pressure transducer method

The engine combustion chamber was fitted with a Kistler Piezo-electric pressure transducer to measure the compression pressure of the misfiring engine working at a given speed and compression ratio. The ignition system was arranged so that each firing cycle was consecutively followed by a misfiring cycle; consequently the Pressure-Time diagram obtained on the oscilloscope screen, consisted of both cycles (see Fig. 9.2-1) and measurements of the misfiring compression pressure was taken.

9.2.1-1. Assumptions

Because of the indirect approach involved in measuring volumetric efficiency by the transducer method, certain assumptions had to be made:

1. No appreciable heat transfer from the induction valve and cylinder wall to the charge occurs,

2. the index of compression (n) is assumed to be 1.35 and constant throughout the process (value suggested by Harrow[6]),

3. the temperature of the residual products of
    combustion left in the clearance volume at
    the end of the exhaust stroke is equal to
    that of the cylinder wall,

4. The pressure and temperature of the charge
    at the induction valve are equal to the
    initial pressure and temperature in the cylinder,

5. The effect of valve overlap is negligible.

The inlet cylinder conditions are taken as a reference of
calculating the mass quantities.

For the flowmeter, it is assumed that the change in
atmospheric humidity does not significantly affect the calibration
curves, and for the IRGA that the exhaust gas, after passing
through the furnace, has completely oxidized; and that the amount
of carbon monoxide dissolving in the water vapour which is present
in the exhaust gas is negligible.

The IRGA provides A/F ratio on a dry basis while both the
transducer and flowmeter give values of volumetric efficiency on
a wet basis, it is being assumed that the moisture in the air
has a negligible effect on the accuracy of η_v measurements.
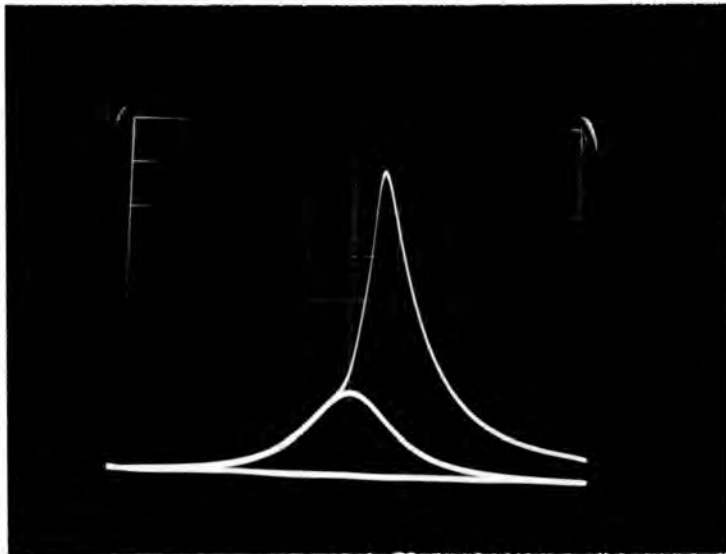
FIG. 9.2.1. P-T diagram showing the firing and
                misfiring cycles super-imposed

When measuring the compression pressure, the volume of the evaporated fuel tends to increase the pressure in the cylinder; however the drop in the charge temperature that is caused by the evaporating fuel is assumed to compensate for this pressure increase.

9.2.2-2. <u>Theory</u>

For the misfiring cycle let:

T : cylinder temperature

T_1: air temperature at inlet to cylinder

T_2: charge temperature at end of compression

P : compression pressure (Gauge)

P_1: inlet pressure to cylinder

m_1: mass of air to fill swept volume at inlet conditions

m_2: mass of air to fill clearance volume at T_2

m_2': mass of residual product to fill clearance volume

m_3: mass of air induced per cycle

n : index of compression (polytropic)

V_1: swept volume

V_2: clearance volume

Total pressure in the cylinder after compression $P_2 = P_1 + P$

For the compression process;

$$\frac{T_2}{T_1} = \left(\frac{P_2}{P_1}\right)^{\frac{n-1}{n}} \qquad T_2 = T_1 \left(\frac{P_2}{P_1}\right)^{\frac{n-1}{n}}$$

also $V_2 = \dfrac{V_1}{\text{compression ratio}}$

using the gas low;

$$P_1 V_1 = m_1 R T_1 \qquad \text{then}$$

$$m_1 = \frac{P_1 V_1}{R T_1} \qquad \text{similarly} \quad m_2 = \frac{P_2 V_2}{R T_2}$$

$$m_2' = \frac{P_1 V_1}{R T}$$

$$m_3 = m_2 - m_2'$$

and (η_V) Volumetric efficiency (transducer) $= \dfrac{m_3}{m_1}$

Calculated example

Barometric pressure $\qquad\qquad\qquad$ = 30 inch Hg

Depression pressure in the inlet system = .118 inch Hg

hence P_1 = 30 - .118

$\quad\quad\quad$ = 29.882 in Hg (1 inch Hg = 0.49 p.s.i.)

$\quad P_1$ = 14.65 p.s.i.

$\quad T_1$ = 75.2°F

$\quad\quad\quad$ = 535.2°R

compression pressure = 180 p.s.i. (Gauge)

$\quad P_2$ = 14.65 + 180

$\quad P_2$ = 194.65 p.s.i.

$$T_2 = T_1 \left(\frac{P_2}{P_1} \right)^{\frac{n-1}{n}}$$

$$= 535.2 \left(\frac{194.65}{14.65} \right)^{\frac{1.35-1}{1.35}}$$

$\quad T_2$ = 1046°R

compression ratio = 7.95, hence -

$$V_2 = \frac{\text{swept volume}}{\text{C.R.}}$$

swept volume = 0.0200 ft^3

- 129 -

$$V_2 = \frac{0.0200}{7.95}$$

$$V_2 = 0.002515 \ ft^3$$

$$P_2 V_2 = m_2 R T_2$$

$$m_2 = \frac{1946.5 \times 144 \times 0.002515}{53.3 \times 1046}$$

$$m_2 = 0.001265 \ lb$$

The temperature T of the residual gas left in the cylinder at the end of the exhaust stroke is assumed qual to the cylinder wall temperature = 80°C or 636°R.

$$m_2' = \frac{14.65 \times 144 \times 0.002515}{53.3 \times 635}$$

$$m_2' = 0.001068 \ lb$$

Hence $\qquad m_3 = 0.001265 - 0.0001068$

$$m_3 = 0.0011085 \ lb$$

and

$$m_1 = \frac{14.65 \times 144 \times 0.0200}{53.3 \times 535.2}$$

$$m_1 = 0.001479 \text{ lb}$$

$$\eta_V \text{ (transducer)} = \frac{m_3}{m_1}$$

$$= \frac{0.0011085}{0.001479}$$

$$\eta_V = 74.9\%$$

9.2.2. <u>Viscous flowmeter method</u>

The engine induction line is fitted with an Alcock viscous flowmeter in which the air passes through a form of honeycomb so that the flow is viscous. The resistance of the element is directly proportional to the air velocity and is measured by means of an inclined manometer. Felt pads are fitted in the manometer connections to damp out fluctuations.

An air filter is fitted to the inlet of the flowmeter. The depression pressure across the filter was measured by a mercury manometer so that pressure corrections could be made when using calibration curves for the meter.

Knowing the atmospheric pressure in the meter and the air temperature which was measured with a thermocouple, direct readings of the air flow (m) in pounds per minute were obtained from the calibration curves for the meter (see Appendix 7).

The mass of air flow per cycle $= m_2$

$$m_2 = \frac{m \times 2}{\text{Engine speed}} \quad \text{(four-stroke engine)}$$

If m_1 is the mass of air to fill the swept volume at induction conditions then:

$$\eta_V \text{ (by meter)} = \frac{m_2}{m_1}$$

m_1 is found as in 9.2-1.

9.2.3. Infra Red gas analysis method

Fig. 9.2.3-1 illustrates the operation of the Luft and Grubb-Parsons type of analyser (see Fig. 9.2.3-2). Radiation from the nichrome heater A, is reflected into absorption tubes B B and then through to absorbing vessels C C which are filled with the gas to be detected. A rotating shutter S allows infra-red light to pass intermittently and simultaneously through the tubes B and a heating effect is produced in each of the receiver chambers C. These
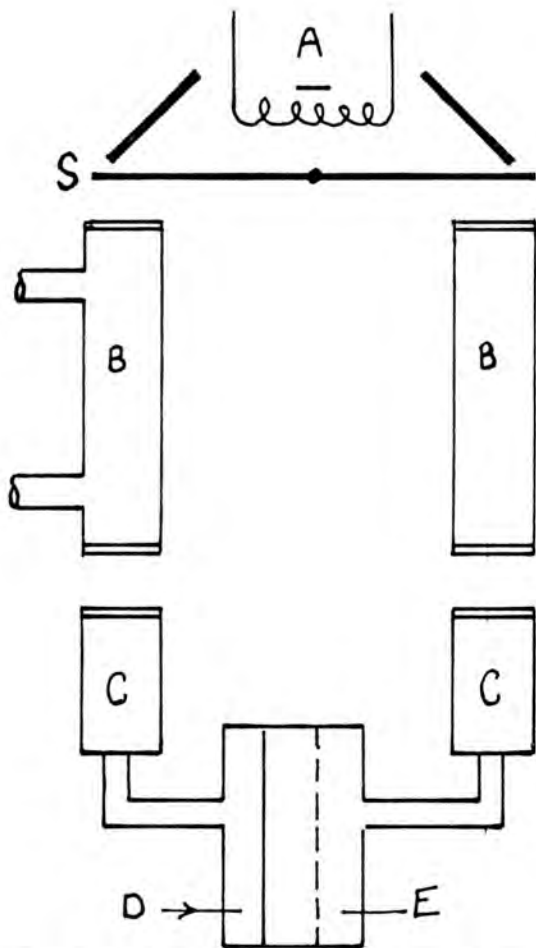
FIG. 9.2.3-1. Illustration of the Infra-Red gas analyser operation

FIG. 9.2.3-2. The Luft and Grubb-Parsons analyser
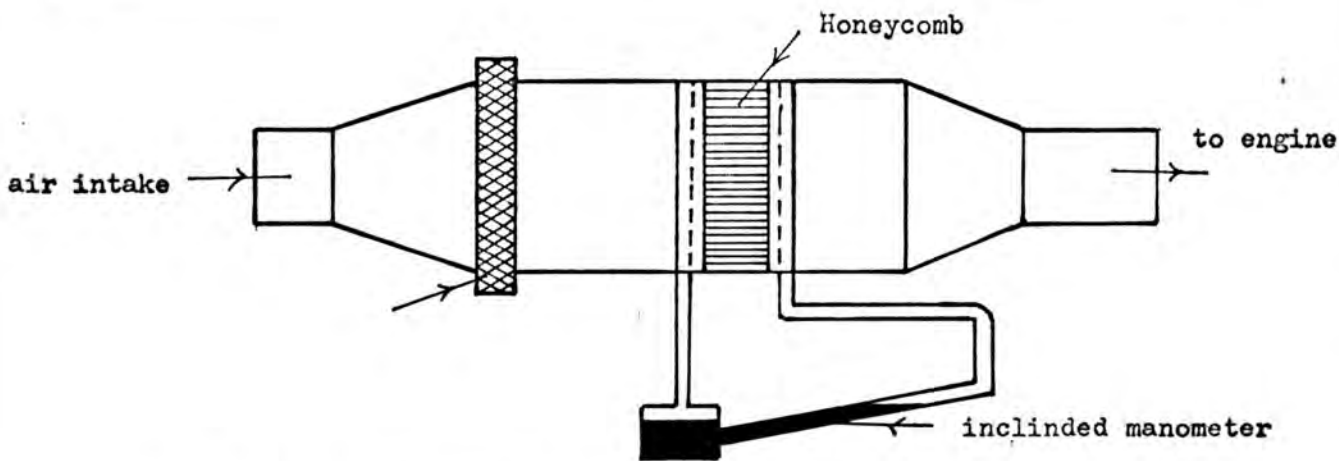
FIG. 9.2.2. Diagrammatic illustration of the Alcock viscous flowmeter

receivers are separated by a thin metal diaphragm D which, in combination with the closely adjacent insulated and perforated metal plate E, forms an electrical condenser. Any deformation of the thin diaphragm resulting from a pressure difference between the two chambers causes a variation of this capacity.

If no absorption occurs in the tubes B, the system remains symmetrical and the heating effect in the two receiving chambers will be the same; thus no pressure difference will arise between them.

When the engine exhaust gas is introduced into one of the tubes B the energy balance is upset since radiation is absorbed by the exhaust gas before it can reach C; consequently a pressure difference between the two cells C is set up each time the shutter S permits radiation to pass. The resulting capacity changes are amplified electronically, and a final indication is obtained on the output meter.

The calibration of the IRGA is shown on Graph 9.2.3 and Appendix 9.

Calculated example

At an engine speed of 1008 r.p.m. and inlet pressure of 30.002 inch Hg,

IRGA Calibration

IRGA Meter reading

Actual % CO₂
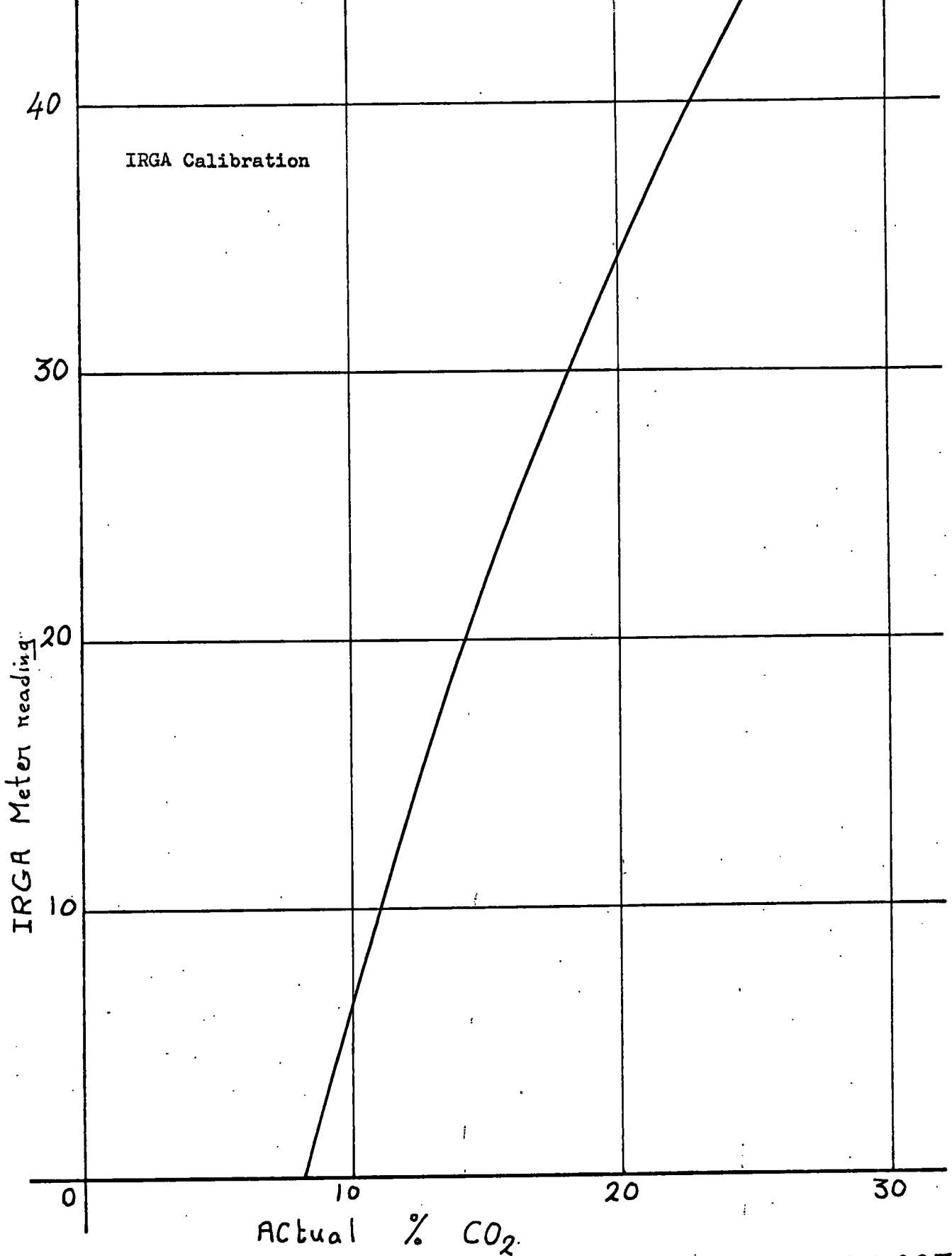
GRAPH 9·23

IRGA meter reading is 27.8

From Graph 9.2.3,

Corresponding % CO_2 in the oxidized

exhaust gas = 17.4%

From calibration tables for the iso-octane fuel

A/F ratio = 12.16

fuel consumption = 98 sec/50 cc.

= 30.6 cc/min.

Specific gravity of fuel = 0.694

Mass of one cubic foot of fuel = 0.694 x 62.5

= 43.4 lb.

Mass of air introduced/cycle =

$$\frac{cc\ fuel/min \times A/F \times 2}{r.p.m. \times (30.5)^3} \times 43.4$$

$$= \frac{30.6 \times 12.16 \times 2}{1008 \times (30.5)^3} \times 43.4$$

= 0.001129 lb

Mass of air to fill swept volume at inlet conditions

= 0.00148 lb

$$\eta_V \text{ (IRGA)} = \frac{0.001129}{0.001478}$$

$$= 76.4\%$$

9.3. Comparison of the Results

The volumetric efficiency of the engine was found by the three different techniques with the engine running at different compression ratios. Graphs 9.4-1, 9.4-2, 9.4-3 and 9.4-5 represent the volumetric efficiency curves obtained by three techniques at engine compression ratios of 79.5:1, 7.22:1, 6.88:1, 5.95:1, 5:1 respectively (see Appendix 6 for results) and engine speeds ranging from 1000 r.p.m. to 2500 r.p.m.

These graphs show that within the experimental error, the volumetric efficiency values obtained by the three techniques are comparable (average difference about 2-3%). All graphs show that the characteristic shape of the η_V curves obtained by the flowmeter and transducer are approximately similar. Generally if the air flowmeter provides an accuracy of about 2% in measuring η_V, then Graphs 9.4-1, 9.4-2, 9.4-3, 9.4-4 and 9.4-5 indicate conclusively that within the assumptions made, the η_V values obtained by the transducer are accurate to an average value of about $\pm 3\%$. The errors were greatest at the engine compression ratio of 7.95:1 and a speed of 2000 r.p.m. (Graph 9.4-1).

Since the measurement of η_V by means of pressure transducers is directly governed by the values of the peak pressure of the misfiring cycle, any quantity affecting the compression pressure will consequently affect the measured value of η_V. The main variables affecting the transducer technique for η_V measurements are:

(a) The heat transfer from the inlet valve and cylinder to the induced fresh charge increases the charge temperature from that corresponding to the inlet conditions, remembering that the η_V calculations are based on inlet conditions.

(b) The heat transfer from the charge to the cylinder wall during compression varies with engine speed, thus slightly altering the value of the polytropic index (n).

(c) The amount and temperature of the residual products left in the cylinder; the temperature of the products vary with engine speed, their mass depends on the final exhaust pressure which also depends on the engine speed.

GRAPH 9.4-1

x Transducer
o Pin flowmeter
▲ IRGA

Compression ratio 7.95 : 1

% Volumetric Efficiency

Engine speed RPM.

- 139 -
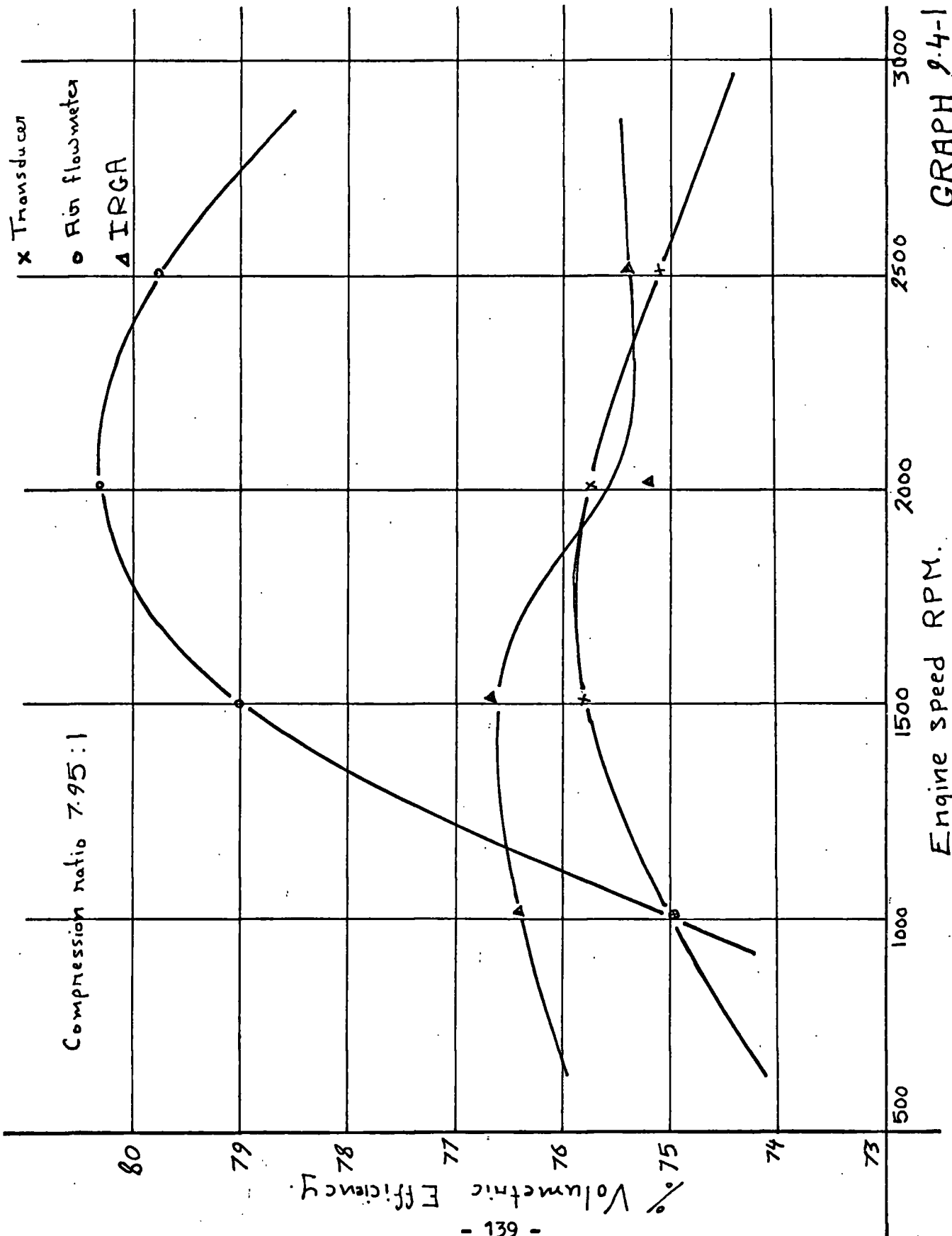
GRAPH 9.4-2

Compression Ratio: 7.22:1

o Air flowmeter
△ IRGA
x Transducer

% Volumetric Efficiency

Engine Speed RPM.
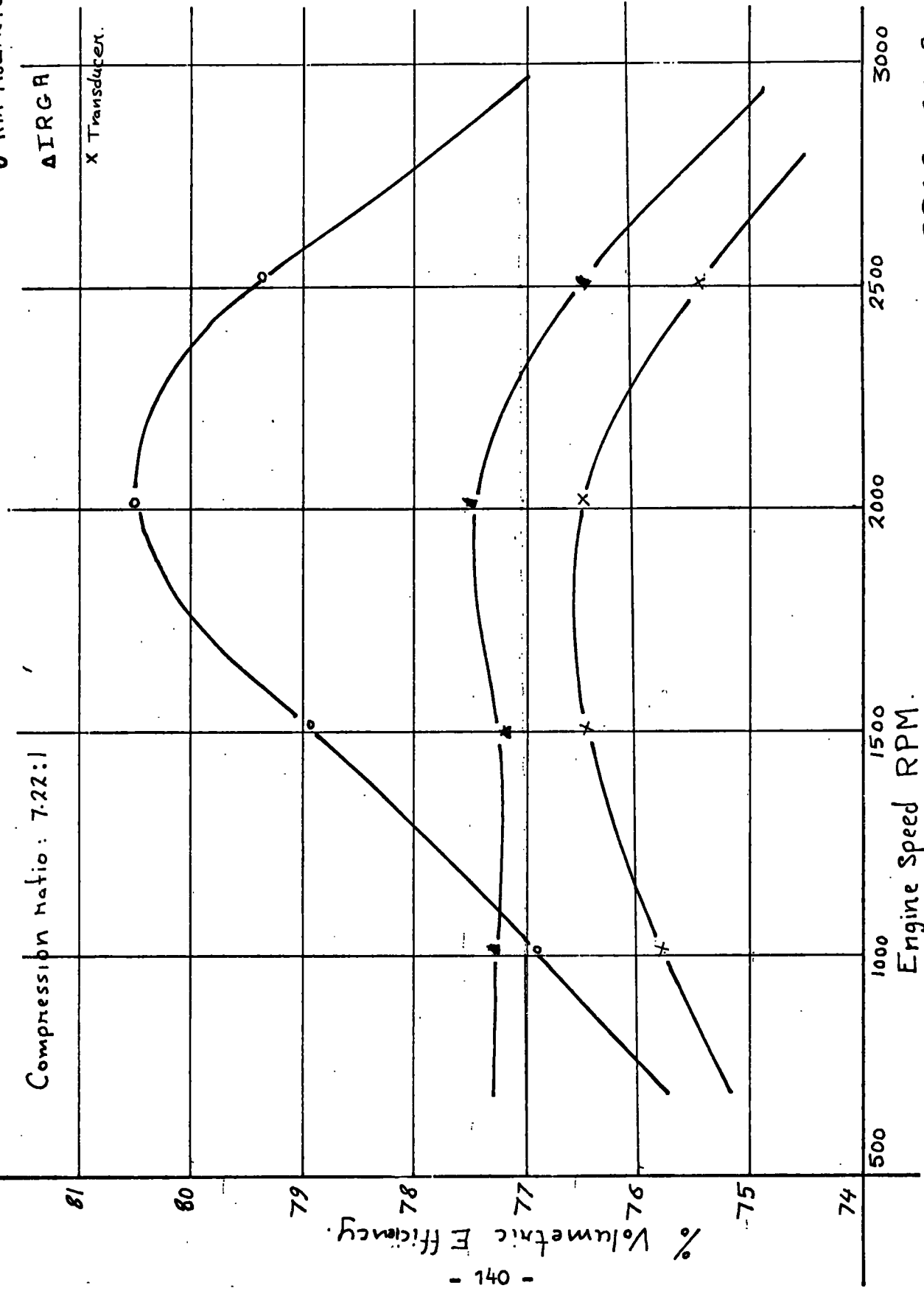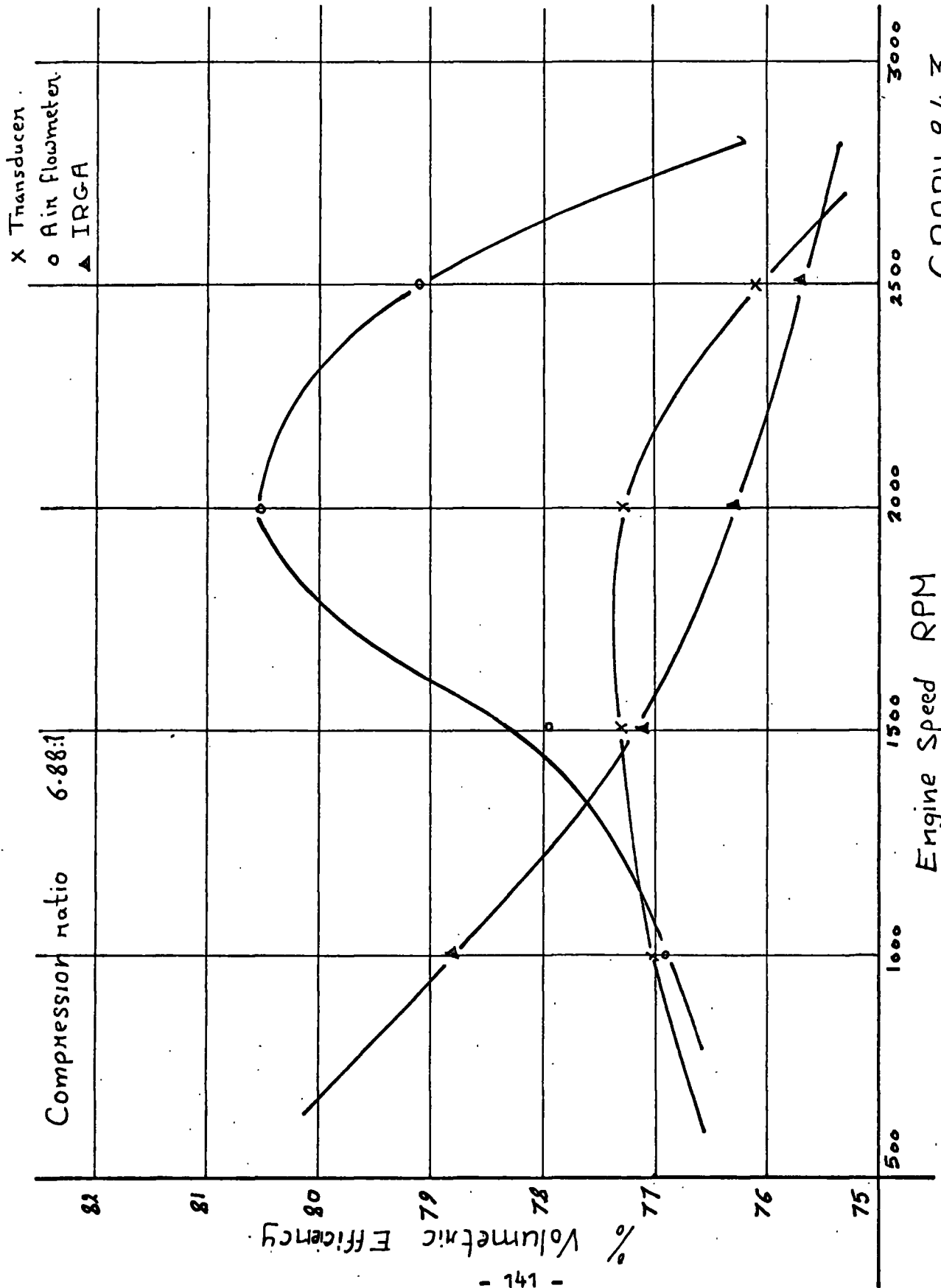
GRAPH 9.4-3

GRAPH 9.4.4.

GRAPH 9.4-5.

Compression ratio 5:1

X Transducer.
● Air Flowmeter.
▲ IRGA.
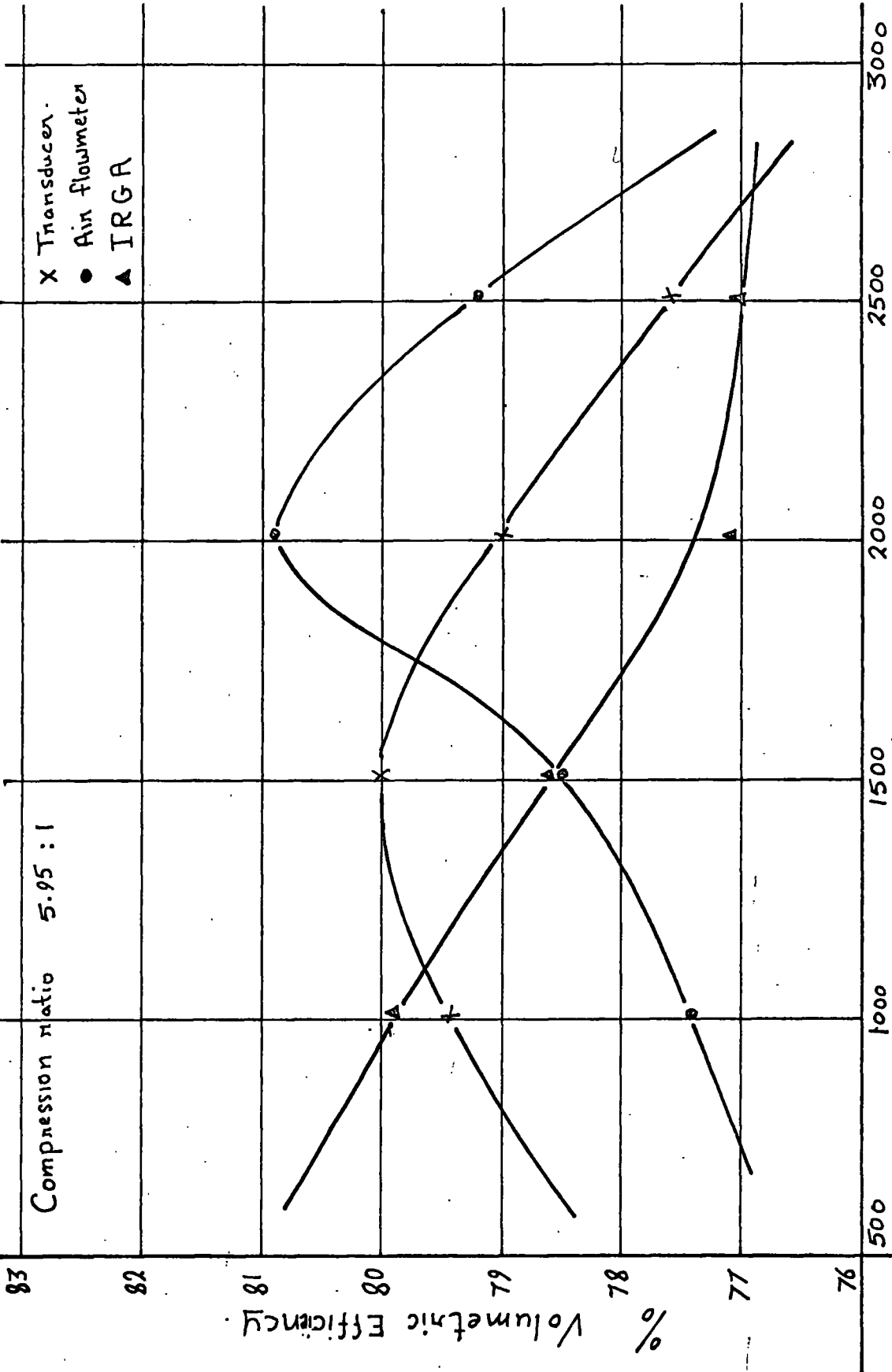
Engine Speed. RPM.

% Volumetric Efficiency.

- 143 -
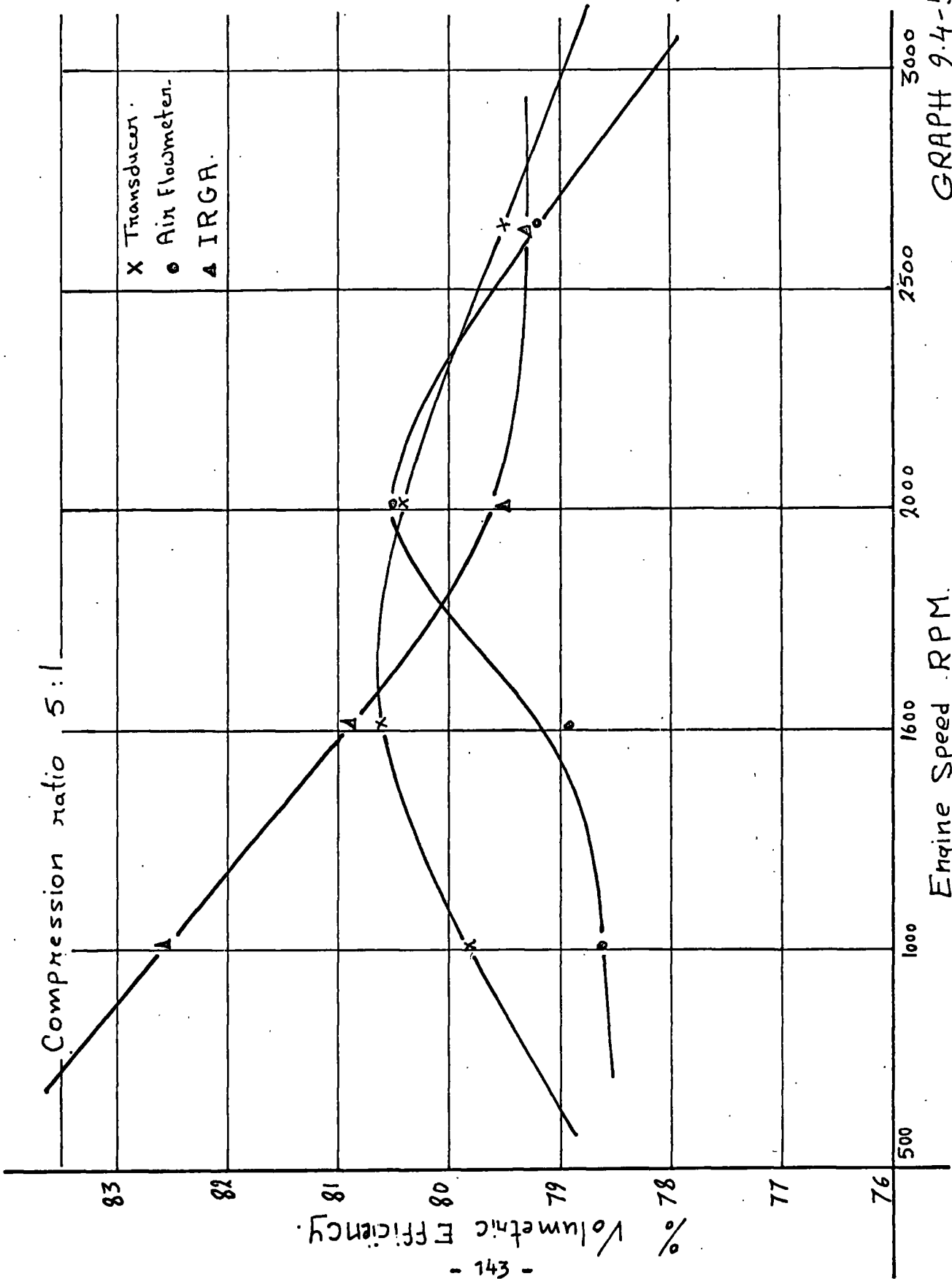
EFFECT OF COMPRESSION RATIO.

GRAPH 9.4.6

Engine Speed RPM.

x Transducer
• Air Flowmeter

% Volumetric Efficiency

5:1   5.95:1   (5:1)   (5.95:1)   (6.88:1)   6.88:1
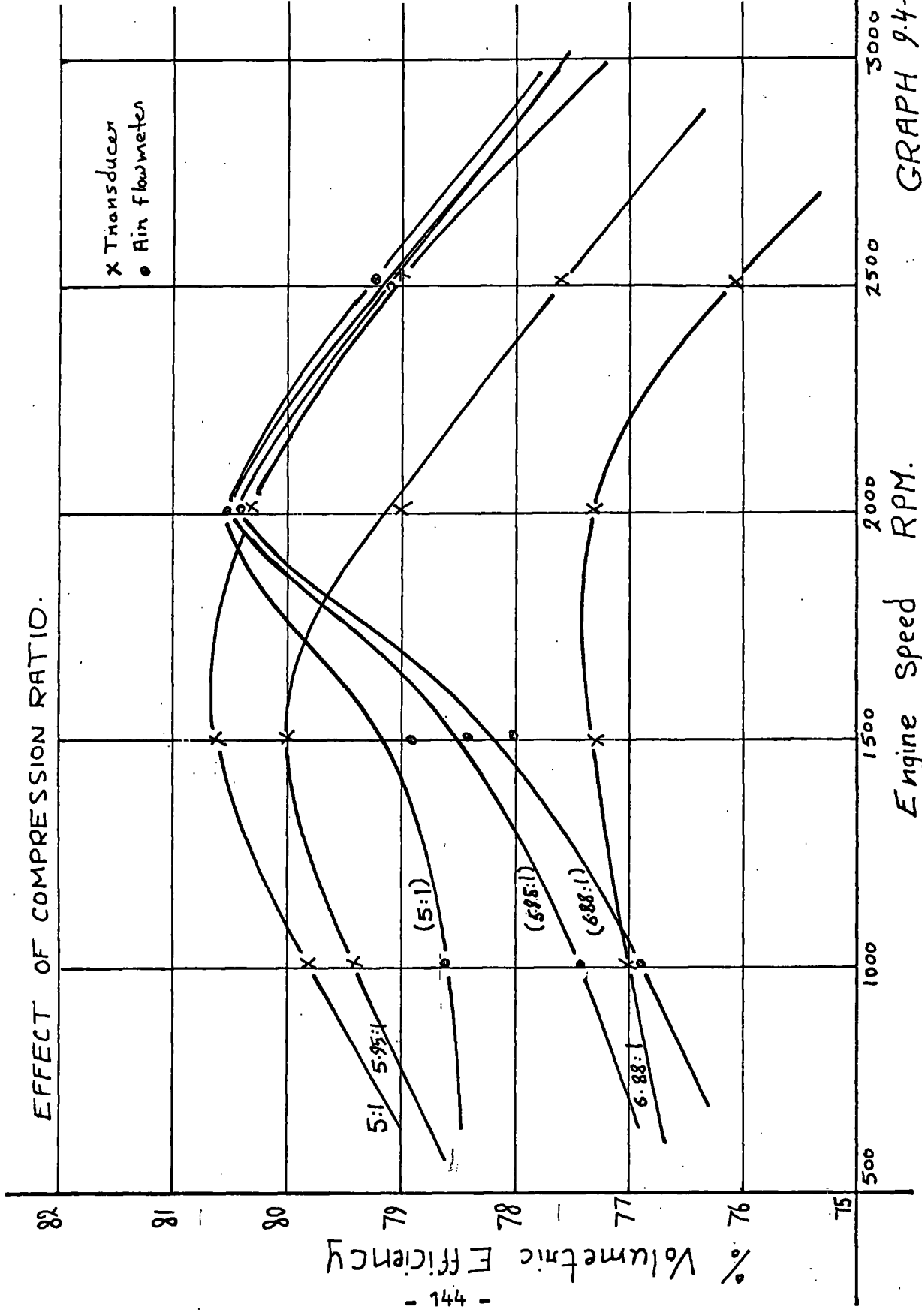
The three techniques generally showed a loss of η_V at the higher engine speeds and compression ratios. Livingood, Rogowski and Taylor[7] have concluded that the pressure losses through the induction valve are considerably higher at the higher engine speeds, which results in a drop of η_V. Graph 9.4-6 shows a loss of η_V at the higher compression ratios and this may be due to the compression temperature being higher at the higher compression ratios; this in turn has the effect of increasing the temperature of the cylinder thus reducing the charge density which amounts to the reduction of η_V.

10.   DISCUSSION AND CONCLUSIONS

10.1.   The Piezo-electric pressure transducers and calibration

The use of Piezo-electric crystals has produced a technique for measurements of various parameters, the transducer often offering clear advantage over other types of transducers.

Much of the development of internal combustion engines depends on the use of indicator diagrams. They give a histogram of the pressure fluctuations which occur within the cylinder. Using different methods, the losses caused by thermodynamic irreversibilities, gaseous energy and mechanical friction may be deduced.

Piezo-electric crystal transducers are generally very satisfactory for all normal uses in internal combustion engines so far as sensitivity and drift are concerned. The engine temperature has no detectable effect on the transducer linearity but it introduces a minor change on the transducer sensitivity. This defect can be eliminated by calibration.

For pressure measurements, the transducer is positioned directly in the cylinder head or cylinder wall because of passage effects which may occur between transducer and reacting gases. (It may also be used to measure the injection pressure immediately in

front of the nozzle holder of diesel engines).

This work shows that for Piezo-electric pressure transducers:

(i) Under static calibration conditions, the sensitivities of the transducers examined are not affected by temperature.

(ii) For the dynamic pressure calibration using the balanced-disc pressure pick-up as a reference, satisfactory results were obtained up to the maximum engine speed of 2750 r.p.m.

(iii) The effect of increasing engine speed is to change the calibration for the Kistler transducer. For the AVL transducer, the sensitivity varies with both engine speed and input pressure. Hence the Kistler transducer is likely to give more satisfactory results.

(iv) The effect of temperature during dynamic operation on the Kistler and AVL transducers is to reduce sensitivity. The AVL transducer was least affected.

(v)   The physical response of the transducer
examined at low pressures can cause
errors in determining low pressure values
on P-T diagrams and it has a significant
effect on the P-V diagram.

Comparison of Graphs 4.2-3 and 4.2-4 which represent the
Kistler transducer dynamic pressure calibration by the two
different techniques described shows that the balanced-disc pick-
up responded with considerable delay. It may be concluded that
the balanced-disc pick-up is only suitable for determining the
peak pressure of the cycle; however, it is not suitable for
obtaining accurate P-T diagrams because this would mean a variable
delay due to mechanical effects leading to erroneous results.

10.2.   The reciprocating engine indicators

The use of a Piezo-electric transducer and an oscilloscope
to obtain a P-T diagram has the following advantages:

(i)   Owing to its negligible inertia, the cathode-
ray, can be employed for displaying elec-
trical oscillations of frequencies exceeding
1000 Kc/s. (Resonant frequency of a Piezo-
electric pressure transducer is about 125
Kc/s).

- 148 -

(ii) Any desired portion of the engine cycle can be selected and magnified on the time-base, thus enabling a very close study to be made of phenomena suoh as ignition lag in diesel engines and detonation in petrol engines, both occurring during such a small crank angle that analysis is practically impossible on the P-T diagram.

(iii) Rapid transients may be examined.

(iv) P-V diagrams can be obtained; the timing signal for the P-T diagrams is to be replaced by one to complement the motion of the piston in the cylinder.

The technique described for detecting top-dead-centre on the P-T diagrams provided an average accuracy of about 0.3° of crank angle. The only difficulty is that the oscilloscope beams which indicate the pressure and T.D.C. must be exactly on the same vertical axis when observed on the screen before photographing; any horizontal drift from this position will introduce errors into the results. It is essential to observe the oscilloscope beams before and after photographing to ensure that no drift has occurred during recording.

The P-V indicator constructed gave a satisfactory signal on the C.R.O. screen (see Fig. 7.7-2). A dynamically calibrated transducer is required for the pressure indication; also a cam with correct profile (see Drawing 7.3-1) should be provided for the accurate indication of the volume signal.

10.3. Passage effects

An investigation into combustion behaviour in a Lister diesel engine demonstrated the necessity for mounting transducers flush with the cylinder wall (or cylinder head). If this precaution is not taken, passage effects are superimposed on the real pressure changes in cylinder pressure.

10.4. The pressure transducer technique for measuring the volumetric efficiency (η_v)

The accuracy of measuring η_v by the transducer is largely dependent on the accuracy of calculating the mass of the residual gases left in the cylinder at the end of the exhaust stroke. The residual product temperature was taken the same as that of the cylinder wall; also the pressure in the cylinder at the end of the exhaust stroke was assumed equal to the inlet pressure to the cylinder. These two assumptions do not hold accurately particularly at the higher engine speed. Better accuracy can be achieved

using a thermocouple to measure the exhaust gas temperature, and

a light spring indicator may be used to estimate the cylinder

pressure during the exhaust stroke.

Generally the transducer method of measuring η_v gave

satisfactory results (average accuracy, $\pm 3\%$) when compared with

the methods of direct air flow measurement and Infra-Red gas analysis.

Static calibration results for Kistler 601A transducer

Amplifier setting:

      CAL FACTOR   - 10
      Range   - 100 p.s.i./Volt

Oscilloscope Setting:

      Variable cal.   - .01 Volt/Div.
      Signal amplification - X1
      D.C. gain   - X1
      Sensitivity setting - maximum

Kistler 601A	output beam deflection (oscilloscope division units)	
Input pressure p.s.i.	Room temp.	80°C
0	0	0
15	0.55	0.6
105	1.18	1.18
155	1.74	1.73
205	2.35	2.35
255	2.9	2.9
305	3.45	3.45
355	4.05	4.05
405	4.6	4.59

Table 4.2-1

Static calibration results for AVL 10 mm transducer

Amplifier setting:

    CAL FACTOR   - 4.13
    Range   - 100 p.s.i./Volt

Oscilloscope Setting:

    Variable cal.   - .01 Volt/Div.
    Signal amplification - X1
    D.C. gain   - X1
    Sensitivity setting   - maximum

AVL 10 mm	output beam deflection (oscilloscope division units)	
Input pressure p.s.i.	Room temp.	80°C
0	0	0
55	0.78	0.78
105	1.5	1.46
155	2.3	2.2
205	3	2.95
255	3.74	3.65
305	4.5	4.5
355	4.9	5.1
405	5.85	5.82

Table 4.2-2

Static calibration of SLM PZ14 transducer

Amplifier setting:

    CAL FACTOR   -   10
    Range   -   100 p.s.i./Volt

Oscilloscope setting:

    Variable cal. setting   -   .01 Volt/Div.
    Signal amplification   -   X1
    Sensitivity setting   -   minimum
    D.C. gain   -   X1

SLM PZ14	output beam deflection (oscilloscope division units)	
Input pressure p.s.i.	Room temp.	80°C
0	0	0
55	0.7	0.73
105	1.35	1.35
155	2	2
205	2.65	2.65
255	3.22	3.26
305	3.9	3.95
355	4.5	4.6
405	5.2	5.23

Table 4.2-3

Results for the dynamic calibration of the
Kistler 601A transducer

Engine speed 500 r.p.m.   Transducer, cooled.

Kistler 601A	output beam deflection (oscilloscope division units)	
Input pressure p.s.i.		
70	.7	.6
120	1.35	1.3
170	2.05	1.95
220	2.67	2.56
270	3.2	3.05
320	3.7	3.6
380	4.4	4.2
420	4.6	4.5

Table 4.2-4

Engine speed 1000 r.p.m.   Transducer, uncooled.

Kistler 601A	output beam deflection (oscilloscope division units)	
Input pressure p.s.i.		
70	1	0.9
120	1.6	1.5
170	2.21	2.1
220	2.8	2.65
270	3.4	3.2
320	4	3.8
370	4.4	4.3
420	4.85	4.85

Table 4.2-5

Engine speed 1000 r.p.m.   Transducer, cooled

Kistler 601A	output beam deflection (oscilloscope division units)	
Input pressure p.s.i.		
70	1.05	
120	1.64	
170	2.25	
220	2.87	
270	3.43	
320	4.1	
370	4.55	
420	4.95	

Table 4.2-6

Engine speed 2000 r.p.m.   Transducer cooled.

Kistler 601A	output beam deflection (oscilloscope division units)	
Input pressure p.s.i.		
70	1.1	0.93
120	1.68	1.5
170	2.3	2.05
220	2.95	2.6
270	3.46	3.2
320	4.13	3.8
370	4.55	4.35
425	5	4.99

Table 4.2-7

Engine speed 2000 r.p.m.   Transducer, uncooled

Kistler 601A	output beam eflection (oscilloscope division units)	
Input pressure p.s.i.		
70	1	
120	1.58	
170	2.28	
220	2.83	
270	3.41	
320	4.0	
370	4.5	
420	5	

Table 4.2-8

Engine speed 2750 r.p.m. Transducer, cooled.

Kistler 601A	output beam deflection (oscilloscope division units)	
Input pressure p.s.i.		
70	1.12	0.9
120	1.75	1.4
170	2.37	1.97
220	2.96	2.56
270	3.54	3.15
220	4.17	3.7
370	4.63	4.18
420	5.05	4.75

Table 4.2-9

Engine speed 2750 r.p.m. Transducer, uncooled.

Kistler 601A	output beam deflection (oscilloscope division units)	
Input pressure p.s.i.		
70	1	
120	1.58	
170	2.28	
220	2.83	
270	3.41	
320	4	
370	4.5	
420	5	

Table 4.2-10

Dynamic calibration of AVL 10 mm transducer

Results obtained when the pick-up disc is moving up only.

Amplifier and oscilloscope settings – same as for the static testing.

Engine speed 1000 r.p.m.

AVL 10 mm	output beam deflection (oscilloscope division units)	
Input pressure p.s.i.	Uncooled	Cooled
50	0.9	1
100	1.8	1.86
150	2.55	2.61
200	3.27	3.4
250	4.1	4.18
300	4.75	4.81
350	5.4	5.43
400	6	6.03

Table 4.2-11

Engine speed 2000 r.p.m.

AVL 10 mm	output beam deflection (oscilloscope division units)	
Input pressure p.s.i.	Uncooled	Cooled
50	0.95	1.0
100	1.78	1.85
150	2.53	2.58
200	3.3	3.4
250	4.08	4.15
300	4.8	4.85
350	5.5	5.56
400	5.98	6.18

Table 4.2-12

Engine speed 2750 r.p.m.

AVL 10 mm	output beam deflection (oscilloscope division units)	
Input pressure p.s.i.	Uncooled	Cooled
50	0.98	1
100	1.87	1.8
150	2.58	2.63
200	3.4	3.45
250	4.15	4.22
300	5	4.86
350	5.58	5.6
400	6.05	6.12

Table 4.2-13

Results for the modified dynamic calibration of
the cooled Kistler and AVL transducers

1.   Kistler transducer

Amplifier setting:

      Amplification   -   X100
      CAL FACTOR   -   X10

Oscilloscope setting:

      Variable cal.   -   .05 Volt/Div.
      Sensitivity   -   minimum

Engine speed 1000 r.p.m.

Kistler Input pressure p.s.i.	output beam deflection (oscilloscope division units)
113	2.61
154	3.6
186	4.4
253	5.9
331	7.7

Table 4.2-14

Engine speed 2000 r.p.m.

Kistler	output beam deflection (oscilloscope division units)
Input pressure p.s.i.	
114	2.72
154	3.6
193	4.61
242	5.62
271	6.28
308	7.07

Table 4.2-15

Engine speed 2750 r.p.m.

Kistler	output beam deflection (oscilloscope division units)
Input pressure p.s.i.	
114	2.72
154	3.7
199	4.81
247	5.9
279	6.6
313	7.45

Table 4.2-16

2.   <u>AVL transducer</u>

Amplifier setting:

    Amplification - X100
    CAL FACTOR   - X10

Oscilloscope setting:

    Variable cal. - .02 Volts/Div.
    Sensitivity   - minimum

Engine speed 1000 r.p.m.

AVL	output beam deflection (oscilloscope division units)
Input pressure p.s.i.	
264	8
236	7
201	6
168	5
134	4
102	3

Table 4.2-17

Engine speed 2000 r.p.m.

AVL	output beam deflection (oscilloscope division units)
Input pressure p.s.i.	
260	8
228	7
197	6
164	5
131	4
98	3

Table 4.2-18

Engine speed 2750 r.p.m.

AVL	output beam deflection (oscilloscope division units)
Input pressure p.s.i.	
257	8
227	7
193	6
162	5
127	4
95	3

Table 4.2-19

APPENDIX 4

Eccentric cam lift calculation

Let cam eccentricity $= \epsilon$

   cam radius $= r$

   cam lift $= \Delta d$

Vertical height of cam above centre of shaft $= d$

   also let $d_o = r - \epsilon$

See Fig. 7.3-1.

At any instant

$$d = r - \epsilon \cos \theta$$

$$\Delta d = r - d_o - \epsilon \cos \theta$$

$$= r - (r - \epsilon) - \epsilon \cos \theta$$

$$\Delta d = \epsilon \ (1 - \cos \theta)$$
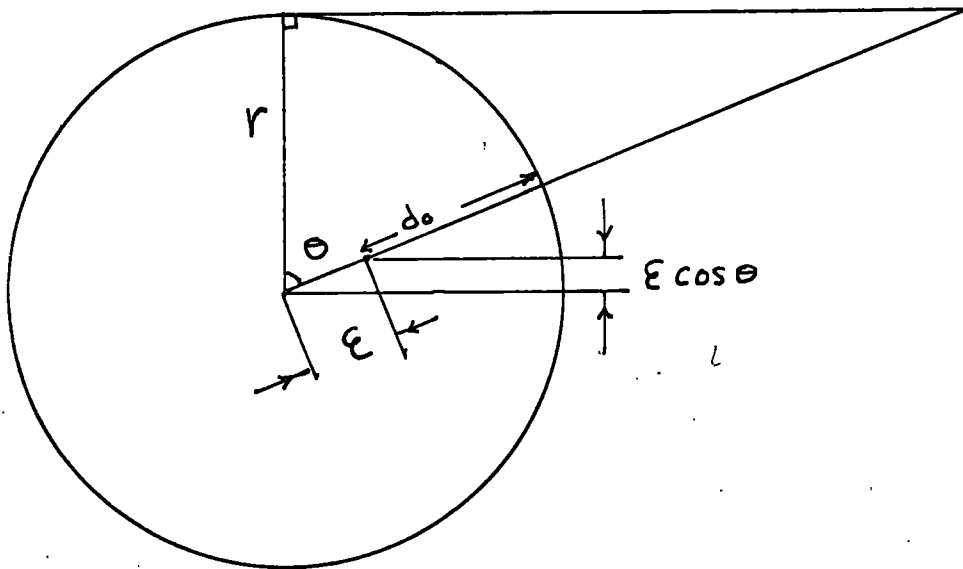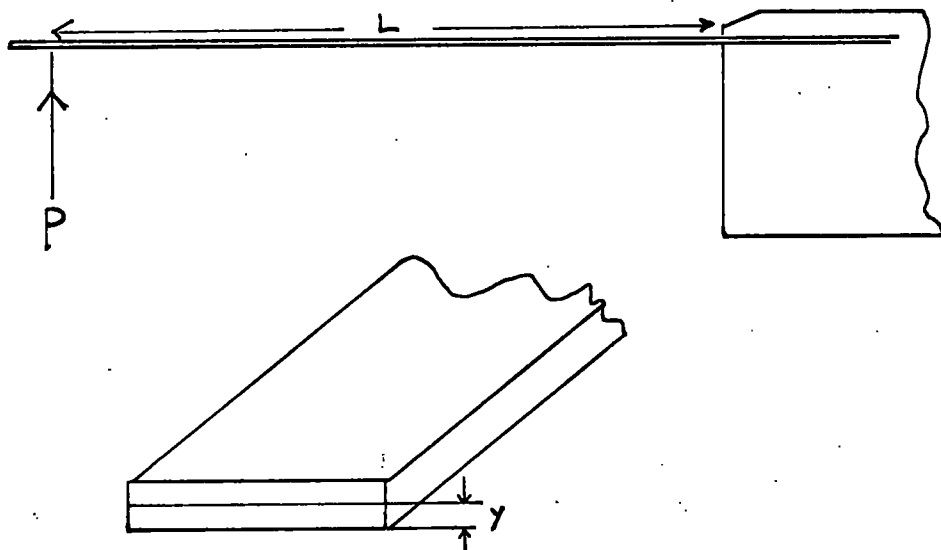
FIG. 7.3-1

FIG. 7.3-2

To compare the eccentric cam lifts Δd with the corresponding piston displacements δd that were found graphically (see drawing 7.3-2), a cam eccentricity of 2.25 inch is used for the calculation giving a maximum lift of 4.5 inches. This is equivalent to the maximum piston stroke.

Table 7.3-1 shows the values of Δd and δd with respect to the crank angle θ. (See also graph 7.3-1).

The required cam profile was drawn on a large scale (X4 full size) in order to achieve a reasonable accuracy. (See drawing 7.3-2).

θ	cos θ	1 – cos θ	Δd	δd
0	0.1	0	0	0
10	0.9848	0.0152	0.0342	0.03
20	0.9397	0.0603	0.136	0.099
30	0.866	0.134	0.301	0.2
40	0.766	0.234	0.526	0.35
50	0.6428	0.3572	0.804	0.54
60	0.5	0.5	1.125	0.8
70	0.342	0.658	1.48	1.1
80	0.1736	0.826	1.86	1.43
90	0.0	1	2.25	1.81
100	-0.1736	1.1736	2.64	2.22
110	-0.342	1.342	3.02	2.63
120	-0.5	1.5	3.37	3.05
130	-0.6428	1.628	3.66	3.44
140	-0.766	1.766	3.97	3.8
150	-0.866	1.866	4.19	4.10
160	-0.9397	1.937	4.36	4.29
170	-0.9848	1.9848	4.46	4.42
180	-0.1	2	4.5	4.5

Table 7.3-1

APPENDIX 5

Calculation for the Wheatstone bridge output signal

Since the output from the bridge is connected to a high impedance amplifier, then the current between the terminals A and B (see Fig. 7.6) is negligible. Hence the current i_2 flows through the resistance R_2 and R_3. Similarly a current i_1 flows through the resistances R_1 and R_4. Hence

$$I_1 = \frac{Eb}{R_1 + R_4}$$

$$I_2 = \frac{Eb}{R_2 + R_3}$$

$$E(CB) = I_1 R_1 = \frac{Eb\ R_1}{R_1 + R_4}$$

$$E(CA) = I_2 R_2 = \frac{Eb\ R_2}{R_2 + R_3}$$

But the voltage drop between AB

$$E(AB) = E(CA) - E(CB)$$

Hence

$$E(AB) = \frac{Eb\, R_2}{R_2 + R_3} - \frac{Eb\, R_1}{R_1 + R_4}$$

$$\therefore\ E(AB) = Eb\ \frac{R_2}{R_2 + R_3} - \frac{R_1}{R_1 + R_4} \tag{1}$$

From the Bending equation for the spring (see Fig. 7.3-1)

$$\frac{f}{y} = \frac{M}{I}$$

f — shear stress
y — distance from neutral axis
I — moment of inertia
M — moment = PL

$$P = \frac{fI}{Ly} \tag{2}$$

For a cantilever deflection P

$$\delta = \frac{PL^3}{3EI}$$

$$P = \frac{3\delta EI}{L^3} \tag{3}$$

From (3) and (2)

$$\frac{FI}{Ly} = \frac{3\delta EI}{L^3}$$

or $f = \dfrac{3\delta E y}{L^2}$

But strain $e = \dfrac{f}{E}$

$e = \dfrac{3\delta y}{L^2}$ L and y: constants

$e = $ constant x δ

Hence the strain in the spring is proportional to δ

$y = .024$ inch

$L = 3$ inch

also using a cam lift δ of 0.2 inch

then $e = \dfrac{3 \times 0.2 \times 0.24}{3^2}$

$e = 0.0016$

For the strain gauge

Gauge factor $= \dfrac{\Delta R}{R} \quad \dfrac{\Delta L}{L}$

where $\dfrac{\Delta L}{L} = e$

Gauge factor = 2.17

Stress free gauge resistance R = 60Ω

ΔR = Gauge factor x e x R

Hence the change in resistance of the strain gauge

ΔR = 2.17 x 0.0016 x 60

= 0.208 ohms

Consequently the resistance of the strain gauge under positive strain

= 60.208 ohms

and the resistance of the strain gauge under negative strain

= 59.792 ohms

From equation (1) the output voltage of the bridge

$$Eg \ = \ 12 \left(\frac{60.208}{60.208 + 59.792} \ - \ \frac{60}{60 + 60} \right)$$

$$Eg \ = \ 0.0202 \ Volts$$

Using a X100 fixed gain amplifier, the bridge output is amplified to 2.02 volts.

This signal gives a range of beam deflection from 0.2 to 30 cm, depending on recorder amplifier sensitivity and amplification used.

APPENDIX 6

Results for the volumetric efficiency measurements
by Pressure transducer and Viscous flowmeter

Barometric pressure - 30 in Hg. Meter temperature - 23°C. Inlet temperature - 24°C.

C.R. 7.95:1

		1007	1505	2008	2502
Engine speed	r.p.m.	1007	1505	2008	2502
Inlet depression	in Hg	-0.118	-0.157	-0.157	-0.157
Inlet pressure to manometer	in Hg	29.882	29.843	29.843	29.843
Gauge factor	-	0.02507	0.02504	0.06149	0.06149
Meter reading	cm	23.2 L.S	34.3 L.S	19.4 M.S	24 M.S
Mass of air flow	lb/min	0.582	0.878	1.192	1.473
Mass of air aspirated/cycle	lb	0.001157	0.001169	0.001185	0.001177
Oscilloscope beam deflection	0.05V/Div	4.18	4.25	4.33	4.38
Compression pressure	p.s.i.	180	182	182	179
Mass of air to fill swept vol.	lb	.001479	.001475	.001475	.001475
Calculated mass of air induced/cycle (transducer)	lb	0.0011095	0.0011197	0.0011197	0.0011197
η_v flowmeter	%	75	79.1	80.3	79.8
η_v transducer	%	75	75.8	75.8	75.6

Table 1

Barometric pressure - 30.02 in Hg.   Meter temperature - 25°C.   Inlet temperature 26°C.

		C.R. 7.22:1			
Engine speed	r.p.m.	1004	1502	2006	2507
Inlet depression	in Hg	-.118	-.157	-.157	-.157
Inlet pressure to manometer	in Hg	29.902	29.863	29.863	29.863
Gauge factor	-	0.02480	0.02477	0.06081	0.06081
Flowmeter reading	cm	22.9 L.S	34.2 L.S	19.5 M.S	24 M.S
Mass of air flow	lb/min	0.568	0.870	1.185	1.458
Mass of air aspirated/cycle	lb	0.001130	0.601158	0.001181	0.001163
Oscilloscope beam deflection	0.05V/Div	3.81	3.82	3.85	3.84
Compression pressure	p.s.i.	163	162	163.5	160
Mass of air to fill swept vol.	lb	0.001470	0.001467	0.001467	0.001467
Calculated mass of air induced/cycle (transducer)	lb	0.0011567	0.0011137	0.001147	0.001127
η_v flowmeter	%	76.9	78.9	80.6	79.4
η_v transducer	%	77.3	77.2	77.5	76.5

Table 2

Barometric pressure - 30.02 in Hg. Flowmeter temperature - 26°C. Inlet temperature 27°C.

C.R. 6.88:1

		1001	1512	2001	2501
Engine speed	r.p.m.	1001	1512	2001	2501
Inlet depression	in Hg	-0.118	-0.157	-0.157	-0.157
Inlet pressure to manometer	in Hg	29.902	29.863	29.863	29.863
Gauge factor	-	0.02463	0.02460	0.06042	0.06042
Flowmeter reading	cm	22.9 L.S	34.5 L.S	19.5 M.S	24 M.S
Mass of air flow	lb/min	.564	.853	1.178	1.449
Mass of air aspinated/cycle	lb	0.001127	0.001130	0.001178	0.001158
Oscilloscope beam deflection	0.05V/Div	3.58	3.55	3.6	3.59
Compression pressure	p.s.i.	154	152	152	149
Mass of air to fill swept vol.	lb	0.001466	0.001464	0.001464	0.001464
Calculated mass of air induced/cycle (transducer)	lb	0.0011284	0.0011313	0.0011317	0.001137
η_v flowmeter	%	76.7	77.1	80.5	79
η_v transducer	%	77	77.3	77.3	76.1

Table 3

Barometric pressure 30.02 in Hg.   Meter temperature 26°C.   Inlet temperature 27°C.

C.R. 5.95:1

		1008	1508	2007	2509
Engine speed	r.p.m.	1008	1508	2007	2509
Inlet depression	in Hg	-0.118	-0.157	-0.157	-0.157
Inlet pressure to manometer	in Hg	29.902	29.863	29.863	29.863
Gauge factor	-	.02463	.02460	.06042	.06042
Meter reading	cm	23.2 L.S	34.5 L.S	19.6 M.S	24.1 M.S
Mass of air flow	lb/min	.572	.867	1.182	1.455
Mass of air aspirated/cycle	lb	.001135	.001150	.001177	.001160
Oscilloscope beam deflection	0.05V/Div	2.95	2.98	3	2.98
Compression pressure	p.s.i.	127	128	126	123
Mass of air to fill swept vol.	lb	0.001466	0.001464	0.001464	0.001464
Calculated mass of air induced/cycle (transducer)	lb	0.0011644	0.0011707	0.0011567	0.0011367
η_v flowmeter	%	77.5	78.5	80.4	79.2
η_v transducer	%	79.4	80	79	77.6

Table 4

Barometric pressure - 30.02 in Hg.   Meter temperature - 27°C.   Inlet temperature 27.5°C

C.R. 5:1

		1009	1506	2011	2516
Engine speed	r.p.m.	1009	1506	2011	2516
Inlet depression	in Hg	-0.118	-0.157	-0.157	-0.157
Inlet pressure to manometer	in Hg	29.902	29.863	29.863	29.863
Gauge factor	-	0.02450	0.02447	0.06010	0.06010
Flowmeter reading	cm	23.4 L.S	34.7 L.S	19.7 M.S	24.2 M.S
Mass of air flow	lb/min	0.574	0.856	1.182	1.453
Mass of air aspinated/cycle	lb	0.001148	0.001150	0.001175	0.001157
Oscilloscope beam deflection	0.05V/div	2.3	2.3	2.35	2.4
Compression pressure	p.s.i.	98	99	98	97
Mass of air to fill swept vol.	lb	0.001461	0.00146	0.00146	0.00146
Calculated mass of air induced/cycle (transducer)	lb	0.0011654	0.0011767	0.0011717	0.0011607
η_v Flowmeter	%	78.5	78.9	80.5	79.2
η_v transducer	%	79.8	80.6	80.3	79.5

Table 5

Inlet temperature 77°F.

Atmospheric pressure 30.12 in Hg

		C.R. 7.95:1			
Engine speed	r.p.m.	1008	1502	2015	2507
Inlet depression	in Hg	-0.118	-0.157	-0.157	-0.157
Inlet pressure	in Hg	30.002	29.963	29.963	29.963
IRGA meter reading		27.8	29.3	30.7	32.3
CO_2 in exhaust gas	%	17.4	18	18.6	19.3
A/F ratio	By mass	12.16	11.67	11.21	10.71
Fuel consumption	cc/min	30.6	47.6	65.2	85.7
Air consumption	lb/cycle	.001129	.001131	.001110	.001120
Mass of air to fill swept vol.	lb	.001476	.001475	.001475	.001475
η_v (IRGA)	%	76.4	76.7	75.2	75.9

Table 6

Inlet temperature 77°F.   Atmospheric pressure 30.12 in Hg.

		C.R. 7.22:1			
Engine speed	r.p.m.	1015	1506	2016	2508
Inlet depression	in Hg	-0.118	-0.157	-0.157	-0.157
Inlet pressure	in Hg	30.002	29.963	29.963	29.963
IRGA meter reading	%	27.8	29.3	30.8	32.5
CO_2 in exhaust gas	%	17.4	18	18.6	19.4
A/F Ratio	By mass	12.16	11.67	11.21	10.64
Fuel consumption	cc/min	30.6	47.6	66.7	85.7
Air consumption	lb/cycle	0.001121	0.001128	0.001135	0.001112
Mass of air to fill swept vol.	lb	0.001476	0.001475	0.001475	0.001475
η_v (IRGA)	%	75.8	76.7	77	75.4

Table 7

- 185 -

Atmospheric pressure 30.1.   Inlet temperature 78.8°F.

		C.R. 6.88:1			
Engine speed	r.p.m.	1005	1507	2005	2503
Inlet depression	in Hg	-0.118	-0.157	-0.157	-0.157
Inlet pressure	in Hg	29.982	29.943	29.943	29.943
IRGA meter reading		26.9	29	30.4	32.3
CO_2 in exhaust gas	%	17	17.9	18.5	19.4
A/F Ratio	By mass	12.51	11.75	11.29	10.64
Fuel consumption	cc/min	30.3	47.6	65.2	85.7
Air consumption	lb/cycle	0.001154	0.001135	0.001123	0.001114
Mass of air to fill swept vol.	lb	0.001473	0.001471	0.001471	0.001471
η_v (IRGA)	%	78.3	77.1	76.3	75.7

Table 8

Atmospheric pressure 30.1 in Hg. Inlet temperature 80.6°F.

			C.R. 5.95:1		
Engine speed	r.p.m.	1010	1510	2006	2502
Inlet depression	in Hg	-0.118	-0.157	-0.157	-0.157
Inlet pressure	in Hg	29.982	29.943	29.943	29.943
IRGA meter reading		26.3	28.2	30.1	32
CO_2 in exhaust gas	%	16.7	17.6	18.4	19.2
A/F ratio	By mass	12.78	11.99	11.36	10.78
Fuel consumption	cc/min	30.3	47.6	65.2	85.7
Air consumption	lb/cycle	0.001173	0.001156	0.00112	0.001129
Mass of air to fill swept vol.	lb	0.001468	0.001466	0.001466	0.001466
η_v (IRGA)	%	79.9	78.6	77.1	77.1

Table 9

Atmospheric pressure 30.1 in Hg. Inlet temperature 82.7°F.

		C.R. 5:1			
Engine speed	r.p.m.	1016	1509	2008	2512
Inlet depression	in Hg	.118	.157	.157	.157
Inlet pressure	in Hg	29.982	29.943	29.943	29.943
IRGA meter reading	%	25.7	27.7	30	32
CO_2 in exhaust gas	%	16.5	17.3	18.3	19.2
A/F ratio	By mass	12.97	12.25	11.77	10.78
Fuel consumption	cc/min	30.9	47.6	66.7	88.2
Air consumption	lb/cycle	0.001208	0.001182	0.001162	0.001159
Mass of air to fill swept vol.	lb	0.001462	0.001461	0.001461	0.001461
η_v (IRGA)	%	82.6	80.9	79.5	79.3

Table 10

APPENDIX 7

IRGA Calibration

The sample tube was purged with a known percentage mixture of dry compressed CO_2 and nitrogen supplied from a series of cylinders. The rate of mixture flow was adjusted at 500 cc/min and the IRGA sensitivity switch was set to give a suitable meter deflection. This procedure was repeated for different known mixture proportions and fixed meter sensitivity, noting the meter deflection in each case. A graph of meter deflection against % CO_2 was plotted (see graph 9.3-3) representing the calibration for the instrument.

To find the air/fuel ratio, the exhaust gas was passed in the sample tube and the meter reading finally observed. From the calibration curve, the % CO_2 in the exhaust gas was found. By using standard calibration curves for the fuel used, the air/fuel ratio corresponding to the CO_2 in the oxidized exhaust gases was found.

IRGA Calibration Results

% CO_2	IRGA Meter Reading
8.5	0.9
12	13.1
16	24.5
25	44.5

For the air flowmeter, calibration tables for the three manometer inclinations were supplied by the manufacturer, who claimed an accuracy of 2%.

REFERENCES

1. W. L. Brown

    Methods of evaluating requirements
    and errors in cylinder pressure
    measurements.
    S.A.E. Journal, Jan, 9-13 1967.

2. Cearay D. Miller

    Slow motion study of injection and
    combustion of fuel in diesel engines.
    S.A.E. Journal (Transaction)
    Vol. 53, No. 12, Dec. 1945.

3. C. S. Draper

    Pressure waves accompanying detonation
    in diesel engines.
    Journal of the aeronautical science.
    Vol. 5, No. 6, April 1938.

4. F. Nagao et al

    Influence of the connecting passage
    of a low pressure indicator on
    recording.
    Bulletin of J.S.M.E.
    Vol. 6, No. 21, Feb. 1963.

5. J. G. Withers

    Effect of passages on the accuracy of
    indicator diagrams.
    The Engineer.
    Vol. 200, p. 860, Dec. 1955.

6. G. Harrow

    Thornton Research Centre
    Shell Research, U.K. Ltd.

7. J. C. Livengood,
    A. R. Rogowski
    and C. F. Taylor

    The volumetric efficiency of four-
    stroke engines.
    S.A.E. Journal.
    Vol. 6, No. 4, Oct. 1952.